

DANISH METEOROLOGICAL INSTITUTE

TECHNICAL REPORT

00-01

STOWASUS 2100

**Regional Storm, Wave and Surge Scenarios
for the 2100 Century:**

**Progress report for the second project year
(1/12 1998 - 31/11 1999)**

Eigil Kaas, Uffe Andersen, Roger Flather, Jane Williams, Piero Lionello,
Piero Malguzzi, Arnt Pfizenmayer, Hans von Storch, John de Ronde,
Marc Philippart, Stephanie Holtermann, Magnar Reistad, Knut Helge Midtbø,
Ole Vignes, Hilde Haakenstad, Bruce Hackett and Ingerid Fossum.

ISSN 1399-1388 (online version)



Copenhagen 1999



**Regional storm, wave and surge
scenarios for the 2100 century**
(Contract no. ENV4-CT97-0498)

Coordinator, Eigil Kaas, DMI

**Progress report for the second
project year (1/12 1998-30/11 1999)**

Content:

Organisational	1
Summary of the project and its progress	3
Individual partner contributions	14
Danish Meteorological Institute (DMI).....	14
Proudman Oceanographic Laboratory (POL).....	20
University of Padua (UP)	29
ISAO-CNR	37
Institute of Hydrophysics (GKSS).....	44
National Institute for Coastal and Marine Management (RIKZ).....	53
The Norwegian Meteorological Institute (DNMI)	63

Regional storm, wave and surge scenarios for the 2100 century

(Contract no. ENV4-CT97-0498)

Progress report for the second project year (1/12 1998-30/11 1999)

This second status report of STOWASUS-2100 consists of three main sections describing

- 1) Organisational and logistic matters. This is a short section listing the project organisation, the official meetings and so on.
- 2) A summary of the entire project and its progress. Some of the figures presented in this part are also shown under the individual partner contributions. The same applies for several parts of the text.
- 3) Individual partner contributions. The authors of these contributions are identical to the scientific investigators at the individual institutions.

Organisational

The 7 partners (all contractors) in the project are listed in table 1 together with the principal investigators. There has been one official project meeting in 1999 held 10-11 June in Bergen Norway.

INSTITUTION	PRINCIPAL (RESPONSIBLE) INVESTIGATOR
Danish Meteorological Institute (DMI)	Eigil Kaas (co-ordinator)
Proudman Oceanographic Laboratory (POL)	Roger Flather
University of Padua (UP)	Piero Lionello
ISAO-CNR	Piero Malguzzi
Institute of Hydrophysics, GKSS	Hans von Storch
National Institute for Coastal and Marine Management (RIKZ)	John de Ronde
The Norwegian Meteorological Institute (DNMI)	Magnar Reistad

Table 1. List of partners and investigators

The project is to a high degree administrated and co-ordinated via an Internet home page which the reader is referred to for more organisational details. It is located at:

<http://www.dmi.dk/pub/STOWASUS-2100/>

The home-page includes 10 sub pages:

1. Description. This page includes a summary of the project and its actual progress.
2. Partners. Provides information about partners and includes addresses, phone numbers, e-mail addresses etc.
3. Partner information. Needed ongoing information to the partners.
4. Work-programme. An http version of the official work-programme approved by the EU-Commission.
5. Meetings. Information about the project meetings, including short summaries.
6. Progress reports. Includes http-versions of the annual reports (of which this is an example).
7. Data. Information about data availability.
8. Project publications. Gives a list of publications produced within the project. Some of these are electronically accessible.
9. Other publications. A reference list including publications which are relevant to STOWASUS-2100.
10. Other projects. Short description of other projects which are interrelated to STOWASUS-2100.

Summary of the project and its progress

INTRODUCTION

The overall objective of STOWASUS-2100 is to study severe storms, surges and waves in the present climate and in a scenario with increased CO₂-concentration. More specifically, the project is a joint atmospheric/oceanographic numerical modelling effort aiming at constructing and analysing storm, wave and surge climatologies for the North Atlantic/European region in a climate forced by increasing amounts of greenhouse gases and to compare with present day conditions. It is investigated whether any systematic anomalies regarding frequency, intensity or area of occurrence are found for these extreme events. Also physical mechanisms responsible for possible scenario anomalies are investigated.

The backbone in STOWASUS-2100 is two 30 year time slice simulations with the ECHAM4 atmospheric climate model at T106 horizontal resolution. The experimental design of these simulations is described in May (1999). The project work is divided into 12 working tasks consisting of analyses of storm activity in these simulations and in different impact scenarios for extreme storms, waves and surges. These scenarios are largely based on simulations with regional wave, storm surge and atmospheric models which are driven by boundary conditions from the T106 backbone simulations.

Some important results obtained during the second project year are

- The storm surge simulations indicate increased 50 year return storm surge levels by some 30-40 cm in the German Bight region in the 2xCO₂ scenario climate relative to the control climate. Smaller increases are seen in many regions in the North Sea and further north in Skagerak and along the Norwegian coast.
- A preliminary analysis of wave simulations shows that the significant wave heights are slightly increased in the Northeast Atlantic and the North Sea region. For certain locations the 99 percentile levels of significant wave heights are increased by almost 10%.
- A quite preliminary results is that there seem to be a tendency for increases in favourable conditions for development in polar lows north of Norway and further east. There is no sign of similar likely changes in Mediterranean convective low pressure systems.

PROGRESS OF THE INDIVIDUAL WORKING TASKS

The individual working tasks are described in detail in the work programme (see e.g. <http://www.dmi.dk/pub/STOWASUS-2100/workprog.htm>). In the following the status of each task after the second project year is described.

Task 1: Statistical analysis of the T106 atmospheric data

This task consists of a statistical analysis of the storm activity in the target region in the two 30 year time simulations and in comparisons with observations as well as with other studies.

According to the work programme this task should only be carried out during the first half year and during the last year of the project. However, since technical problems (see below) has caused a considerable delay of task 2, it was decided partly to move the task 1 work of the last year to the

second year. This will leave more time to finish task 2 during the last project year. The analysis in task 1 during the second year included:

1. a comparison between the storm climate in the T106 resolution with that in the original coupled T42 model (ECHAM4/OPYC) providing SSTs for the T106 simulations,
2. a critical look at the length of the simulations (2x30 years),
3. an update of the statistical analysis to include 5 winter months instead of the original 3 month period (all the results below are based on this expanded period which gives more stable statistics)

500 hPa variability

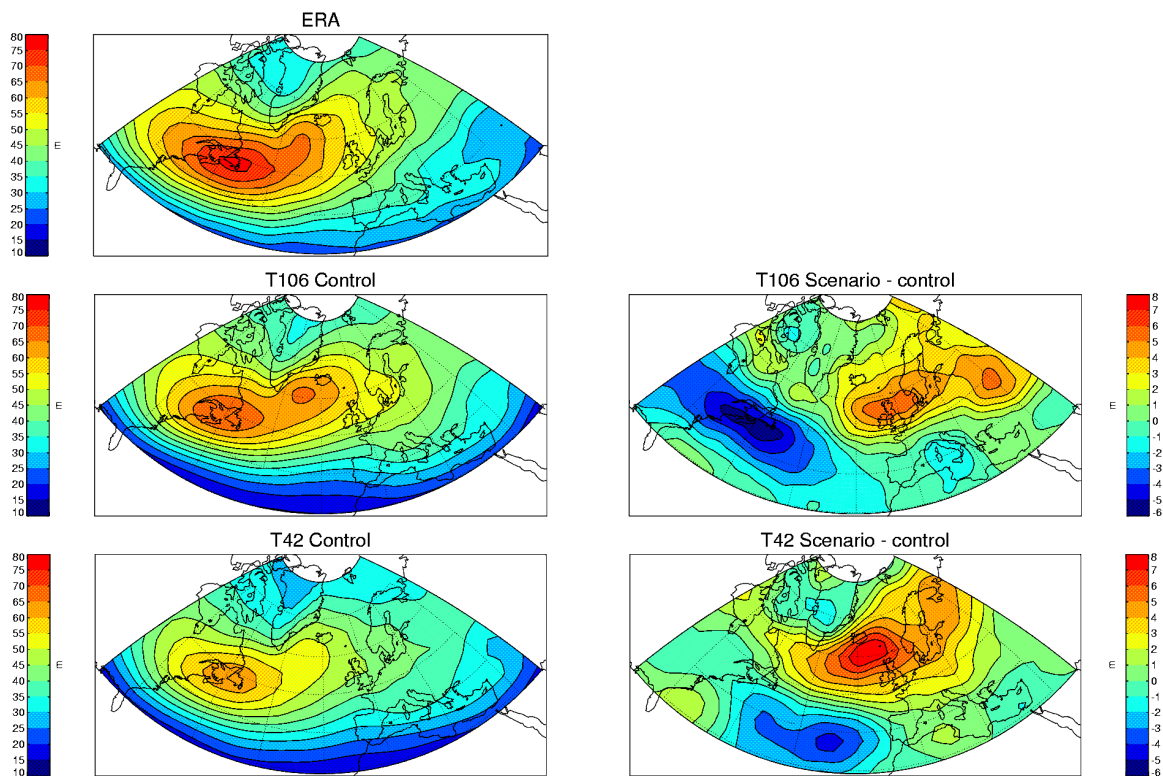


Fig. 1. The storm track intensity (the 500-hPa short term variability) from a) the ERA data, b) the control run in T106 resolution, c) the difference between the scenario and the control run in T106 resolution, d) the control run in T42 resolution and e) the difference between the scenario and the control run in T42 resolution.

Concerning item 1, both simulations in T106 and T42 resolution agree on enhanced storm track intensity over northern Europe in the scenario run - see figure 1. There are, however, differences in the regional details of the response pattern and there seem to be tendency that the climate change signal over western Europe is stronger in T42 than in T106. Furthermore, the strongest winds speeds over ocean in the T106 control simulation are generally marginally stronger than in the T42 resolution model (not shown). This is believed to be a consequence of the higher resolution and hence the shorter time steps. However, local effects might play a role in this.

The length of climate simulations are usually limited due to the models huge consumption of computer power. However, if the simulations are too short the internal climate variability will be larger than the changes (i.e. the signal) between control and scenario simulations. Beersma et al. (1997), for instance concluded that two 5 years simulations were too short to detect statistical significant climatic changes and this was one of the basic arguments for setting up STOWASUS-2100. Therefore an analysis - using Hotelling T^2 test - was performed to investigate the minimum length needed for climate simulations. The main conclusion is that 8 years of data is sufficient to obtain significant changes in sea level pressure for the original T42 coupled simulation while 18 years must be included before the changes in the T106 resolution are significant. The difference is probably related to the overall stronger pressure response in the T42 than T106. For the short term variability of the 500 hPa height (storm tracks), the corresponding numbers are 22 and 29 years. Based on these findings it is concluded that the chosen simulation period of 30 years is marginally sufficient for the purpose of the project.

All the work in task 1 will soon appear as DMI scientific report (Andersen et al. 2000) which describes the analysis methods in more detail.

Task 2: Baroclinic developments - case and process studies

In this task a number of selected cases will be studied. This is done by re-simulating the storms with a high resolution regional climate model (HIRHAM). The basic purpose is to investigate which mechanisms dominate in defining the most extreme developments.

According to the Work Programme the selected storms should already have been simulated in the HIRHAM model both with the control and the scenario climatology. So far the HIRHAM model has been set up and a few storms from the control run have been simulated. However, there has been a serious problem with the version of the model used: the wind field has an unrealistic noisy structure near the surface. Quite some effort has been put into explaining this odd behaviour. A serious error was recently identified in the horizontal diffusion and it is believed to be responsible for the noise. The error has now been corrected but test runs have to be completed. It is important to note, that the error was only present in that particular version of HIRHAM used here. It is related to the parallelization of the code.

Task 3: Polar lows

In this task it is investigated whether one can expect an increasing or decreasing number of polar lows in the scenario climate. The idea is to first set up an objective synoptic scale criteria to identify these system as they cannot be simulated explicitly at T106 resolution. Statistics for the criteria in the ERA-data and in the T106 control and scenario simulations are then compared. Furthermore, individual cases will be simulated with the HIRHAM regional model.

During the second project year the construction of the indeks, which is based on a special form of the quasi-geostrophic omega equation, was completed. The occurrence of polar lows in the (T106) ERA data identified with the index were first compared to known events in the winters 1982-1985. This comparison revealed that the index is not suited for identifying individual polar lows but that it may be quite reasonable in defining the statistical occurrence of polar lows, given the larger scale atmospheric flow.

The number of polar lows detected with the index over the ocean north of Norway and further east in the T106 control simulation is 122, however, with some redundancy since one event may be counted a few times. The same number for the scenario is 166 which must be considered a significant increase.

The next step to take place during the last project year will be to simulate a set of selected cases with the HIRHAM model. The entire task was delayed a little due to basic problems in defining the objective selection criteria.

Task 4: Intense cyclogenesis in the Mediterranean

In this task so called Mediterranean storms are analysed. These storms that are highly convective are quite similar to polar lows, and at variance to tropical depressions they need a synoptic forcing. The work consists of defining a set of cases which will be used as input for the wave and surge models (tasks 6 and 10). Furthermore, an objective index, equivalent to but different from that for polar lows, will be set up to identify the likelihood for development of strong Mediterranean storms. The work also includes simulation of a few individual cases with the regional atmospheric model BOLAM.

During the second project year the selection of cases was completed. This was done by tracking individual storms and analysing the strength in terms of anomalous centre pressure and maximum geostrophic wind at sea level. Figures 2 and 3 show the distributions of number of cyclones with different maximum depths for each of the two measures of strength. It can be seen that the results are somewhat inconclusive since the tail of the distribution based on maximum depth indicates a worsening of the storm climate, while the opposite is the case when the selection is based on geostrophic wind.

NUMBER OF CYCLONES vs MAXIMUM DEPTH in hPa

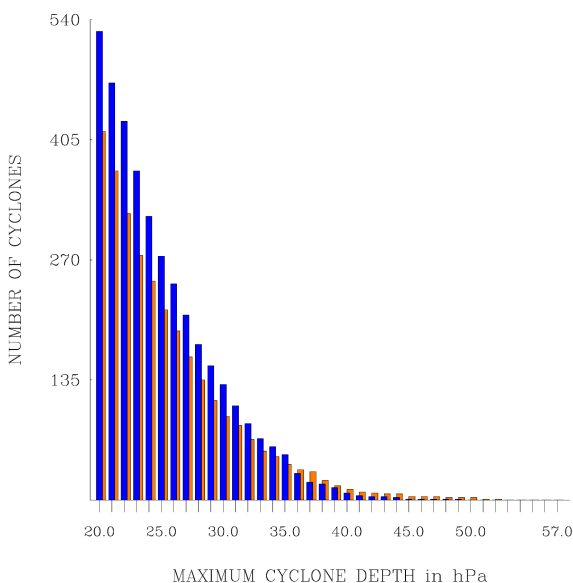


Fig. 2. Cumulated distribution of number of simulated cyclones in the present (blue) and doubled CO₂ (orange) scenario. The abscissa shown the anomalous maximum cyclone depth in hPa.

NUMBER OF CYCLONES vs MAXIMUM DEPTH in hPa

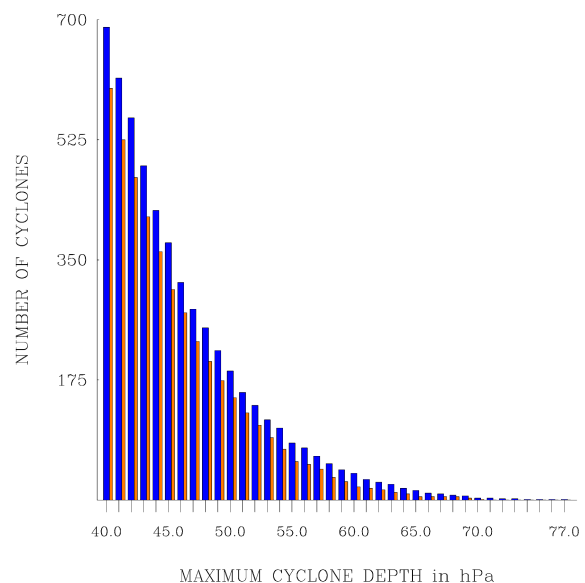


Fig. 3. As Fig. 2, but based on maximum geostrophic wind at sea level.

The final version of the objective index for identifying potential cases of strong convective cyclogenesis in the Mediterranean has now been defined and applied to the T106 control and scenario simulations. Figure 4 shows that the number of cases in the CO₂ case is smaller at all threshold values (except for one case with very high index) than in the control. One may conclude

that, on average over the season tested (1 October to 30 January), the frequency and the intensity of those systems should diminish in the climate of the 21st century. This is most likely because the number of the synoptic precursors is expected to be smaller and the surface fluxes of sensible heat weaker.

One control and one scenario case have been selected using the objective index. These cases were then simulated with the BOLAM model. Both cases turned out to develop into Mediterranean lows, indicating that the index constitutes a good indicator.

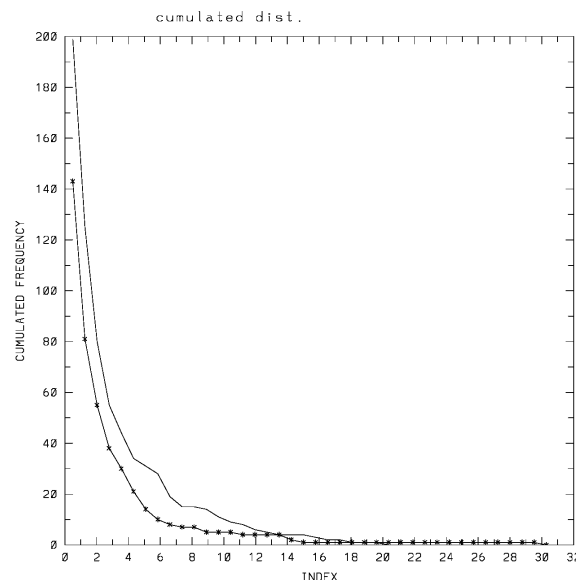


Fig. 4. Cumulated distribution of the index (see text) for the CTR (thin line) and the CO₂ (starred line) scenario.

According to the original work plan, the simulation of individual cases should serve the purpose of identifying systematic differences between climatic scenarios concerning frequency and intensity of Mediterranean systems. It has been realised, however, that a few tens of cases are not enough for that, given the extreme variability presented by Mediterranean systems and the large number of degrees of freedom involved. It has therefore been decided to devote a larger part of the high resolution simulations to train the statistical wind downscaling which is a very important step in order to be able to run the 30 year simulation of surges and waves (tasks 6 and 10). The high resolution simulations for this purpose will be performed in the beginning of the last project year.

Task 5: Surge statistics based on 30 year T106 time slices: North-western European shelf seas.

This task includes simulations at POL with the 35 km model (NEAC) and with the 12 km model (NISE) nested into NEAC. All simulations with NEAC cover the coloured region in figure 5 while the NISE simulations only cover the southern part of the North Sea, the Irish Seas and the English Channel. The NEAC simulations are forced by astronomical tide only, by tide and "observed" forcing during the years 1955-1997 (hindcast based on a DNMI 50 km gridded analysis of sea level pressure) and by tide and the forcing from the T106 30 year control and 30 year scenario. The NISE simulations are similar, but don't include the 1955-1997 hindcast period.

The task has been almost completed in 1999, but due to the problems with the T106 data (mentioned in the last status report), detailed analysis of the simulations and reporting in terms of articles/reports have not yet been carried out. The results obtained are considered a main result in the project. Figure 5 shows the 50 year return surge for the scenario simulation minus the tide only simulation. The method used to obtain this statistic is similar to that described in Flather and Smith (1998) and is based on the "r largest" method (Tawn, 1988). Figure 5 is based on the 10 largest independent surges each winter and a fit to a Gumbel distribution. The simulated surge climatology in the control (and scenario) is comparable to observed climatology at individual locations (not shown). Figure 6 shows the main result, namely that the 50 year return surge is 30-40 cm higher in the German Bight region in the scenario than in the control and also that there are smaller increases at many other coastal locations. The figure is based on 20 cases each winter which turned out to be needed to obtain stable statistics.

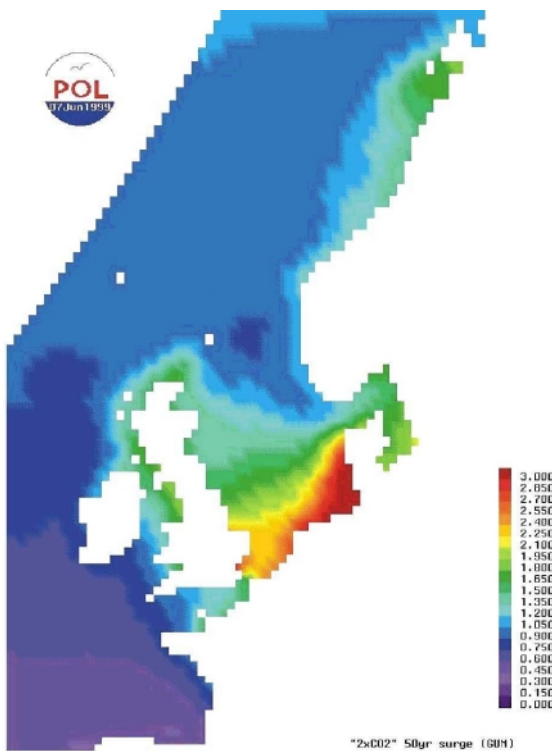


Fig. 5. 50 year surge in meters ("2xCO₂") based on 10 largest independent surges per year and fit to a Gumbel distribution

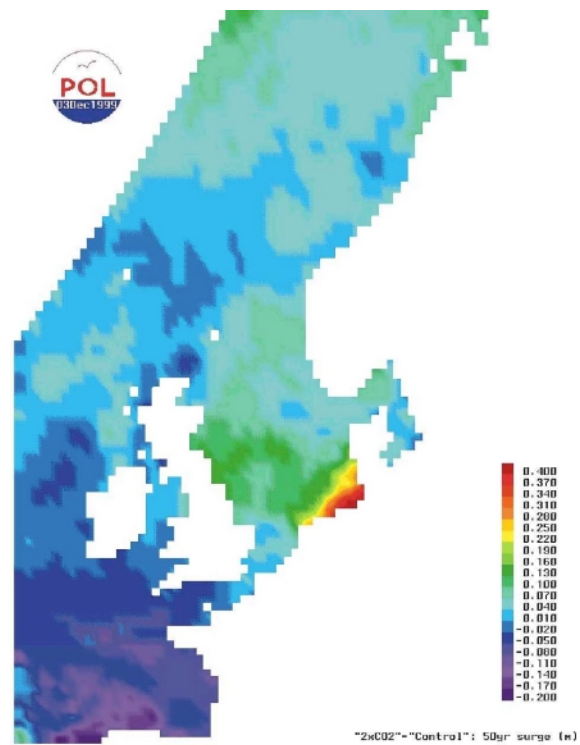


Fig. 6. Difference in 50 year surge ("2xCO₂" - "control"), based on 20 largest surges per year and fit to a Gumbel distribution.

The high resolution simulations with the NISE model have also been finished and show essentially the same feature as in Fig. 6, although with more details. The completion of the NISE model runs provides the necessary source of open boundary forcing for high-resolution "local" models, to be run as part of Task 7.

The work is delayed, however not seriously, due the problems with the driving T106 data. The conclusion of the task during the final project year will include further studies on the method to identify 50 year return surges. Furthermore, detailed reporting will be carried out.

Task 6: Surge statistics based on 30 year T106 time slices: The Adriatic Sea.

This task include simulations of surges in the Adriatic region. A major obstacle consists of downscaling the atmospheric forcing from T106 resolution to the needed regional forcing.

So far a downscaling algorithm has been developed and applied to a few months of the European Re-analyses (ERA). For these months the barotropic version of the POM model has been run with direct T106 ERA forcing and with the downscaled forcing. The results indicate that the downscaling improves the Venice surges when compared observations.

The task is considerably delayed relative to the original work programme. This is basically due to delays and problems in defining an appropriate downscaling of the wind forcing. The long 30 year control and scenario simulations will be performed during the last project year.

Task 7: Downscaling of surge statistics to estimate local variations

The purpose of this task is to develop a specific downscaling approach relating surge levels in deep water (North Sea) to surge levels in the Wadden Sea and other local areas (English Channel or Irish Sea, Skagerak and mid Norwegian coast). A considerable part of the includes an investigation of the most feasible way to perform the downscaling for the Wadden sea.

During the last year the feasibility studies for the Wadden sea have been finished and it was concluded that the most appropriate downscaling is to run full 30 year winter simulations with a nested configuration of modes from RIKZ: the Dutch Continental Shelf Model (DCSM) => Southern North Sea model (ZNZ). The DCSM model has a resolution of 1/8 longitude and 1/12 latitude. The ZNZ model is a curve-linear model ranging in resolution from 300m to 10000m.

The following simulations are planned with this nested model:

1. 30 storm seasons 'control' scenario, surge only
2. 30 storm seasons 'control' scenario, tide + surge
3. 30 storm seasons '2*CO₂' scenario, surge only
4. 30 storm seasons '2*CO₂' scenario, tide + surge
5. test run (storm season 2088 - 2089), surge only

By the end of 1999 half of the computations were carried out. The forecast is that all the computations will be finished in the middle of January 2000.

The work on Wadden Sea surges in task 7 follows the time schedule, i.e. the final surge scenarios will be available in late spring 2000.

For the other local areas to be investigated with very high resolution models (1-5 km resolution) from POL and DNMI (ECOM3D) the work is a about half a year behind the schedule. This is mainly due the problem of the first version of the T106 data. It is, however, anticipated that it will be possible to finish the simulations and the needed analyses before the end of project.

Task 8: Influence of resolution of atmospheric forcing on surge statistics: North-western European shelf seas.

This task includes a series of sensitivity experiments where individual cases are run with the very high resolution surge models from POL and DNMI for a few sensitive areas. The simulations will be forced with very high resolution atmospheric model (HIRHAM) output (task 2 and 3) and be compared to the simulated surges in tasks 5 and 7 which are based on the more coarse atmospheric forcing (T106).

The work in this task has not started yet and is therefore delayed by half a year. The delay is due the problems with the original T106 data and with running the HIRHAM model (see task 2).

Task 9: Case studies: The Adriatic Sea.

In this task the regional atmospheric model BOLAM, forced with the ECHAM T106 boundary conditions, will be run for a few cases. This dynamical downscaling of the T106 will be used as direct atmospheric forcing of the POM ocean model (barotropic version). The surges simulated this way will be compared to surges simulated in task 6 to investigate how important the more realistic BOLAM forcing is relative to the statistical downscaling of the atmospheric wind forcing.

So far 21 cases have been selected from both the T106 control and the scenario simulations. Simulations of these cases with the regional atmospheric BOLAM model will provide the needed training predictands for the statistical downscaling of T106 winds into high resolution winds fields which shall drive the two 30 year Adriatic simulations (task 6). In task 9 the direct BOLAM output for a few of the cases will be used as input to the surge model and the simulated surges in these cases will be compared to corresponding cases in the two 30 year simulations. So far two cases (one from the control and one from the scenario) have been simulated this way for the entire Mediterranean, and they both resulted in surges in the Venice area. The comparison with the same cases from the 30 year simulations will be done when these are available during the last project year.

Task 10: Wave simulations in the Mediterranean

This task is equivalent to tasks 6 and 9, but for waves. Thus 2 times 30 year time slice simulations will be performed with the WAM model. The forcing will be taken from the same statistical downscaling of the winds which is used in task 6. As for task 6 a few test months of downscaled atmospheric re-analyses (ERA) have been used to drive WAM. When the waves simulated with downscaled wind forcing are compared to observations it is seen that the under-evaluation of waves when driving directly (i.e. non-downscaled) with ERA is much reduced. Similarly, two cases (the same as in task 9) from the control and scenario were successfully simulated using direct output from BOLAM.

The full 30 year control and scenario simulations awaits the final downscaling of the wind forcing and takes place during the last project year.

Task 11: Wave scenarios for the northern seas

This task is equivalent to tasks 5 and 7, but for waves. The work includes long simulations with the WAM model forced directly by winds from the time slice simulations. In the original work plan it was planned to run for only some 2 times 10 years at resolutions 50 and 150 km. But efficient coding and parallelization has made it possible to perform two full 30 year control and scenario simulations covering the area in figure 7. The simulations were finished during the second project year - somewhat ahead of schedule - and figure 7 shows the long term difference in significant wave height. Small increases are seen over large domains in the northern and eastern part of the model area. More important, table 1 shows that the 99 percentile of the significant wave heights are increased by almost 10 percent for some locations in the north-east area. This indicates that high wave heights here are more frequent in the 2xCO₂ scenario than in the control.

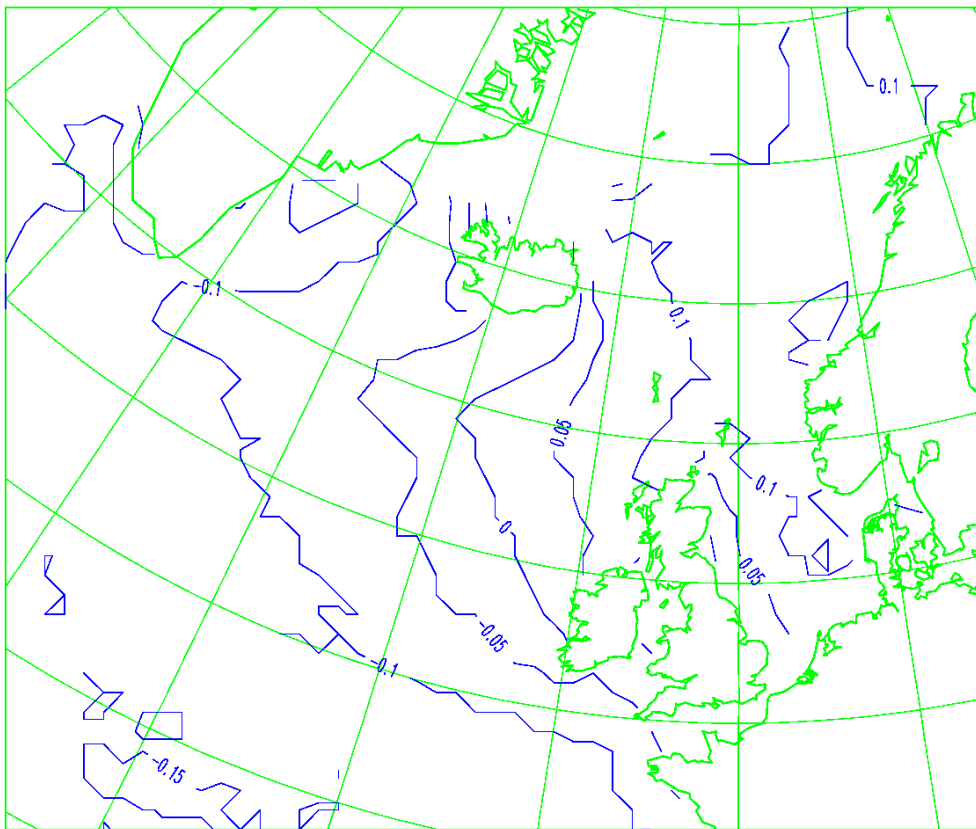


Fig. 7. The difference between average significant wave height in the 2XCO₂ run and the control run for the 30 years. Equidistance 0.05m.

Wave height statistics Ekofisk (56.5 N, 3.2 E)				
	Mean	50%	90%	99%
Ctr. year 1-30	2.09	1.7	4.1	6.7
CO ₂ year 1-30	2.19	1.8	4.3	7.0
Obs. 1980-98	2.07	1.8	3.8	6.2
Wave height statistics Gullfaks (61.2 N, 2.3 E)				
	Mean	50%	90%	99%
Ctr. year 1-30	2.89	2.5	5.4	8.5
CO ₂ year 1-30	3.02	2.6	5.6	8.8
Obs. 1980-98	2.74	2.4	4.9	7.6
Wave height statistics Mike (66.0 N, 2.0 E)				
	Mean	50%	90%	99%
Ctr. year 1-30	2.87	2.5	5.3	8.2
CO ₂ year 1-30	3.00	2.6	5.5	8.9
Wave height statistics Ami (71.5 N, 19.0 E)				
	Mean	50%	90%	99%
Ctr. year 1-30	2.42	2.0	4.5	7.6
CO ₂ year 1-30	2.53	2.1	4.7	8.3

Table 1: Statistics of significant wave height (m): Mean values, 50, 90 and 99 percentiles for control run, 2XCO₂ run. For Ekofisk and Gullfaks also for observations from years 1980-1998.

The work during the last year will mainly be devoted to careful analyses of the wave simulations. Furthermore, the data will very soon be delivered to GKSS to serve as input for the wave generator (task 12). It was decided to give higher priority to running the full 30 year time slices at relatively high resolution than to run selected cases at very high resolution. At the moment it has not been decided whether the WAM will be rerun for a few cases. It will depend on the results from tasks 2 and 3.

Task 12: Ocean wave generator.

The purpose of this part of the project is to generate very long synthetic time series of wave heights at individual locations. So far the construction of a wave generator for 3-hourly wave heights and direction conditioned on the monthly mean air pressure state has been finalised. An autoregressive model is used to describe the monthly sea level pressure as input for the wave generator. This part of the wave generator is conditioned on the CO₂ concentration, i.e. the change in monthly mean pressure distribution in the scenario relative to present climate. The wave generator was trained/build using observed sea level distribution data and wave hindcasts from the WASA project (WASA group, 1998). The wave generator has been tested for the scenario period relative to the control period for a specific location (near platform EKOFISK). The top panel in figure 8 shows the long term difference (scenario minus control) in mean sea level pressure in winter and the lower panel the panel the associated change in the wave distribution near EKOFISK. It can be seen that the change in pressure is associated with a slight decreases of the lower percentiles (2 - 8 cm) and an increase for the higher percentiles (13-17 cm) for the distribution of wave heights in north - south direction. This means a minor increase in the height of south- and northward waves. For the distribution in west - east direction a complete shift about 40 cm is expected, i.e. fewer waves and decreased extreme values for westward waves and more waves and increased extreme values for eastward waves. Investigations for the mean wave heights and intra-monthly wave frequency for the directions show that we have to expect an increase of the mean eastward wave heights and also an increase of the duration of these waves.

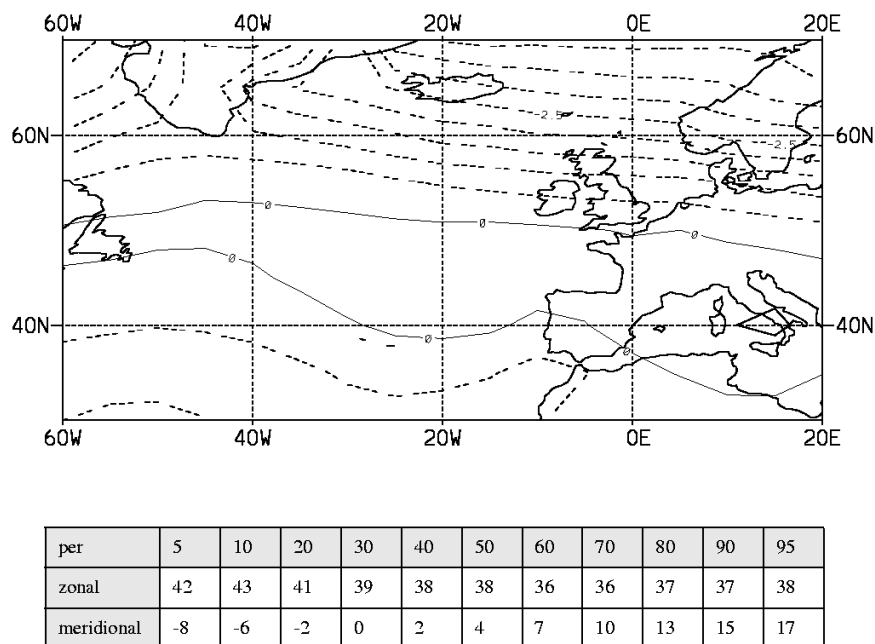


Fig. 8. Mean SLP difference (top) between the control and 2*CO₂ run for the winter (ONDJFM) and the connected change of the percentiles of the wave distributions (bottom).

In the last project year the final wave generator will developed using input in terms of monthly variations in sea level pressure from the T106 time slice experiments and the corresponding 30 year wave simulations performed in task 10 and 11.

DEVIATIONS FROM THE WORK PROGRAMME

There are no fatal deviations from the original work programme. However, certain tasks are somewhat delayed and others accelerated as described above. Similarly, a few tasks are modified slightly.

INFORMATION TO THE PUBLIC

The severe storms that hit Europe in December 1999 have attracted considerable public interest in the subject of a possible changing storm climate. Thus, as in example, the STOWASUS-2100 and some of its basic results concerning changes in storm activity have been presented by the coordinator in a 25 minute long, direct TV broadcast (prime time) on the Danish public TV. (DR-1, "Profilen", 7/12 1999), and it has been mentioned in several Danish newspapers.

REFERENCES

Andersen, U., W. May, E. Kaas, P. Malguzzi, P. Lionello and F. Dalan, 2000: Changes in the storm climate in the North Atlantic / European region as simulated by GCM time slice experiments at high resolution, Planned *DMI Scientific Report*.

Beersma, J., K. Rider, G. Komen, E. Kaas and V. Kharin, 1997: An analysis of extra-tropical storms in the North Atlantic region as simulated in a control and 2xCO₂ time-slice experiment with a high resolution atmospheric model, *Tellus*, **49A**, 347-361.

Flather, R.A. and Smith, J.A. 1998. First estimates of changes in extreme storm surge elevation due to doubling CO₂. *The Global Atmosphere and Ocean System*. **6**, 193-208.

May W., 1999: "A time-slice experiment with the ECHAM4 A-GCM at high resolution: The experimental design and the assessment of climate change as compared to a greenhouse gas experiment with ECHAM4/OPYC at low resolution." *DMI Scientific report No. 99-2*. (Available from the address: (<http://www.dmi.dk/f+u/publikation/SR99-2.PDF>))

Tawn, J. A. 1988. An extreme value theory model for dependent observations. *Journal of Hydrology*, **101**, 227-250.

The WASA Group, 1998: Changing Waves and Storms in the North Atlantic? in: *Bulletin of the American Meteorological Society*, **79**, No.5, 741-760.

STOWASUS-2100

Contract no. ENV4-CT97-0498



Danish Meteorological Institute (DMI).

Contribution to progress report for the second project year (1/12 1998-30/11 1999)

By Eigil Kaas and Uffe Andersen

Introduction

The role of DMI is to:

- co-ordinate the project
- deliver data from the ECHAM4 time slice experiment to the partners
- perform statistical analyses of the North Atlantic storminess in the scenario and control experiments
- perform case studies of baroclinic developments using the high resolution model HIRHAM. The study will focus on the influence from the background climatology on the developments on storms with special emphasis on the influence of water vapour.

Task 1: Statistical analysis

Following the Work Programme the initial statistical analysis of changes in the climate between the control and the scenario simulations were completed last year. The T106 data are the backbone in the present project and all the project results regarding surges and waves (tasks: 5-12) rely on this atmospheric driving. Therefore we decided to deviate somewhat from the original work programme and speed the further analysis of the T106 atmospheric output which was originally planned for the last year. This change in priority is also partly due to the delay of task 2 (see below) which means that more time will be left for task 2 during the last project year. The new statistical analyses have been done with special emphasis on

4. a comparison between the storm climate in the T106 resolution with that in the original coupled T42 model (ECHAM4/OPYC) providing SSTs for the T106 simulations.
5. a critical look at the length of the simulations (2x30 years)
6. an update of the statistical analysis to include 5 winter months instead of the original 3 month period (all the results below are based on this expanded period which gives more stable statistics)

Comparison between T106 and T42

The results for the T106 resolution model were compared to the results from a T42 resolution with the same model but in coupled mode. Though both simulations in T106 and T42 resolution agree on enhanced storm track intensity over northern Europe in the scenario run, they show somewhat different patterns. (Figure 1) While the simulation in T106 resolution has a SW-NE see-saw pattern with decreasing storm activity over New Foundland, the changes in the simulation in T42 resolution are more directed in the N-S direction with increasing values south-east of Iceland and increased values in the Atlantic Ocean between 30 deg N and 45 deg N.

The highest of the 0.1% percentile winds speeds over ocean in the T106 resolution control simulation seems to be marginally stronger than in the T42 resolution model - see figure 2. This is believed to be a consequence of the higher resolution and hence the shorter time steps. However, local effects might play a role in this.

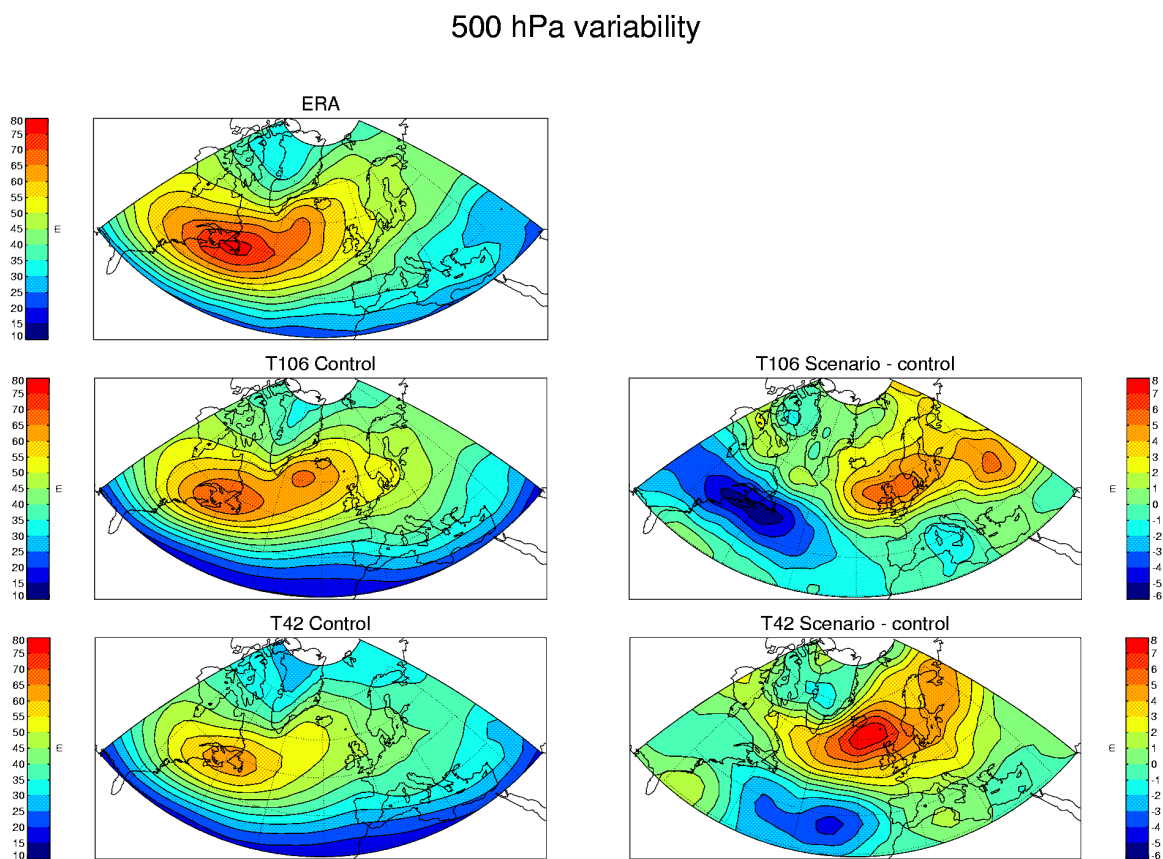


Fig. 1. The storm track intensity (the 500 hPa short term variability) from a) the ERA data, b) the control run in T106 resolution, c) the difference between the scenario and the control run in T106 resolution, d) the control run in T42 resolution and e) the difference between the scenario and the control run in T42 resolution.

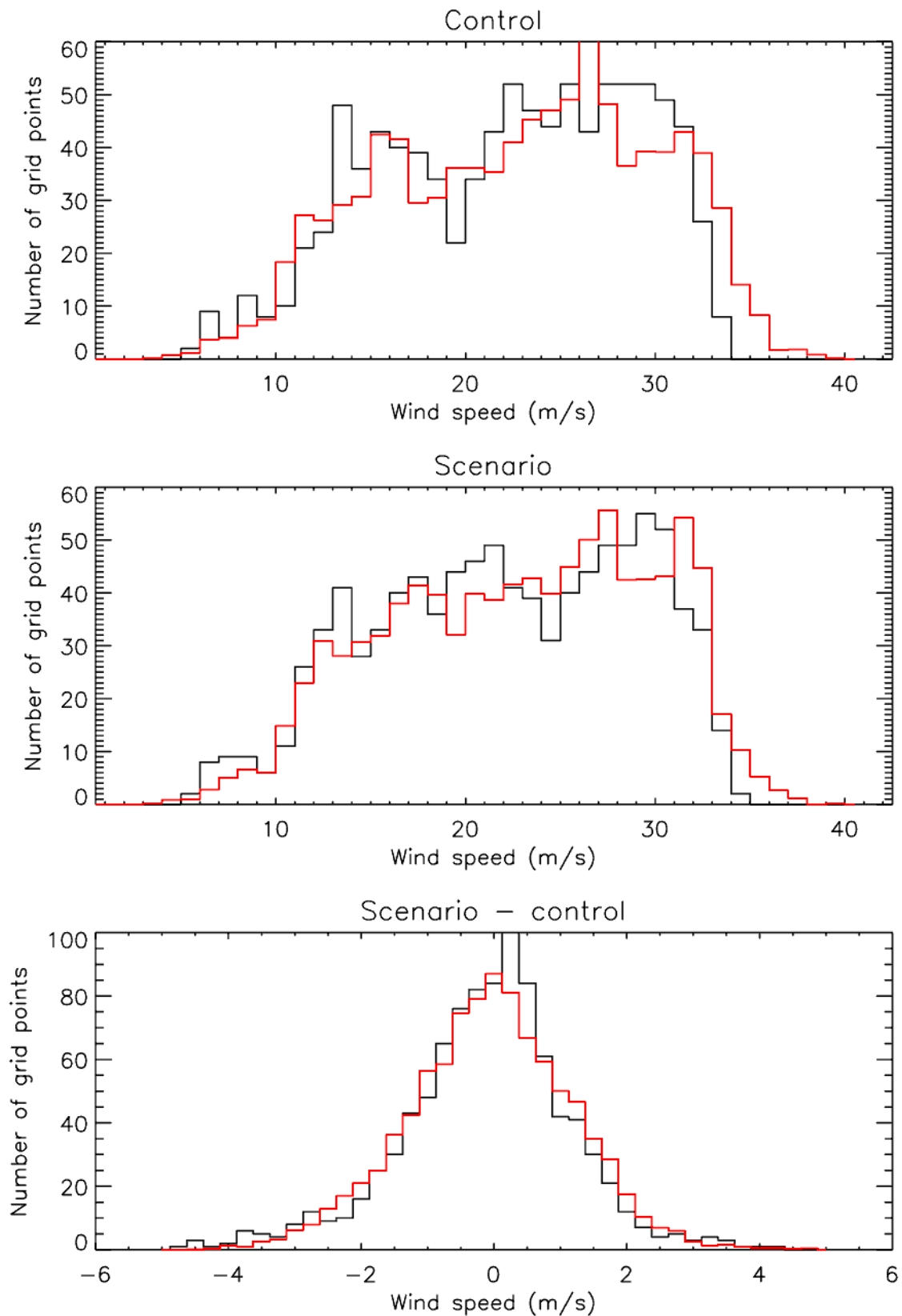


Fig. 2. Histogram of the mean value of the 10m maximum winds exceeding the 0.1 percentile for both the T42 (black lines) and the T106 (red lines) resolutions. a) the control runs, b) the scenario runs and c) the differences between the scenario and the control runs. The number of grid points from the T106 resolution is scaled to the numbers in the T42 resolution.

Length of simulations

An other important reason for performing more statistics is that the length of simulations is an important factor in climate research. Length of simulations are usually limited due to the models huge consumption of computer power. However, if the simulations are too short the internal climate variability will be larger than the changes (i.e. the signal) between control and scenario simulations. Beersma et al. (1997), for instance concluded that two 5 years simulations were too short to detect statistical significant climatic changes and this was one of the basic arguments for setting up STOWASUS-2100.

To estimate how long our simulations should be to obtain statistical significance of the detected changes between a control and a scenario run, the sea level pressure and the variability of the 500 hPa geopotential height were investigated further. The parameters were reduced by using empirical orthogonal functions (EOF) and Hotellings T^2 test were applied to detect the significance level. This was done for different intervals with varying length of the simulations.

Changes in the sea level pressure were significant after 8 years of simulated time in the T42 resolution while it took 18 years before the changes in the T106 resolution were significant. The necessity of a much longer time series in the T106 resolution has probably to do with the much stronger response in the T42 resolution, which comes mainly from systematic differences between the two models in the simulation of the present-day climate.

In the T42 resolution the significance level for the variability of the 500 hPa geopotential height is reached after 22 years, which is substantially longer than for the significance level of the sea level pressure. For the T106 resolution the significance level is only just to be reached after 29 years of simulation.

The results from the statistical analysis referred here are explained in more detail in a note which is planned to be printed as an internal report at DMI.

Task 2: Baroclinic developments:

25 storms in the North Sea and 25 in the Norwegian Sea have been selected from the control simulation. The selection criteria was the number of grid-points within the area with wind speeds exceeding their 1% percentile.

According to the Work Programme the selected storms should already have been simulated in the HIRHAM model both with the control and the scenario climatology. But there has been a serious delay for this task due to reasons explained below.

So far the HIRHAM model has been set up and a few storms from the control run have been simulated. However, there seems to be a problem with the version of the model used. The near surface wind field (1000 hPa, 2 and 10 meter wind) has a noisy structure and during the simulation (approximately 1 to 3 days) and the total sea level pressure is increased in the HIRHAM simulation as compared to the control simulation. The simulation of a storm in ECHAM4 and HIRHAM is shown in figure 3, but we only show the 925 hPa winds to avoid the noise at lower levels.

Quite some effort has been put into explaining this odd behavior. A serious error was recently identified in the horizontal diffusion and it is believed to be responsible for the noise. The error has now been corrected but test runs have not been completed yet. It is important to note, that the error

was only present in that particular version of HIRHAM used here. It is related to the parallelization of the code

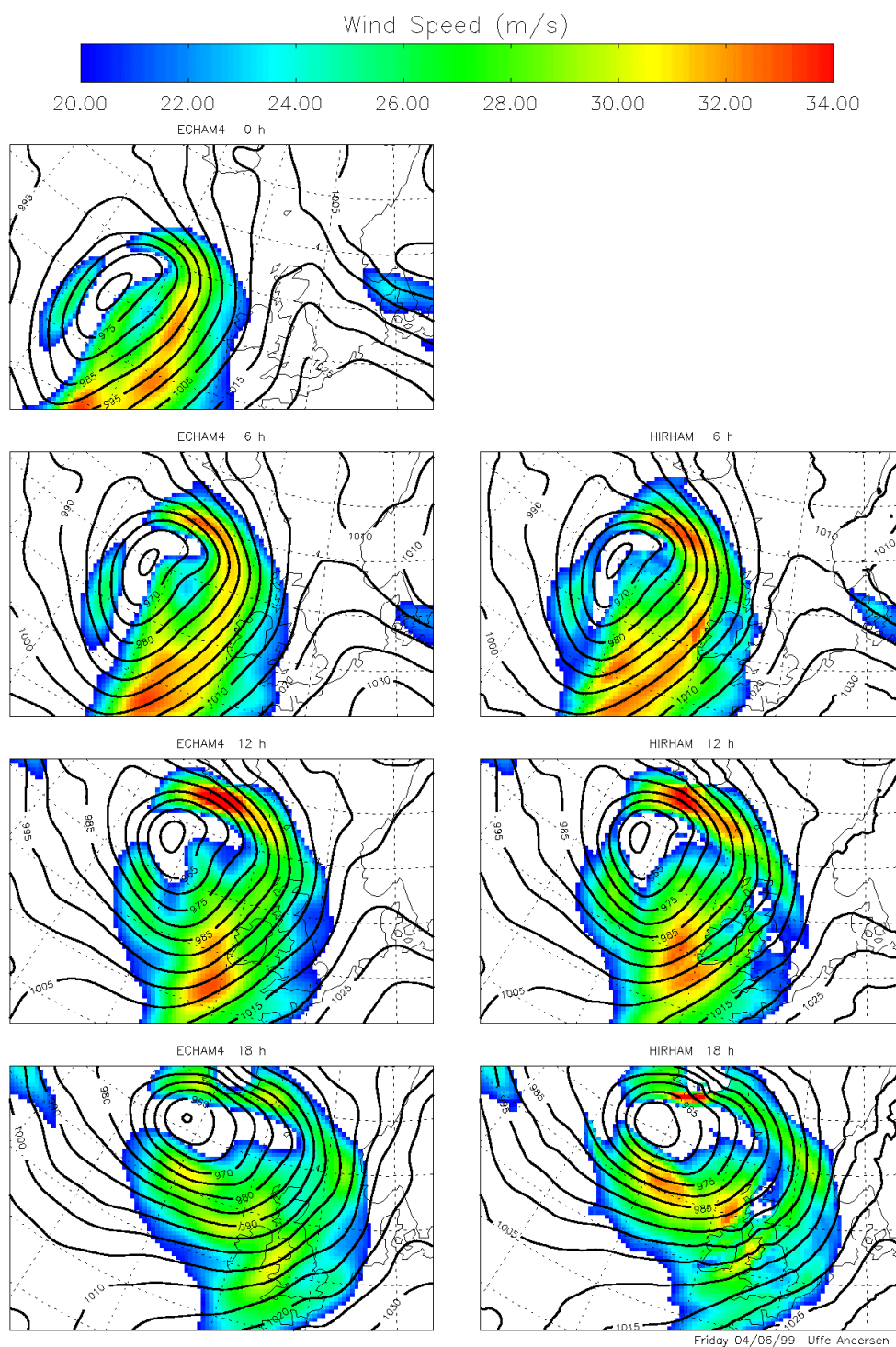


Fig. 3. A storm in the North Atlantic simulated by ECHAM4 in T106 resolution (a,b,d,f) and the same storm simulated in HIRHAM (c,f,g). In the HIRHAM simulation the ECHAM4 simulation were used as boundary conditions. Sea level pressure (contour lines, hPa) and the 925 hPa wind speed (colors, scale at top) are shown for each 6h interval.

In order to detect the difference in the climatology to be used in the simulations with HIRHAM more statistical analysis has been done on different fields: Temperatures : 2m, 200hPa, 300hPa, 850hPa; geopotential height of 500 hPa Zonal wind from 200 hPa and 850 hPa. Calculation of the correlation of these parameters using EOFs are started but not yet finished.

The simulations of the storms will be done in the control scenario and will start 1 to 3 days before the storm reach the North Sea or the Norwegian Sea. Conditions such as depth of low, maximum wind speeds and track of cyclone will be monitored. The simulations will be redone with the climatology from the control run changes to the climatology of the scenario run. When the storms are simulated with the scenario climatology some precautions must be taking. If the scenario climatology is added uncritically to the simulation, conditions that are unfavourable for low pressure systems to develop might show up. To prevent this the added change in climatology should be smooth and consistent.

The simulation of the storms will also be done with a 'dry' version (i.e. no release of latent heat during condensation) of the model. Other experiments has shown that release of latent heat strengthen the developments of the cyclones.

According to the work plan the simulations should have been completed by now. Due to the problems with the HIRHAM model this has not been done. The simulations are expected to be finished within 6 months.

Task 3: Polar lows

See the contribution from DNMI.

The final simulation with HIRHAM will be done by DNMI instead of DMI. For comparison DMI will, however, run one case.

References

Andersen, U., W. May, E. Kaas, P. Malguzzi, P. Lionello and F. Dalan, 2000: Changes in the storm climate in the North Atlantic / European region as simulated by GCM time slice experiments at high resolution, Planned DMI Scientific Report.

Beersma, J., K. Rider, G. Komen, E. Kaas and V. Kharin, 1997: An analysis of extra-tropical storms in the North Atlantic region as simulated in a control and 2xCO₂ time-slice experiment with a high resolution atmospheric model, Tellus, 49A, 347-361.

STOWASUS-2100

Contract no. ENV4-CT97-0498



Proudman Oceanographic Laboratory (POL).

Contribution to progress report for the second project year (1/12 1998-30/11 1999)

By Roger Flather and Jane Williams

Background

POL is contributing to investigations of changes in storm surge statistics associated with increasing CO₂ in tasks 5, 7 and 8. The work to date contributes to Task 5: “Surge statistics based on 30 year T106 time slices – North West European shelf seas from 35km and 12km models”, and Task 7: “Downscaling of surge statistics to estimate local variations”.

The last report (Flather and Williams, 1998) described the set-up and running of a new model called NEAC covering the NE Atlantic and European shelf seas (43°N to 70°N and 15°W to 20°E) with resolution of ~35km. The following runs had been completed:

1. Tide only 1955-1999 and 2060-2089.
2. Tide + surge with DNMI met forcing for years 1955-1997 (to determine “present day” surge climate).
3. Tide + surge with ECHAM4 climate model forcing for years 1970-1999 (representing “control”) and for the 30 years representing the scenario.

Surge components were derived by subtracting tide from the corresponding tide + surge solutions, and initial analyses of extremes were undertaken. Extreme surge elevations were derived using an approach based on the “r largest” method (Tawn, 1988) similar to that described in Flather and Smith (1998). The 10 largest independent surges were extracted for each year of the “present day” NEAC solution (Run 2 – Run 1) and from the NEAC “control” run (Run 3 – Run 1). A Gumbel distribution was fitted and exceedence probabilities were derived. The 50-year return period surge elevation was considered as an appropriate extrapolation from the 30-year data sets.

Progress with NEAC modelling and analysis

Met. forcing data problems

During the project meeting in Venice, September 1998, some problems with the climate data were reported. These occurred during post-processing by DMI of the ECHAM4 data, causing discontinuities near the Greenwich meridian (0° E) most marked in surface atmospheric pressure but also affecting winds and consequently results from NEAC Run 3, above. In February 1999 corrected ECHAM4 forcing data were received at POL from DMI. NEAC was first re-run for one year to assess the effect of the corrected data on the surges. Differences of O(±5cm) were found

between results with corrected and original data on either side of the Greenwich meridian. Since NEAC Run 3 provides the basis for subsequent comparison with model results from the “2xCO₂” scenario, it was decided to re-run NEAC for the 30 years with the corrected “control” data to ensure consistency.

Comparison between the “control” and “present day” results

Comparison between the “control” and “present day” results provides an indication of how well the climate model reproduces the real storm climatology. The 50-year extreme surge elevation distribution from the “control” run agreed closely with that from the “present day” solution over most of the model domain, but there were differences in coastal regions. One possible explanation for this was the definition of “land” and “sea” in the ECHAM4 model and its effect on winds in coastal areas. If this was the cause, then it should be possible to adjust the ECHAM4 forcing to give results in very close agreement with those based on real (“present day”) met data.

Tests were carried out using the ECHAM4 land-sea mask to apply a more appropriate drag coefficient (arbitrarily chosen as 0.00492) to calculate the surface stress. NEAC was re-run for the 30-year “control” period with this adjustment. Analysis to produce extreme surge estimates showed even larger deviations in coastal areas, suggesting that the underestimate was not due to this cause, and, although further investigation would have been desirable, it was decided to continue the STOWASUS work with the original unadjusted ECHAM4 forcing.

Further NEAC runs

To complete the set of surge results, NEAC was run as follows:

4. Tide + surge with ECHAM4 climate model forcing for years 2060-2089 (representing the “2xCO₂” scenario).

DMI advised us not to use data for months 8, 9 and 10 in year 19 because of a problem with the ECHAM4 “2xCO₂” dataset. Climatic monthly means were calculated using the 30 years of data and substituted for the problem months prior to the 30-year model run (NEAC Run 4).

Another problem arose in that the data tape received with corrected “control” data also contained “2xCO₂” data. These data were found to be different from the set used in the NEAC Run 4, above, although no notification was given that this was actually the case. Comparison of results using the two data sets showed that the original “2xCO₂” data were also affected by the same problem around the Greenwich meridian. For consistency, it was therefore necessary to re-run the 30 years of NEAC Run 4 with the new corrected “2xCO₂” forcing data.

Analysis of results - changes in extreme surge elevation

After the computing of hourly surge residuals by subtracting the model tide, the 10 largest surges per year were extracted. A Gumbel distribution was fitted and the 50-year surge values were derived. Figure 1 shows the distribution for the corrected “2xCO₂” solution.

The difference in 50-year surge (“2xCO₂” – “control”) is shown in Figure 2. The largest values are on the Dutch and Danish coasts, where values peak at approximately +30cm, suggesting an increase in the 50-year surge. However, the distribution is spatially noisy and it was felt necessary to make further investigations.

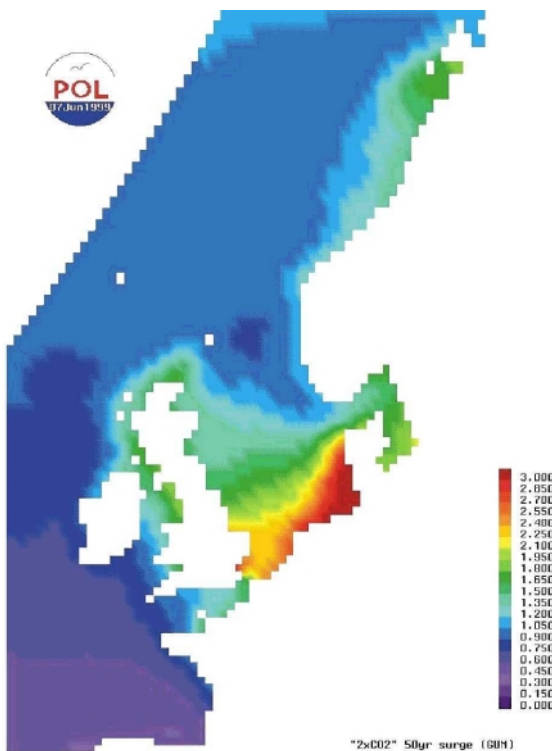


Fig. 1. 50 year surge in meters ("2xCO₂") based on 10 largest independent surges per year and fit to a Gumbel distribution

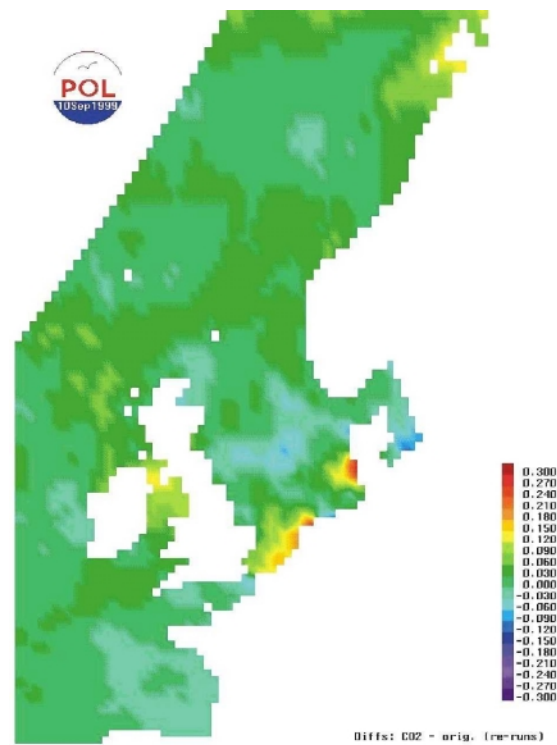


Fig. 2. As Fig. 1 but for the difference between ("2xCO₂" and "control").

A possible source of the "noise" is in fitting the distribution (Gumbel in this case) to the data. To test this, an alternative, the Generalised Extreme Value (GEV), distribution was used. This method gives a distribution of differences (Figure 3) which is quite different from that obtained using Gumbel. There is still a maximum on the west coast of Denmark but located further north, and the second maximum on the Dutch coast is removed. Clearly, the results are very sensitive to the statistical fit of a chosen distribution to the model data. In principle, the Gumbel distribution, which has two free parameters to be determined by the fit, should be more robust than GEV, which has three.

To study these aspects in more detail, hourly time series of surge elevation were extracted from the "control" and "2xCO₂" 30-year runs at selected coastal locations (Figure 4). The 10 largest maxima in each year were extracted using a 60-hour surge event window. Gumbel and GEV distributions were fitted and the 50-year return period surge heights were derived. The results are shown in Table 1. For most locations, taking account of the standard errors in fitting the extreme value distribution, the 50-year extreme surges for "2xCO₂" are not significantly different from those for the "control". However, changes can be seen in the tail of the distributions, which represent the most extreme events. An example of this can be seen in Figure 5. At Bergen, the largest computed surge occurred in the "control" run with more frequent smaller surges in the "2xCO₂" case. At Esbjerg, however, the maximum surge in the "2xCO₂" solution is much bigger than the maximum from "control" and there are generally more large surges with "2xCO₂". This tends to support the increase west of Denmark shown in the model distributions (Figures 2 and 3).

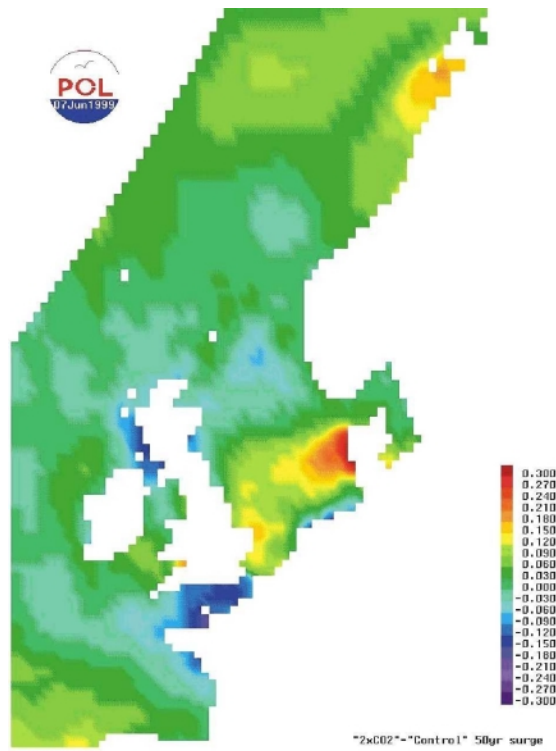


Fig. 3. Difference in 50 year surge ("2xCO₂" and "control") based on 10 largest independent surges per year and fit to a Generalised Extreme Value (GEV) distribution

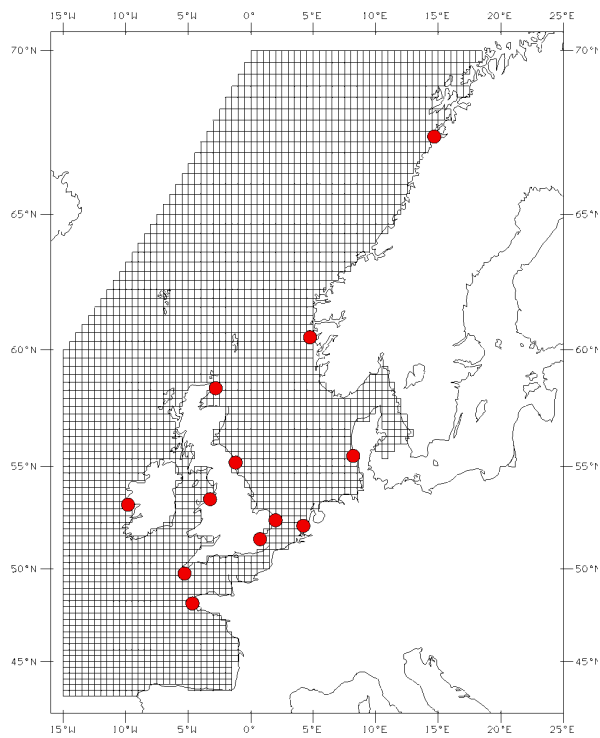


Fig. 4. Locations selected for individual extreme value analysis.

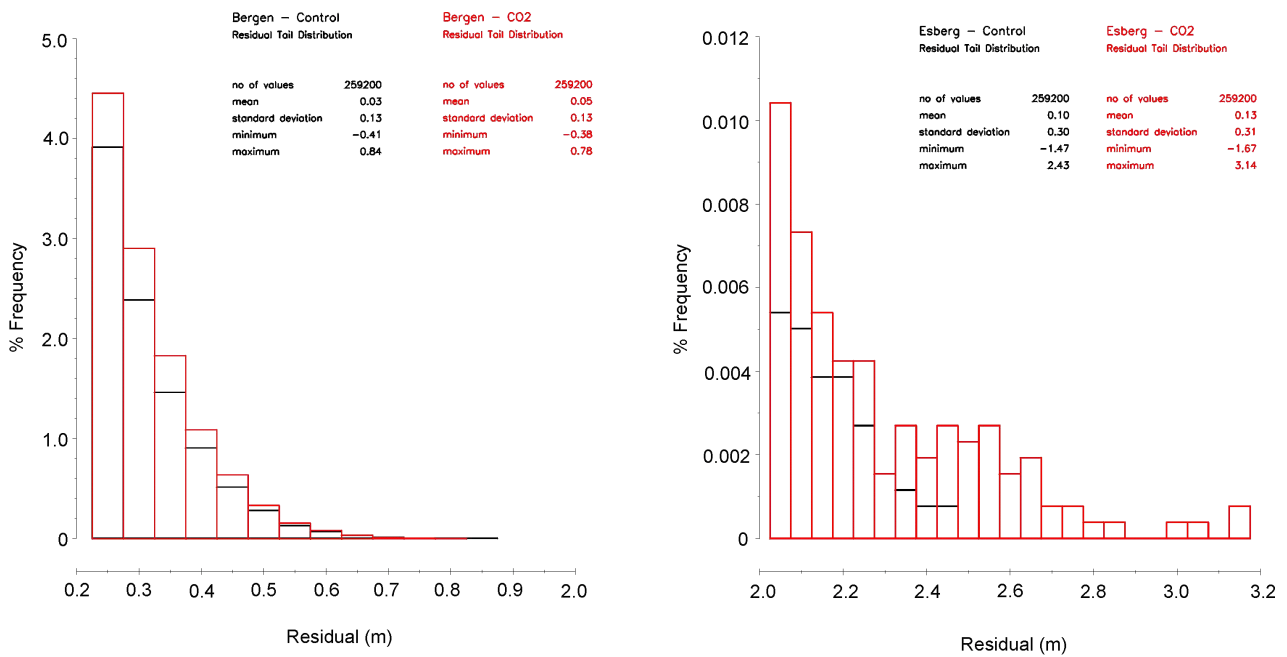


Fig. 5. Extreme statistics for Esbjerg

Port	Gumbel		GEV	
	“Control”	“2xCO ₂ ”	“Control”	“2xCO ₂ ”
Bergen	1.01 (0.04)	1.01 (0.03)	0.78 (0.02)	0.78 (0.03)
Bodø	0.62 (0.02)	0.59 (0.02)	0.51 (0.03)	0.49 (0.03)
Brest	0.69 (0.03)	0.69 (0.03)	0.61 (0.05)	0.52 (0.03)
Esberg	3.44 (0.14)	3.46 (0.13)	2.43 (0.09)	2.88 (0.15)
Galway	0.88 (0.03)	0.85 (0.03)	0.75 (0.05)	0.73 (0.04)
Hook of Holland	2.36 (0.09)	2.37 (0.09)	2.13 (0.17)	2.26 (0.19)
Lowestoft	2.20 (0.09)	2.21 (0.09)	1.93 (0.14)	2.08 (0.16)
Liverpool	1.52 (0.06)	1.64 (0.06)	1.30 (0.08)	1.34 (0.08)
Newlyn	0.75 (0.03)	0.75 (0.03)	0.64 (0.04)	0.59 (0.03)
Sheerness	2.39 (0.10)	2.42 (0.10)	2.14 (0.16)	2.26 (0.18)
Wick	1.35 (0.05)	1.32 (0.05)	1.14 (0.07)	1.14 (0.06)

Table 1. 50-year surge heights (m), based on 10 largest yearly maxima with 60-hour event window, with standard error in brackets.

Since improvements in fit could result from a larger data set, the 20 largest surges per year were extracted from the hourly model data sets. The Gumbel analysis as above was re-applied using the

20 largest values from each of the 30 years and the resulting 50-year extreme surge was re-calculated for every model grid point. The difference in 50-year surge ("2xCO₂" – "control") is shown in Figure 6. Using 20 values instead of 10 gives a less noisy distribution with maxima in the German Bight of over 40cm.

Percentile analysis was also applied to the hourly output of both runs and the differences between 99th percentiles was plotted (Figure 7). This does not require a fit to data of a statistical distribution and so eliminates uncertainties associated with that fit, consequently giving a less noisy distribution. Although the largest 99th percentile is much smaller than the estimated 50 year extreme, there are encouraging similarities between this and the difference in 50 year extreme computed using Gumbel with 20 surges per year (Figure 6).

Further investigation of these important aspects is planned.

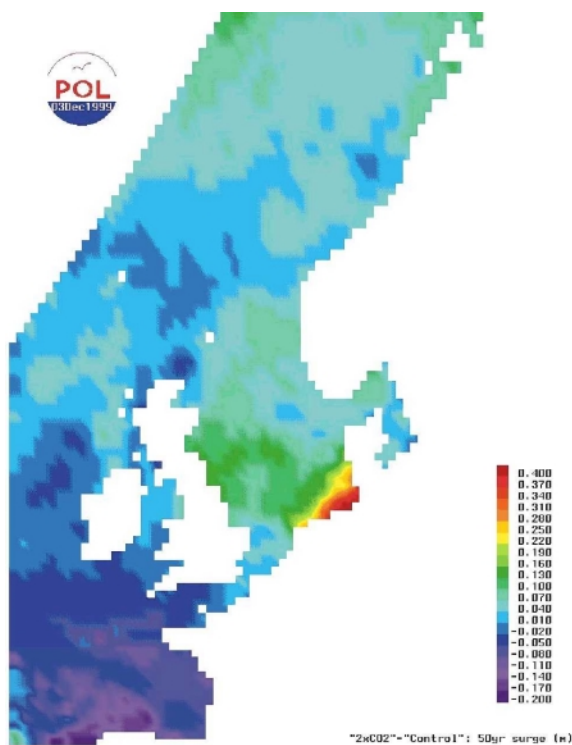


Fig. 6. Difference in 50 year surge ("2xCO₂" - "control"), based on 20 largest surges per year and fit to a Gumbel distribution.

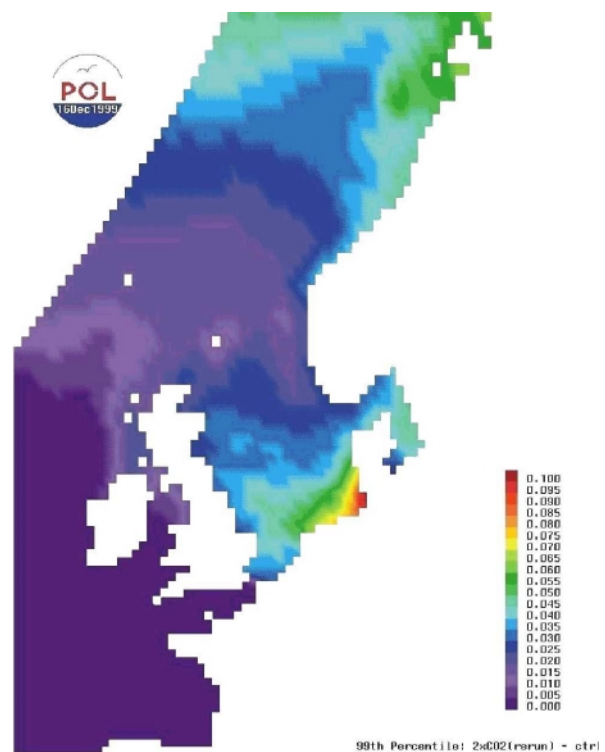


Fig. 7. 99th percentile "2xCO₂" minus "control".

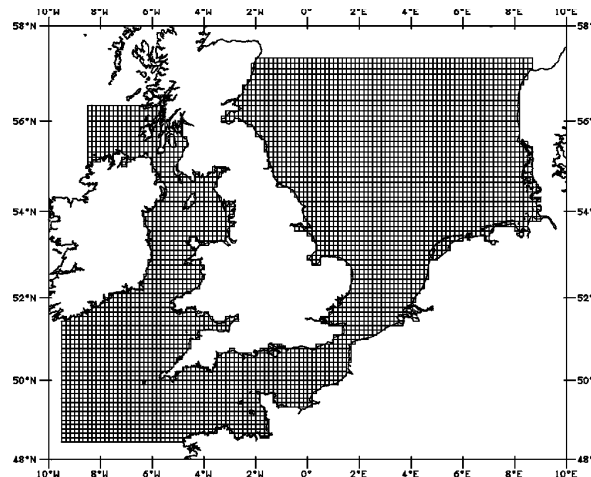


Fig. 8. NISE model grid

Application of a new 12km model

A new 12km model covering the North and Irish Seas and English Channel (NISE) has been set up. It uses open boundary input of 26 tidal constituents and surge elevations interpolated from corresponding NEAC results. The model has 82 rows and 115 columns with origin at 57.3888°N and 9.5833°W. NISE is thus a sub-set of the UK operational surge forecast model, CS3. An interface has been set up to allow NISE to be driven by met forcing from the ECHAM4 data sets. Figure 8 shows the NISE model grid.

The following runs of NISE have been completed:

1. Tide only 1970-1999 and 2060-2089.
2. Tide + surge with ECHAM4 climate model forcing for years 1970-1999 (representing “control” scenario).
3. Tide + surge with ECHAM4 climate model forcing for years 2060-2089 (representing “2xCO₂” scenario).

From each run, complete NISE model fields (sea surface elevation and components of depth mean current) at hourly intervals were stored for subsequent analysis. Run 1 provides tidal predictions which can be subtracted from the “tide + surge” results (Runs 2 & 3), to give the storm surge component which is used in the extreme analysis.

The 20 largest surges per year were extracted and 50-year return period surge heights were derived using a Gumbel distribution using 10 and 20 largest surges as described above. The difference in 50-year surge (“2xCO₂” - “control”) based on 10 largest surges is shown in Figure 9. The equivalent result with 20 largest surges per year is shown in Figure 10. These distributions are similar to those from the coarser grid NEAC model, with more detail in some areas.

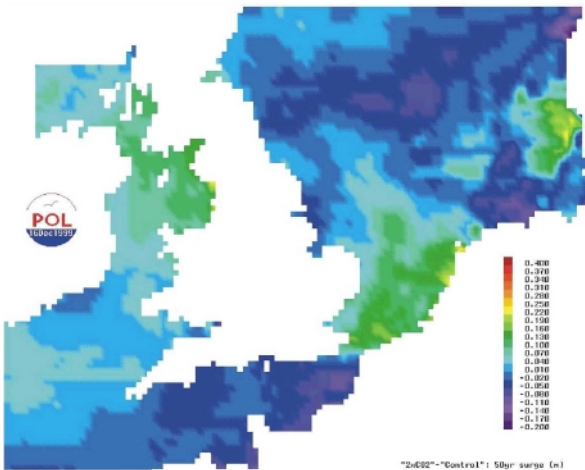


Fig. 9. As Fig. 2, but based on results from the NISE model.

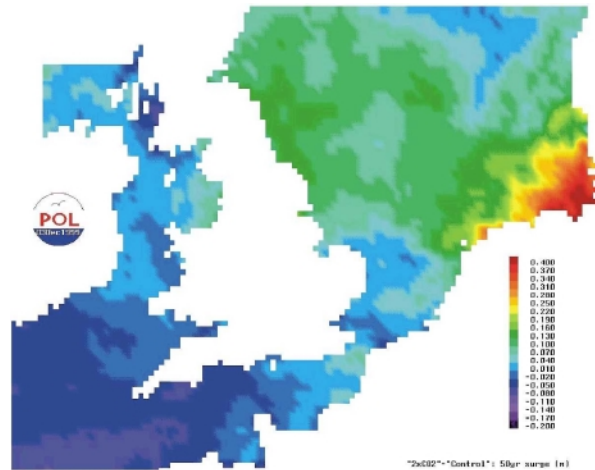


Fig. 10. As Fig. 6, but based on results from the NISE model.

Percentile analysis was also undertaken. The difference in 99th percentile (“2xCO₂” - “control”) and is shown in Figure 11.

The intention is to investigate further, minimise or at least quantify the uncertainties and seek to improve the estimates of differences between “control” and “2xCO₂” extremes obtained.

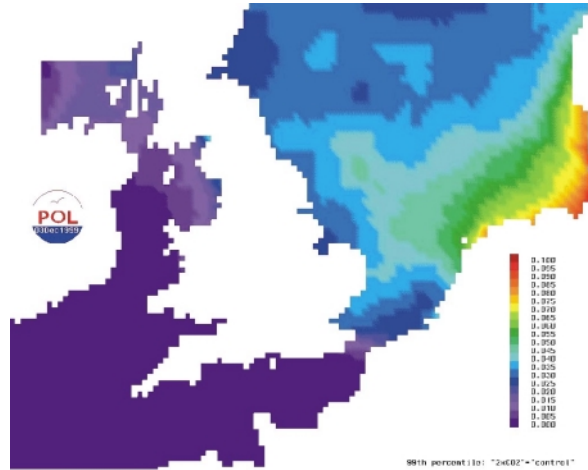


Fig. 11. As Fig. 7, but for the NISE model.

Provision of data to Partners

DNMI

- Data from a subset of the NEAC model grid comprising hourly surge elevations from the “present day”, “control” and “2xCO₂” runs were supplied on DAT tapes.

RIKZ

RIKZ had problems reading and processing data as supplied by DMI. Therefore, we:

- extracted, processed, and formatted ECHAM4 forcing data and supplied to RIKZ on CD-ROM;
- plotted fields of interpolated ECHAM4 wind and pressure data and provided these to RIKZ for validation purposes.

In addition,

- timeseries of hourly data (total water levels and surge elevations) from the “control” and “2xCO₂” NEAC runs were extracted, formatted and written to CD-ROM to provide boundary data for the RIKZ DCSM model.
- Plots of timeseries of these parameters at specified points were also made and provided for data verification.

Progress and future work

Progress was delayed due to the necessity to re-run the NEAC model twice and re-analyse the results. Also, the preparation of data for partners with associated support has taken time.

The completion of the NISE model runs provides the necessary source of open boundary forcing for high-resolution “local” models, to be run as part of Task 7. Discussion with partners is now required in order to agree model runs required for Task 5 and should take place during January 2000.

Logistics

Roger Flather and Jane Williams (née Smith) attended the project meeting in Bergen.

References

- Flather, R.A. and Smith, J.A. 1998. First estimates of changes in extreme storm surge elevation due to doubling CO₂. *The Global Atmosphere and Ocean System*, **6**, 193-208.
- Flather, R.A., Smith, J.A., Richards, J.D., Bell, C. & Blackman, D.L. 1998. Direct estimates of extreme storm surge elevations from a 40-year numerical model simulation and from observations. *The Global Atmosphere and Ocean System*, **6**, 165-176.
- Flather R.A. and Williams, J.A. 1998. Contribution to: Progress report for the first project year (01/12/97 – 30/11/98). STOWASUS-2100: Regional storm, wave and surge scenarios for the 2100 century. EU ENV4-CT97-0498. 45 pp.
- Tawn, J. A. 1988. An extreme value theory model for dependent observations. *Journal of Hydrology*, **101**, 227-250.

STOWASUS-2100

Contract no. ENV4-CT97-0498



University of Padua (UP).

Contribution to progress report for the second project year (1/12 1998-30/11 1999)

By Piero Lionello

Introduction:

The contribution of UP for the first year was concentrated on the implementation of the wave and surge models and on the analysis of the quality of their results when the models are forced with fields at the T106 resolution in the Mediterranean and Adriatic Sea. During the second year the contribution consisted mainly in:

- 1) the development of a procedure for statistical downscaling of the wind fields over the Adriatic Sea and
- 2) in the simulation of wave and surge fields over the whole Mediterranean with a high resolution model for selected intense and representative events.

It was initially observed that, because of the coarse resolution of the input wind fields produced by the time slice experiment, no relevant improvement of the results is obtained by running a higher resolution model limited to the Adriatic Sea and the implementation in the whole Mediterranean was preferred. However, a downscaling of the driving wind fields over the whole Mediterranean Sea proved difficult because of the complicated topography that is present and, consequently, the high resolution simulations were again limited to the Adriatic, as initially planned in the project.

Task.4 Mediterranean Analysis and task.1 statistical analysis of T106 data

(Note that the Task4 is carried on in co-operation with the partner ISAO, Bologna)

A set of programs for the analysis of the formation and evolution of cyclones in the Mediterranean Sea (described by meteorological models at T106 resolution) has been applied systematically to the Control and CO₂ scenarios. The details of the method and the analysis of the results are discussed in a DMI report under preparation. Here, only the main outcomes are presented.

The analysis of the control and CO₂ simulations produced two lists of low pressure systems whose intercomparison allows the identification of systematic differences between the two climatic scenarios. Figure 1 shows the cumulated distributions (blue bars control, orange bars CO₂) for the most intense cyclones in terms of anomalous centre pressure. Each bar indicates the number of cyclones whose intensity DP exceeds the relative threshold. It can be noticed that the control experiment is characterized by a larger number of cyclones, at least in the range up to 35 hPa. However, the tail of the cumulated distribution, shown enhanced in figure 2, presents a predominance of very strong cases in the CO₂ scenario. This result suggests an increase of extreme cyclonic events in the CO₂ scenario, although the statistical significance of the differences should be further investigated.

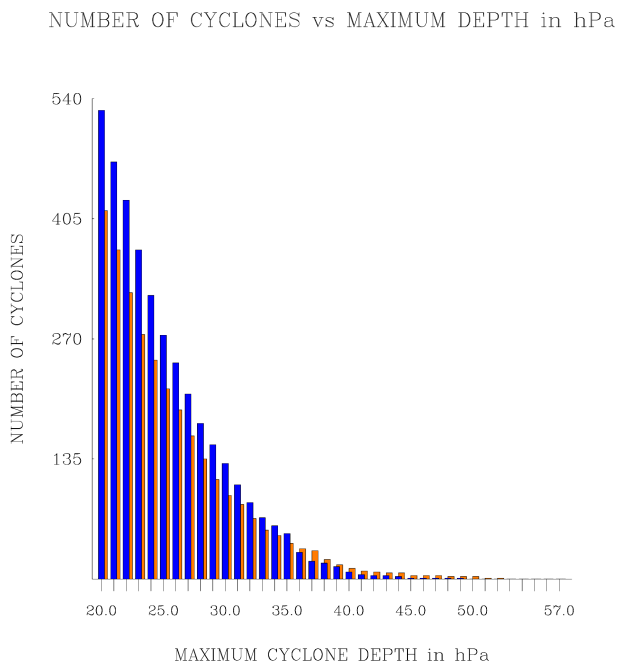


Fig. 1. Cumulated distribution of number of simulated cyclones in the present (blue) and doubled CO₂ (orange) climatic scenarios. The abscissa reports the maximum cyclone depth in hPa.

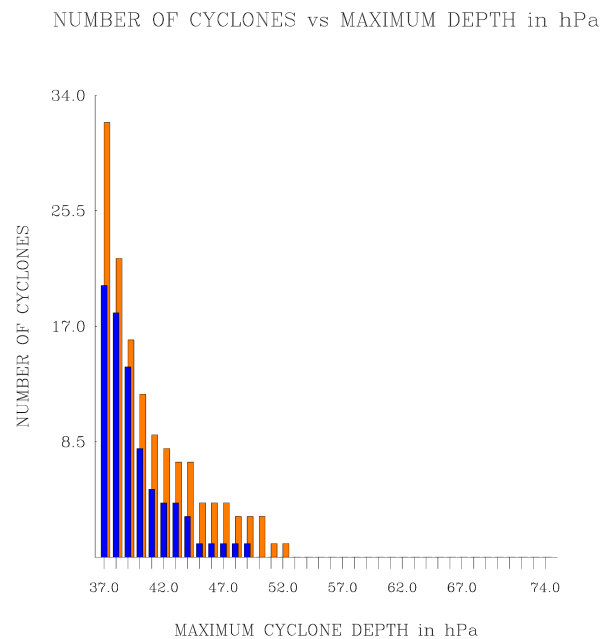


Fig. 2. Enlargement of the tail of the cumulated distribution of Fig. 1.

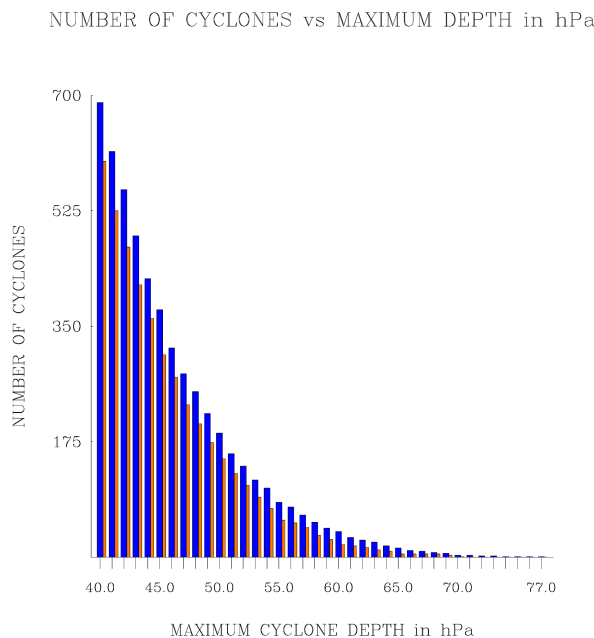


Fig. 3. Same as Fig. 1, but based on maximum geostrophic wind at sea level.

An alternative way to estimate the intensity of the low pressure systems is given by the computation of the maximum geostrophic wind at sea level, which is essentially proportional to the gradient of the pressure field. Figure 3 shows the cumulated distribution of the most intensive systems, ranked accordingly to the maximum intensity of the geostrophic wind. Consistently with the above results,

the control scenario presents more cases for each threshold value. However, this characteristic extends up to the end of the tail of the distribution, with no increase in the number of very intense events in the CO₂ scenario.

The seasonal distribution of the number of cyclones in the 30 year period is presented in figure 4 for low pressure systems exceeding 20 hPa. The two scenarios present a similar annual cycle, with the stormy season going from November to April. The seasonal distribution of the extreme events (depth greater than 37 hPa) reflects the increase of activity in the CO₂ scenario (see figure 5) . It is interesting to notice that the increase is mostly concentrated in the period from February to March.

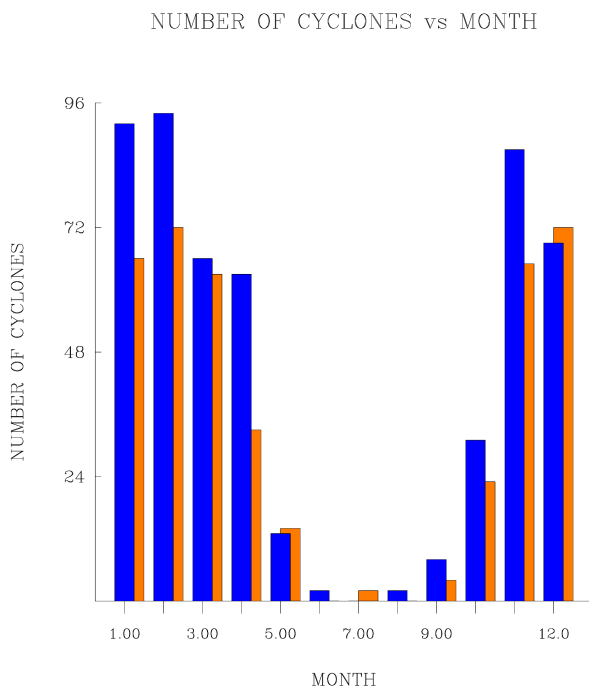


Fig. 4. Monthly distribution of number of cyclones with maximum depth greater than 20hPa in the present (blue) and doubled CO₂ (orange) climate scenarios.

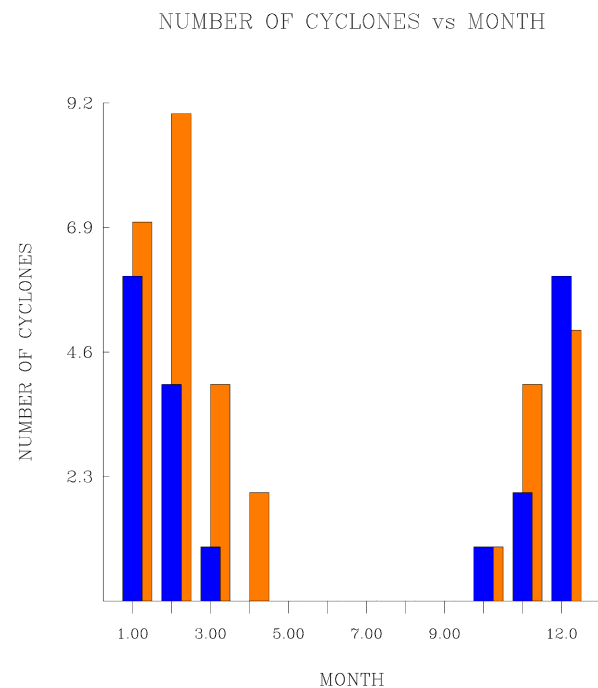


Fig. 5. Same as Fig. 4, but for cyclones having maximum depth greater than 37 hPa.

Figure 6 shows the normalised density of initial points of the cyclone trajectories, in the control (left) and CO₂ (right) scenarios. Only cyclones whose maximum intensity is greater than 20 hPa are considered. This panel gives an indication of the preferred location for cyclogenesis in the Mediterranean area. The maximum of density located on the western boundary of the domain indicates that many cyclones come from the northern Atlantic storm track. There are however two restricted areas south of the Alps where depressions form, presumably by the well known mechanism of lee cyclogenesis. This last feature, which is essentially unchanged in the CO₂ scenario, is also seen in the statistics of observed cyclogenesis in the Mediterranean area, giving, therefore, a strong indication about the realism of the T106 climate simulation.

The list of cyclones produced by this analysis is important in this study also because it provides the full set from which the subset of the storms for the high resolution simulations will be selected. Such subset is used in task 4,9 and 10 for the high simulation experiments. Presently, 11 cases of the Control scenario and 10 cases of the CO₂ Scenario have been selected. The high resolution simulation has been completed for the 11 "control" cases and for 5 "CO₂" cases. The results are

shown in the discussion of task 9 and 10. Moreover, these high resolution simulations will be used for a further refinement of the downscaling procedure.

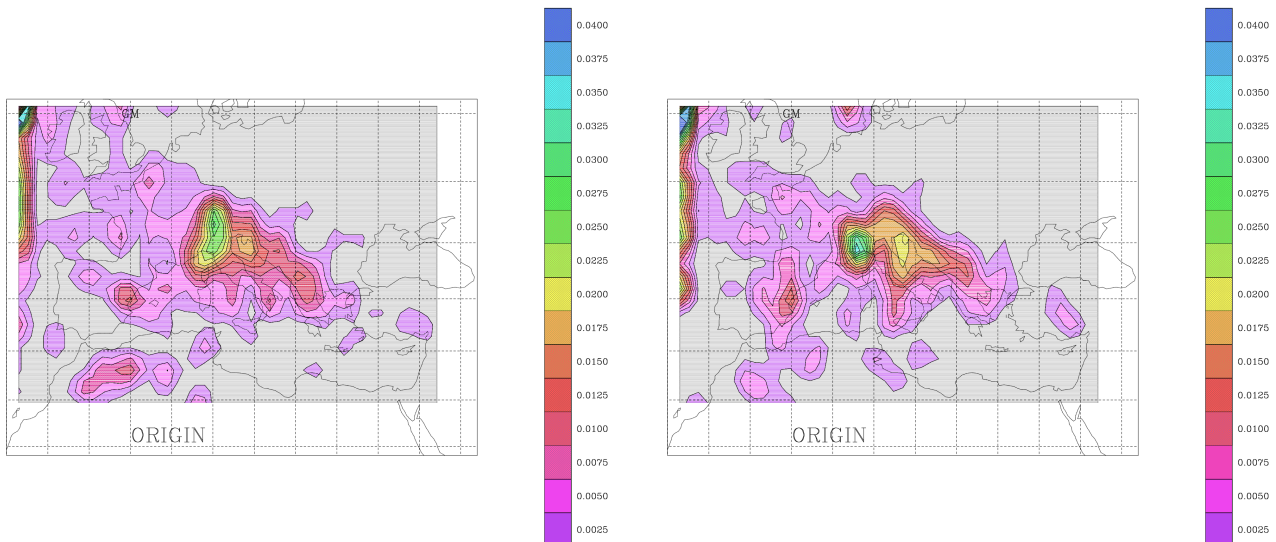


Fig. 6. Present (left panel) and doubled CO₂ (right panel) scenarios: probability of cyclogenesis per model grid point for cyclones exceeding 20hPa. The maximum at the western boundary indicates cyclones originated outside the area.

Task.6 Adriatic Sea surge and task 10 Waves in the Adriatic

Because of the difficulty of producing downscaled wind fields over the whole Mediterranean region, the work adopted the plan of the original proposal, abandoning the idea of simulating the whole Mediterranean Sea and focusing on the Adriatic Sea. The shallow water model (the barotropic component of the POM model) has been implemented in the Adriatic Sea with a 1/12th degree resolution.

The downscaled wind fields have been obtained by BOLAM in a former study that simulated a set of large surges and consequent coastal floods in the Adriatic Sea. The statistical downscaling is based on PCA pre-filtering and subsequent CCA analysis. The global predictor is the ECMWF re-analysed sea level pressure distribution over the large area denoted as "GCM ERA" in figure 7, while the downscaled winds were produced in the area denoted as "BOLAM". Figure 8 shows an example of the LAM wind field and the corresponding field downscaled from ERA data. In general the structure of the LAM wind field is reproduced adequately by the downscaling, though a tendency to the underestimation of the peak values is present.

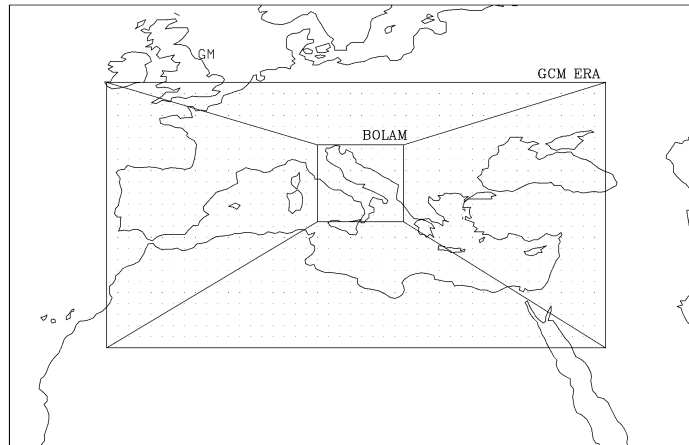


Fig. 7. area used for the wind downscaling: the predictor is the sea level pressure defined on the area "GCM ERA" and the predicand is defined in the area "BOLAM".

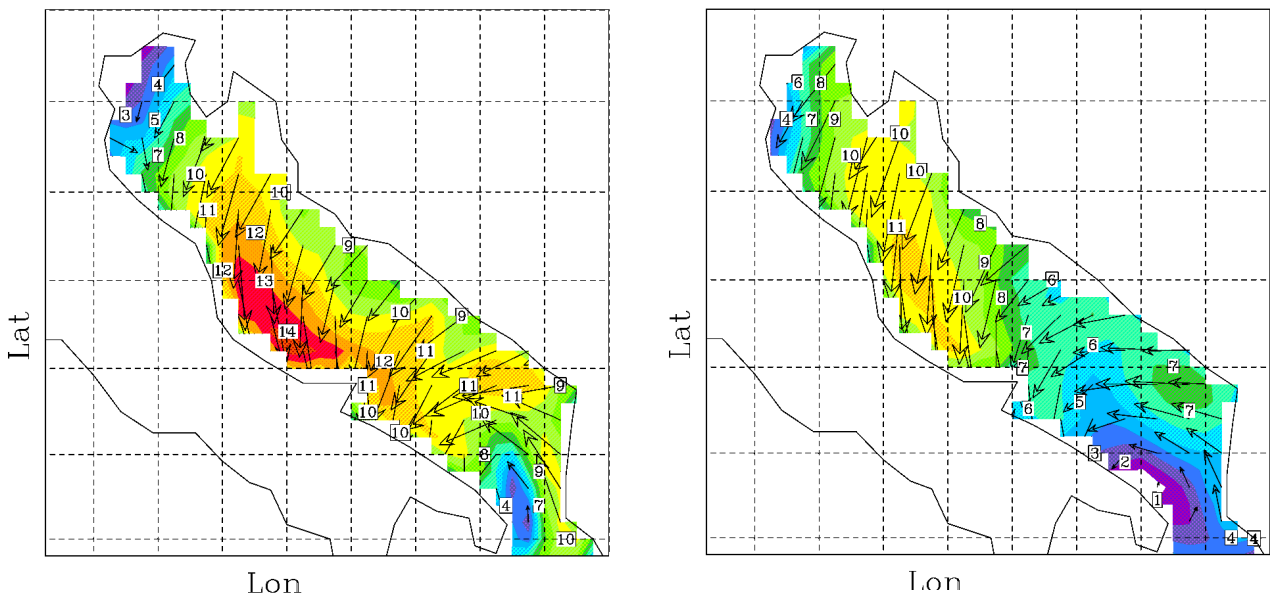


Fig. 8. Left panel: LAM wind field used for T106 downscaling. Right panel: corresponding downscaled wind field.

The quality of the downscaled winds has been investigated by using the ERA data that have been produced with T106 resolution, and which, therefore, have the same representation of the Mediterranean orography that is present in the control and CO₂ global experiment used in this project. These ERA data cover a period that does not overlap with any of the cases used for the development of the statistical downscaling and it is therefore a fully independent dataset.

The downscaled winds have been used for forcing the WAM model in the Adriatic Sea. The results show that the downscaling reduces substantially the underevaluation of the significant wave height, and, though it does not fully compensate for model errors, it improves effectively the quality of the model results. Figs. 9a-b and 10a-b show the observations (black line with circles), the results obtained with T106 winds (blu line) and with the downscaled winds (red dashed line), at Pescara(

fig 9a-b) and Venice (fig 10a-b), for a two months long period. Similar improvements are expected in the computations of the wave fields produced by the Control and CO₂ scenarios.

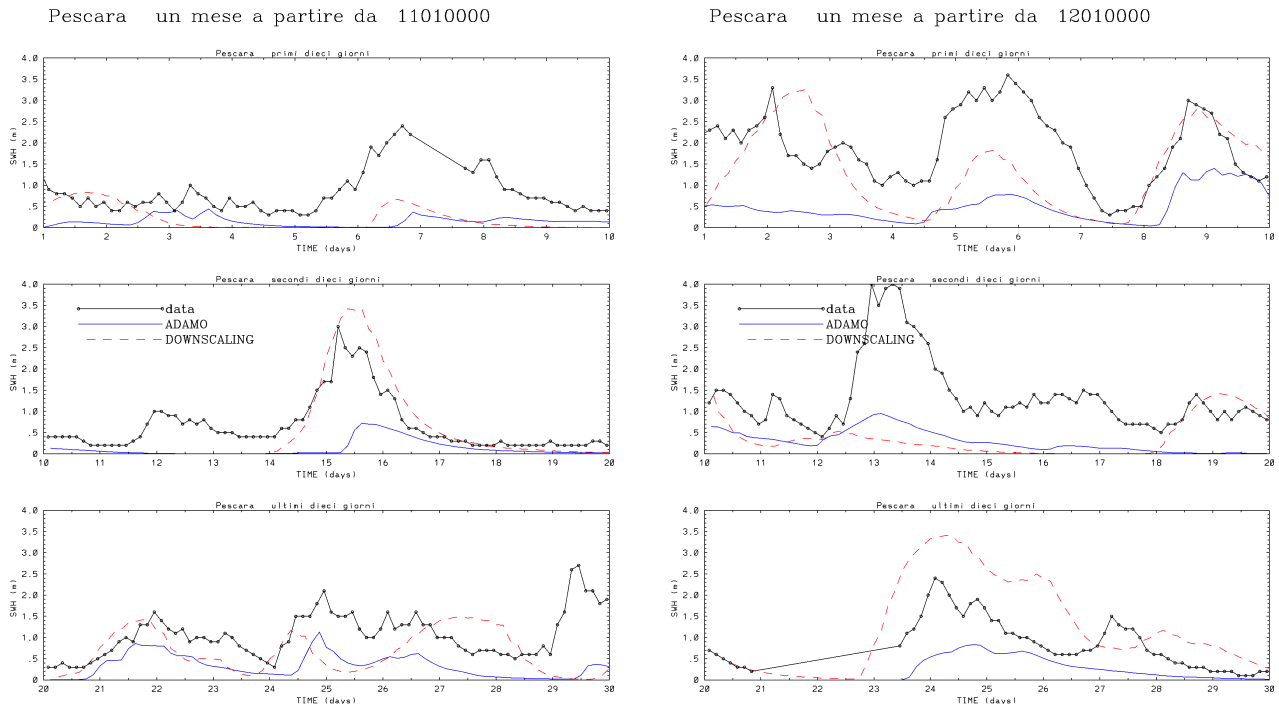


Fig. 9. Left panels: significant wave height observations at Pescara (circles), results of WAM with T106 forcing (continuous blue line) and with downscaled winds (dashed red line) for November 1990. Right panels: as left panels but for December 1990.

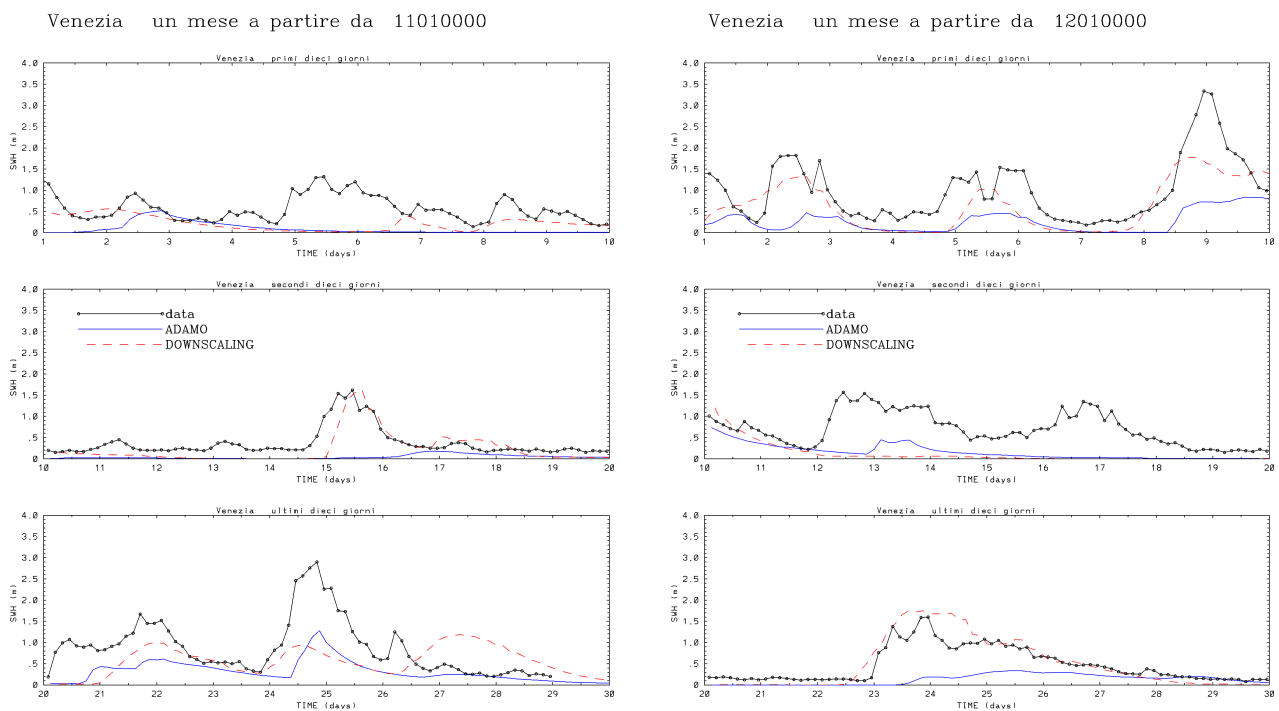


Fig. 10. As Fig. 9 but for Venice

A preliminary experiment with the surge model shows similar results, though a further refinement of the boundary conditions at the southern open end of the Adriatic sea is required, in order to reproduce the response of the basin to the large scale gradient of the sea level pressure over the whole Mediterranean Sea.

Task 9 Case studies: the Adriatic Sea and Task.10 Waves in the Mediterranean

The wave field evolution is simulated in the Mediterranean sea using WAM at the resolution 1/6th deg as part of the MIAO model simulation. The wave field evolution is available at this high resolution for selected cases. These cases have been selected from the dataset resulting by the analysis carried out in task.4, requiring the presence of a deep low pressure system located in a position where it was expected to produce a high wave field and/or surge. The selection has been subjectively oriented to identify storms with different trajectories in order to represent the various possible meteorological situations. Figure 11 shows the computed fields of a high resolution simulation (control experiment, 15th year, January, day 20) where a complex computed structure of the wave field with high peak values is present. The surge has also been simulated for the same cases at a high resolution (1/12 degs) in the whole Mediterranean Sea. Results are shown in figure 12 for the same situation described by figure 11.

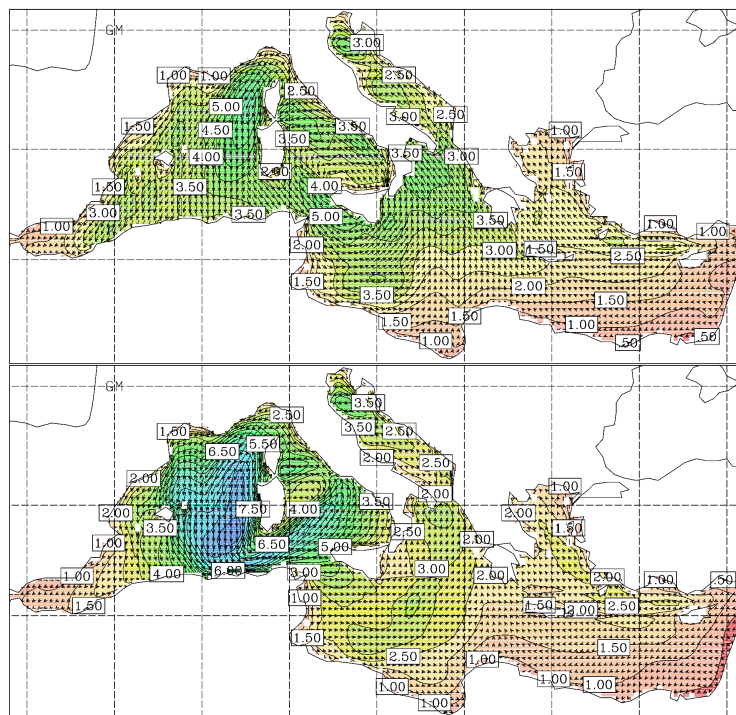
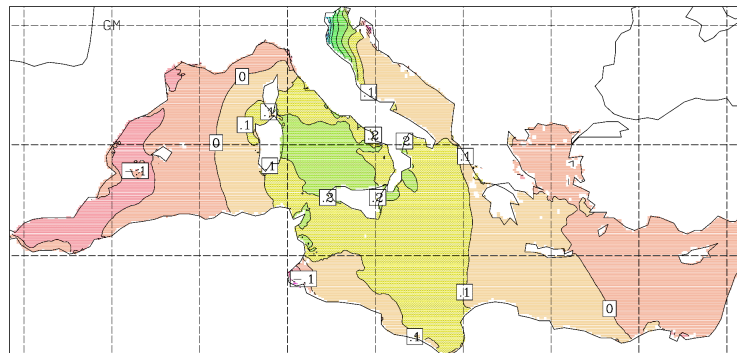
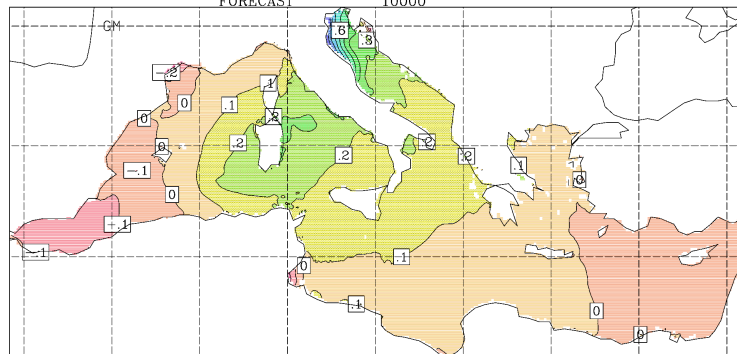


Fig. 11. High resolution wave field at a 12 hour interval for the control experiment, year 15, January, day 20.



INITIAL DATE 150120 0
FORECAST 10000



INITIAL DATE 150120 0
FORECAST 10900

Fig. 12. same as Fig. 11 but for sea surface elevation.

STOWASUS-2100

Contract no. ENV4-CT97-0498



ISAO-CNR

Contribution to progress report for the second project year (1/12 1998-30/11 1999)

By Piero Malguzzi

Introduction

During the season going from October to January, in which the sea surface temperature of the Mediterranean is sensibly larger than that of the air flowing above it, warm core mesoscale cyclones may form over the sea due to diabatic processes. These phenomena (hereafter referred to as *Mediterranean lows*), which have been only recently recognized and studied in the literature (see, for instance, Pytharoulis et al, 1999), bear a close resemblance to polar lows and, on a larger scale, to tropical lows. In association to the development of a Mediterranean low, severe weather conditions are experienced, in the form of strong surface winds over sea, high waves and severe precipitation events which may cause floods especially along coastal areas.

At variance with tropical depressions, Mediterranean lows need a “synoptic” forcing, usually in the form of a cut-off or a maximum of potential vorticity in the middle to upper troposphere, to develop. Numerical experimentation of observed case studies has revealed that the intensity of such a systems is determined primarily by the intensity of the sea surface turbulent fluxes of sensible and latent heat, both fluxes being equally important in determining the depth of the low system. The flux of latent heat sustains convection, which forces directly the dynamics through the release of latent heat during the condensation of water vapor.

Given the small spatial scale involved (the low level cyclone core has a typical radius of the order of 100 km), the T106 climate model is not capable to resolve Mediterranean lows dynamics with the necessary accuracy. It is therefore impossible to assess whether these phenomena will be more frequent or intense in the CO₂ scenario by looking directly at the T106 climate simulations. However, the T106 model may be able to reproduce the conditions favorable to the development of Mediterranean lows, and the research in the second year of the project has mainly focussed on the identification and search of those conditions by inspection at the long time series of various meteorological parameters obtained by the T106 simulations.

Work progress and results

We looked at systematic differences, between the present and CO₂ scenario, in the number of synoptic precursors (upper level cut-off lows), intensity of surface fluxes of sensible and latent heat, and conditions for convective instability. In both scenarios, the period going from 1 October to 30 January has been selected for each simulated year. During this period of the year, the frequency of

observed Mediterranean lows is maximum due to the relatively warm sea surface temperature. The following meteorological parameters have been considered for both scenarios:

- 1- Sea surface temperature
- 2- Air temperature at 2 m
- 3- Specific humidity at 2 m
- 4- Mean sea level pressure (P_{MSL})
- 5- Geopotential height at 500 hPa (Φ_{500})
- 6- Temperature at 500 hPa

Parameters 1 to 4 are used to compute the sea surface turbulent fluxes of sensible and latent heat (F_S and F_Q , respectively). The fluxes computation was made over the grid points depicted in figure 1, which are a subset of the T106 Gaussian grid covering the Mediterranean sea. Sea grid points where the orography at the T106 resolution was greater than 150 m have been excluded from the fluxes computation. Figures 2 and 3 show, respectively, the sensible and latent heat fluxes in the control (CTR, upper panel) scenario and the difference CO_2 - CTR (lower panel), averaged over the period 1 October – 30 January. It can be seen that the sensible heat fluxes are significantly reduced in CO_2 , while evaporation is increased appreciably only over the Aegean sea.

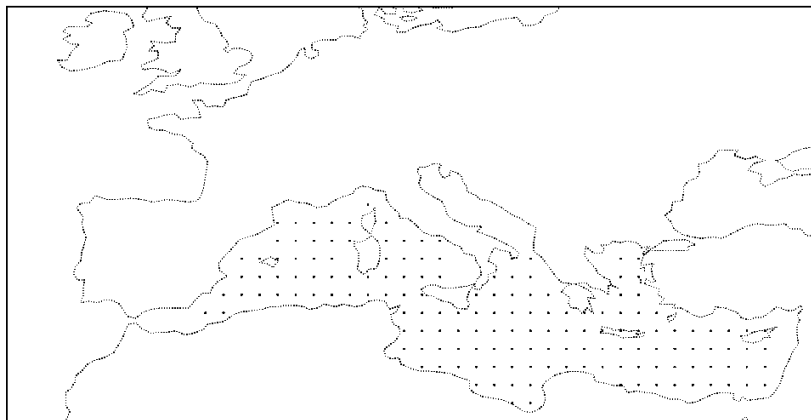


Fig. 1. Portion of T106 Gaussian grid used to compute surface fluxes

Mediterranean lows are driven by convection. In order to estimate systematic changes in the potential of convection over the Mediterranean, we computed a sort of “convection index” defined as the difference between the temperature of a air parcel, raised adiabatically from the sea surface to the 500 hPa level, and the environmental air temperature at that level (indicated hereafter with the symbol ΔT). A positive difference means that that air parcel is positively buoyant, thus increasing the chances for convection. Figure 4 shows the time average of the convection index for the CTR (upper panel) and its average changes in CO_2 (lower panel). Thus, on average, the T106 climate model predicts increased (decreased) chances for convection in the western (eastern) Mediterranean.

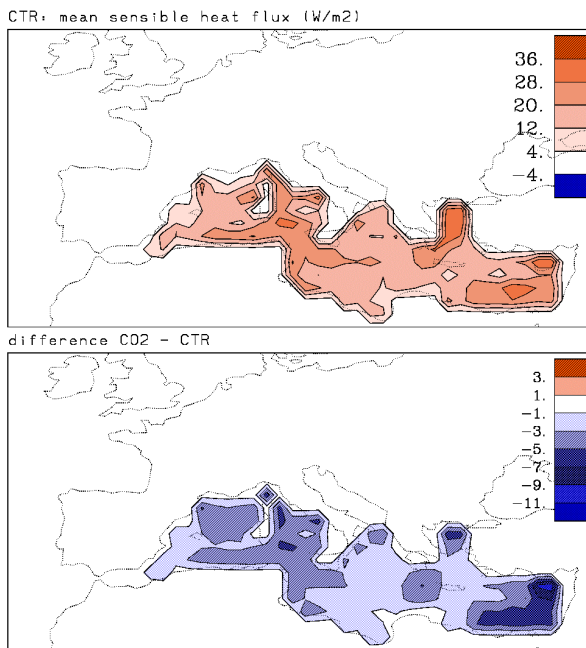


Fig. 2. Sensible heat flux averaged over the period 1 October - 30 January. Upper panel refers to CTR, lower panel to the difference CO₂ - CTR. Units are W/m². Positive values indicate upward fluxes.

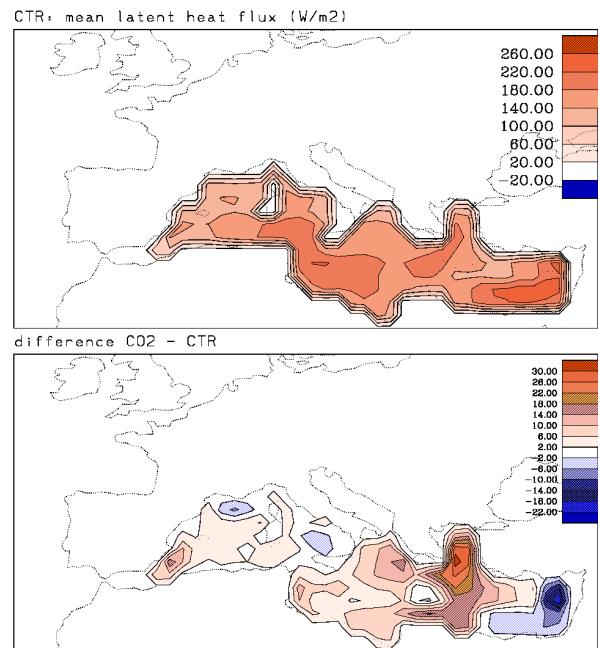


Fig. 3. Same as Fig. 2, but for latent heat flux.

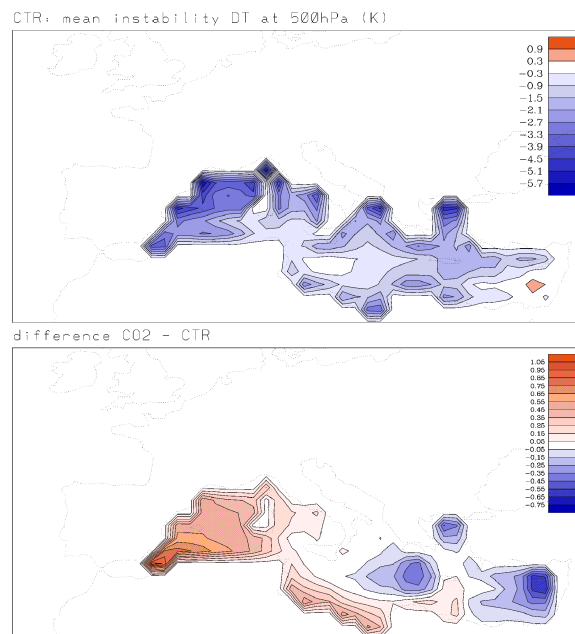


Fig. 4. Same as Fig. 2, but for the temperature difference between lifted parcel and environmental air at 500 hPa. Units are K.

By computing the 1000 hPa geopotential height with the help of the hydrostatic relationship, we computed the 500-1000 hPa thickness averaged over the period of interest. This field gives an idea of the average temperature structure in the lower troposphere. Figure 5, upper panel, reports the

average thickness in CTR. The modifications expected in CO₂ are reported in the lower panel of the same figure. The results indicate an increase of the meridional gradient of temperature over central Europe and a decrease over the Mediterranean. Consequently, the average baroclinicity is displaced to the north, reducing the potential for the development of baroclinic waves and upper level troughs, which are the precursors of the Mediterranean systems.

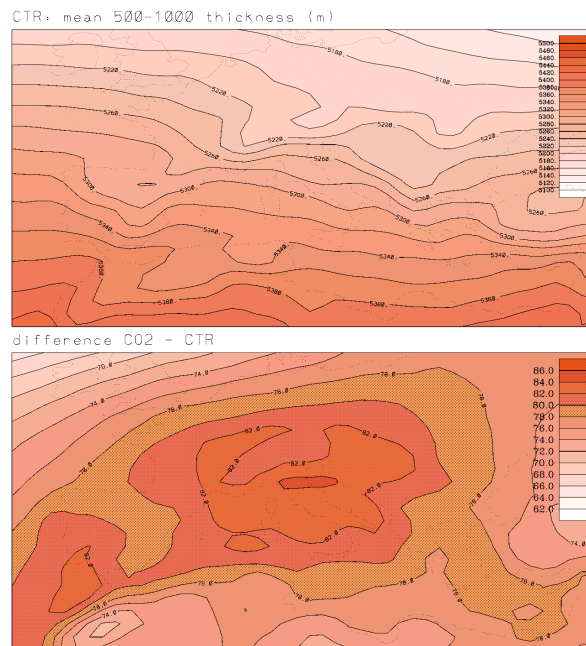


Fig. 5. Same as Fig. 2, but for the 500-1000 hPa thickness. Units are m.

In summary, by looking at the individual factors determining the potential for the development of Mediterranean lows, we may conclude that, on average over the period 1 October to 30 January, the frequency and the intensity of those systems should diminish in the climate of the 21st century, mainly because the number of the synoptic precursors is expected to be smaller and the surface fluxes of sensible heat weaker. This expectation is corroborated by the smaller number of cyclogenesis observed in the T106 simulation over the Mediterranean area (see results in common with UP and planned DMI technical report). It seems possible that some more intense cases could occur over the Aegean sea in the CO₂ scenario, due to the increase of latent heat fluxes over that region.

In order to select case studies of Mediterranean lows to be analyzed with the help of a high resolution model on a limited area, we have defined a multiplicative index which takes into account all the physical processes described above. The index is defined, at a certain instant, as the following product

$$I = C \bullet \max_A (F_T) \bullet \max_A (F_Q) \bullet \max_A (\Delta T) \bullet \max_A (\nabla^2 \Phi_{500}) \bullet \max_A (\nabla^2 P_{MSL})$$

where the maximum is computed over the area A depicted in figure 1, and where C is an arbitrary constant. Positive values of the above index refer to cases in which we observe, contemporaneously over the area considered, upward values of surface turbulent fluxes, potential for convective instability, and positive vorticity in the middle and lower stratosphere. High values of the index should, therefore, select the most favorable cases for the development of Mediterranean lows.

The index has been computed at each available instant of the T106 simulations (once every 6 hours) of the period under examination. The time interval of ± 3 days, centered around the time corresponding to the maximum value of I , defines the initial and final dates of the stronger case. The dates of the second stronger case have been defined analogously, by searching the maximum value of I in the remaining set of instants after the exclusion of the first case. In order to avoid overlap of cases, it is required that the second maximum differs of at least 6 days from the first one. The above procedure is repeated over the entire time series, both in CTR and CO₂, obtaining a ranking of cases in decreasing order of the index value. Figure 6 shows the cumulated distribution of I (number of cases with I greater than the threshold reported in abscissa) in the CTR (continuous line) and CO₂ (continuous-starred line) scenarios. The number of cases found in CO₂ is smaller at all threshold values, except for one case with very high index. This result is found to be stable with respect to variations in the index formulation and case selection.

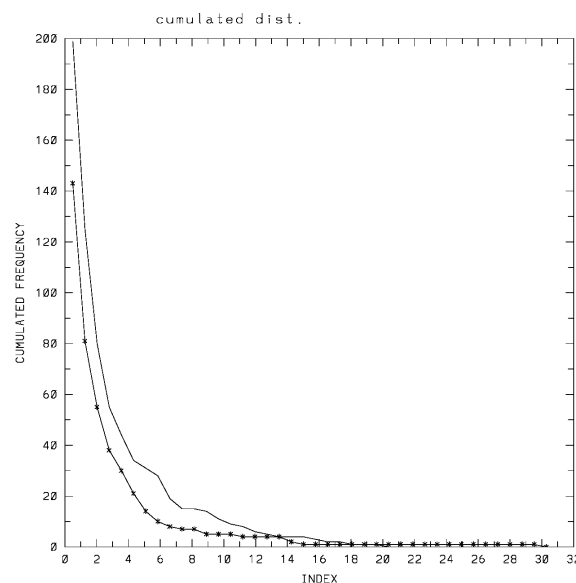


Fig. 6. Cumulated distribution of the index (see text) for the CTR (thin line) and the CO₂ (starred line) scenario.

In order to prove that the cases selected in this way have the potential to develop into Mediterranean lows we must resort to high resolution numerical modeling. In fact, Mediterranean lows present a mesoscale structure that cannot be resolved by the T106 climate model. Two high resolution experiments (30 km resolution) were performed by employing the mesoscale model BOLAM, nested in the T106 data. In both cases, in the high resolution model we observed a deeper cyclogenesis than in the T106 model, with stronger surface winds.

The first case starts the 25th of December of year 31 of the CO₂ scenario and corresponds to the case with the highest value of the index. The synoptic situation of this case is characterized by an upper level cut-off moving eastward over the eastern Mediterranean. Over the sea, a small scale cyclone forms over the Sicily channel and moves eastward towards the Aegean sea. The cyclone intensifies very rapidly during the 26th of December, reaching the maximum intensity at 18 UTC of that day, east of Greece (see figure 7). The same case study has been run without surface fluxes of sensible and latent heat, in order to prove that the shallow cyclone is indeed forced by diabatic processes. The result of this second run (not shown) indicates a much weaker development at low levels.

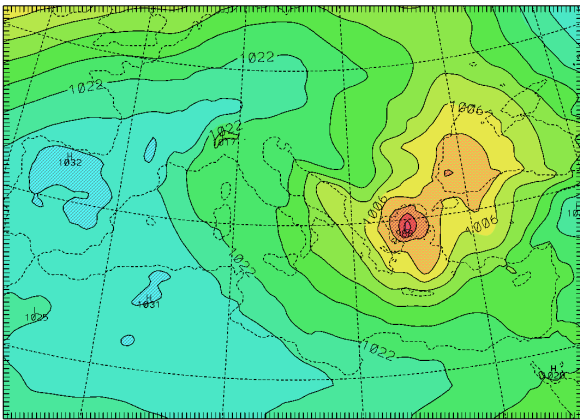


Fig. 7. Mean sea level pressure simulated by the high resolution BOLAM for the CO₂ case starting at day 25, month 12, year 31. Units are hPa.

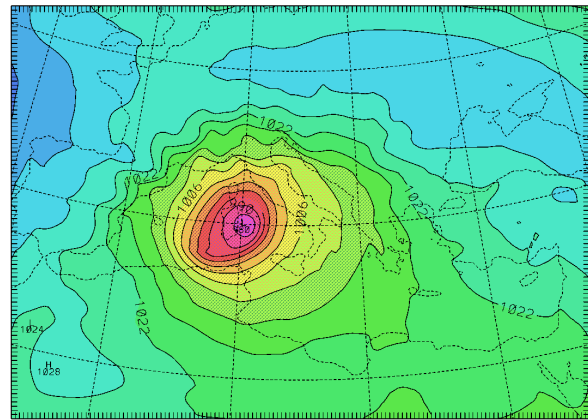


Fig. 8. As Fig. 7, but for CTR case starting at day 20, month 1, year 15.

The second case study that was analyzed belongs to the CTR scenario and starts the 15th of January of the simulated year 20. This case is the third most intense one according to the index selection. During the first two days of integration, an impressive development took place east of the Sardinia island, in association with a slow moving trough at high levels (see figure 8). Again, the same simulation performed without surface fluxes show a less intense cyclonic development at low levels.

From the high resolution simulations of these two cases we can tentatively draw the following conclusions. The cases corresponding to high values of the index I present indeed the potential for developing small scale, intense diabatically forced cyclones. At the same time, we have shown that the T106 climate contains the physical conditions that, at sufficient model resolution, may lead to the development of Mediterranean lows with strong intensity.

Activities in common with UP and modifications of work plan

In collaboration with the University of Padova, we have selected 21 case studies from the T106 simulation (see UP contribution for the list of cases) corresponding, in both climatic scenarios, to situations of strong Mediterranean cyclogenesis and strong surface winds. All the selected cases have been analyzed with the help of the coupled atmosphere-ocean model at high resolution, nested in the T106 data. The main purpose of this work is to provide the statistical basis for the downscaling of the 10m wind, needed for the 30 year surge and wave simulation over the Mediterranean and, in particular, the Adriatic sea.

According to the original work plan, the high resolution simulations of selected case studies should serve the purpose of identifying systematic differences between climatic scenarios concerning frequency and intensity of Mediterranean systems. We think, however, that few tens of cases are not enough for that, given the extreme variability presented by Mediterranean systems and the large number of degrees of freedom involved. We have therefore decided to devote a large part of the high resolution simulations to teach how to make wind downscaling (which is a very important step in order to be able to run the 30 year simulation of surge and waves), and to run few selected cases

concerning Mediterranean lows, mainly with the goal of validating other kinds of analysis aiming to the same goal. The work illustrated in the previous section provides a clear exemplification.

References

Pytharoulis I., Craig, G.C., Ballard, S.P. Study of the hurricane-like Mediterranean cyclone of January 1995. *Physics and Chemistry of the Earth*, Vol. **24**, n **6**, 627-632.

STOWASUS-2100

Contract no. ENV4-CT97-0498



Institute of Hydrophysics, GKSS.

Contribution to progress report for the second project year (1/12 1998-30/11 1999)

By Arnt Pfizenmayer and Hans von Storch

Progress of the work and deviations from the work plan.

We are mostly according to the work plan. We have designed a wave generator for 3-hourly wave heights and direction conditioned on the monthly mean air pressure state. An autoregressive model is used to describe the monthly sea level pressure as input for the wave generator. This part of the wave generator is conditioned on the CO₂ concentration. We finally get an output which is only depending on the CO₂ concentration. A complex testing and validation procedure is in work. A description of the full model is given in the first part of the progress report.

Additional to the work plan we have examined some actual question in climate research. We investigate the probability of anthropogenic influence in the recent wave climate with the central part of our wave generator. A summary of the paper (Pfizenmayer & von Storch, 2000) is given in the second part of the report.

A conditional first-order autoregressive wave-generator

A statistical model was developed to describe the daily statistics of ocean waves at a selected location in the North Sea. With its help we can produce long, realistic, synthetic time series for climate impact studies.

As input data we used observed monthly mean sea level pressure (SLP) over the North Atlantic and Europe and 3-hourly wave heights and direction (1954-1994) at one selected grid point in the North Sea (close to oil platform Ekofisk) from a 40-year hindcast performed in the WASA project (WASA group, 1998). The grid box has a longitudinal extension of 0.7 deg. and a latitudinal extension of 0.5 deg., the location is 56N, 3E. To condition our model on the CO₂ concentration we are using the T106 time-slice experiments from DMI. For all data we use the winter half year (ONDJFM).

Downscaling of the atmospheric circulation to the monthly wave statistic

In a first step the monthly distributions of wave heights for the meridional (fig. 1) and zonal direction were modelled using a statistical downscaling technic. Here we use a multivariate technique, namely redundancy analysis (RDA), that calculates patterns of two different fields that are coupled, so that for the predictant field (monthly wave statistic) the amount of the represented variance is maximized. Details about RDA can be found in von Storch and Zwiers (1999).

As a predictor for the wave climate we have chosen the monthly mean SLP field. This field is representative for the atmospheric circulation and is related to the surface wind through the geostrophic relation. Surface waves are a response to the forcing of this wind field. Another factor is remote wind forcing as this plays a role for the determination of the wave climate in the North Sea. Bauer and Buerger (1998) examined the history and the memory of wind forcing for waves in the North Sea. Waves in the North Sea are on average one day old, indicating a short wind duration and a short fetch for the evolving waves. Only extreme events originating in the NE Atlantic, coming through the North Sea, are around 6 to 7 days old. Consequently we assume that the complete monthly wave statistic can be mostly handled without a time lag to the monthly SLP. To describe the monthly wave statistic we used different percentiles of the wave distribution (fig. 1). For the zonal direction negativ values are for westwards waves and the positive values represent the eastward waves. Each direction is represented by 11 percentiles.

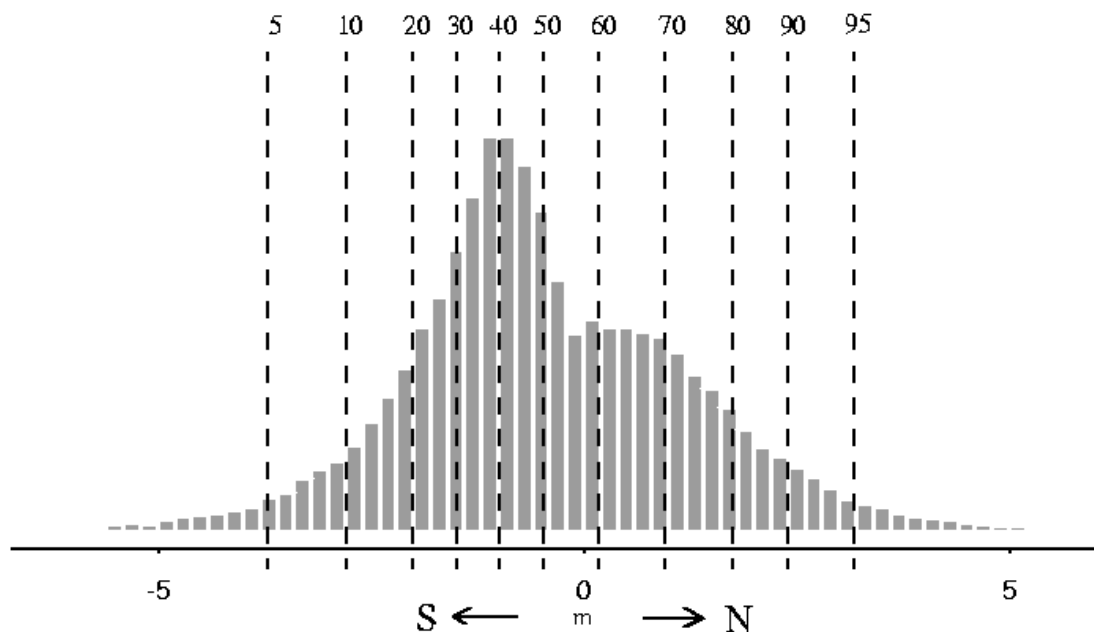


Fig. 1. Wave distribution in meridional direction for the winter half year and the different percentiles used for the statistical model for a grid box close to oil platform Ekofisk.

The RDA model is fitted with data from 1955 to 1964, for the reconstruction of this century and for the climate experiments we used the whole period of available wave data (1955-94).

The first RDA pair (Fig. 2, top) describes 45% of the explained variance of the monthly wave distribution. The time coefficients are correlated with 0.94. The first SLP pattern is characterized by a low-pressure system over Scandinavia and a high-pressure system west of Ireland. The associated pattern for the wave distribution shows an increase of all percentiles in zonal direction and a decrease in meridional direction. That means higher eastward waves, smaller and less westward waves and also more and increased southwards waves. When such an SLP pattern prevails, more low pressure systems pass Scandinavia in a southwestward direction. Consequently we get more northwesterly winds behind the front of cyclones over the North Sea. The pattern with the negative sign represents a situation with low pressure systems passing southwards off England. Therefore we expect southeast wind for Ekofisk.

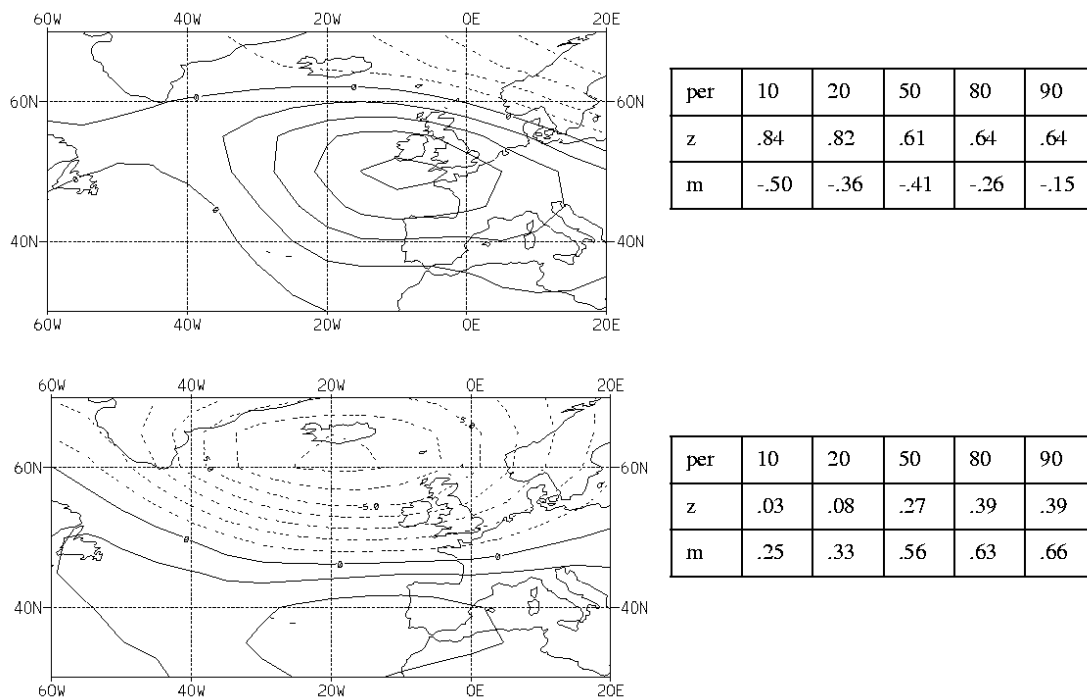


Fig. 2. The two pairs of redundancy pattern of observed winter (ONDJFM, 1955-64) SLP (hPa) in the North Atlantic sector (left) and selected percentiles for the intra-monthly wave distribution for zonal (z) and meridional (m) direction (right). Top (first pair); The correlation between the time coefficients is 0.94. The pattern for the wave distribution explains 45% of the variance. Bottom (Second pair): The correlation between the time coefficients is 0.88. The pattern for the wave frequency explains 33% of the variance.

The second RDA pattern pair (Fig. 2, bottom) is correlated with 0.88 and exhibits a small increase in eastward and a decrease in southward directions for the wave probability. In this case the SLP pattern is dominated by a high pressure system over the North Atlantic. On the east side of the anticyclone we get a southward airstream for the North Sea. In the opposite case the northerly winds are weakened, so we get a decrease of southwards and westwards waves.

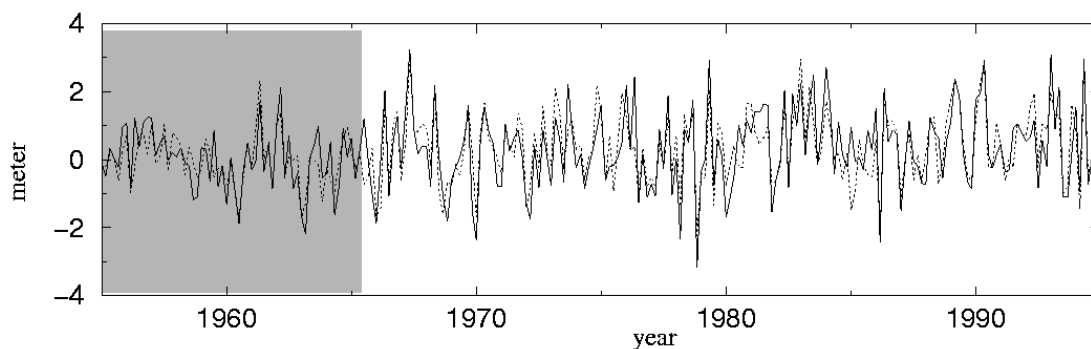


Fig.3. Time-series of the 90% percentile of the intra-monthly waves in zonal direction, as derived from "observed" (solid) and estimated from the monthly mean air-pressure field (dotted). The fitting period is shaded.

The model is validated in an independent period by comparing observed intramonthly percentiles of wave directions with estimated values. In Figure 3 the solid line is the "observation" (i.e. data from the WASA hindcast simulation) and the dashed line is the modelled time series for the 90% percentile in zonal direction. We use two conventional measures of skill for the comparison, the correlation skill score and the percentage of represented variance. The results for all percentiles are shown in Fig. 4. The good agreement demonstrates that the mean atmospheric pressure state is a good indicator for the wave climate.

per	5	10	20	30	40	50	60	70	80	90	95
zonal	.67	.76	.81	.84	.86	.88	.88	.89	.87	.81	.76
meridional	.67	.71	.75	.73	.72	.77	.78	.78	.76	.73	69

per	5	10	20	30	40	50	60	70	80	90	95
zonal	35	56	63	70	74	77	78	79	75	65	55
meridional	42	50	55	49	47	53	57	59	57	53	48

Fig. 4. Correlation skill score (top) and explained variance (bottom) for each percentile of the monthly wave distribution in the independent period (1965-1994).

First-order autoregressive model conditioned to the monthly wave statistic

In a next step 3-hourly wave heights for each direction were modelled using an autoregressive first-order process. In the whole period (1955-94) the autocorrelation parameter is fairly independent of the seasons and independent of the direction so a constant value of 0.94 was used. The autocorrelation parameter between both time series is also constant and is around 0.08.

To determine the monthly error, we used the calculated percentile from the statistical model. For this we need to reconstruct the estimated anomalies of the percentiles with the observed seasonal anomalies. To estimate the values between the available percentiles we use a linear interpolation. For the extreme values we decided to use a fixed minimum and maximum estimated from the observations relatively to the 50% percentile.

Using diagnostics such as autocorrelation functions, quantiles, spectrum and distribution functions the wave generator was validated against the observed wave statistics in the independent period. A complex testing and validation procedure of the model is in work.

Condition to the CO₂ concentration

In the last step we need synthetic timeseries as input for our statistical downscaling model. Here we also use an autoregressive model, whereas the parameters are conditioned on the CO₂ concentration. For this we project our relevant RDA patterns for the SLP from our RDA model on the time slice experiments from the DMI.

The difference for the first and second RDA pattern for their standard deviation, and mean values for each month is shown in Fig. 5. To investigate the evolution between 1*CO₂ and 2*CO₂ we used a transient climate experiment (ECHAM4-OPYC3).

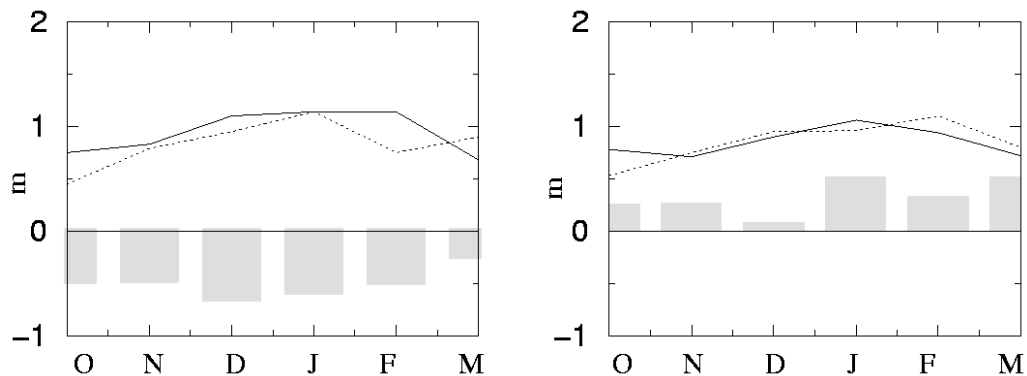


Fig. 5. The standard deviation of the RDA - coefficients for the control (solid) and $2 \cdot \text{CO}_2$ (dashed) experiment for each month. The grey bars are the mean difference between both runs. left: derived from the first RDA - SLP pattern, right second RDA pattern.

We found that the change in the mean values could be regarded as a linear function depending on the CO_2 concentration, for each month and RDA pattern. For the standard deviation no such relationship could be detected. We used a seasonal cycle for the standard deviation and a seasonal cycle conditioned to the CO_2 concentration for the mean value for our autoregressive model (fig 6, 2.).

A problem was to define the autocorrelation from month to month and between the RDA patterns. No significant change between both climate experiments could be found. In the moment we therefore define all autoregressive coefficients to be 0. More analysis of this problems will be carried out.

Implementation of the model

The concept of the wave generator is shown in Figure 6.

1. choice of a CO_2 -concentration (fixed or transient).
2. the parameters of the autoregressive model are determined from the CO_2 concentration.
3. output are synthetic time series of RDA-coefficients.
4. these time series are used as input for our statistical model.
5. statistical model produces as output a description on the monthly wave statistic
6. autoregressive model is conditioned to the monthly statistic
7. final output are time series (3-hourly) for wave height and direction.

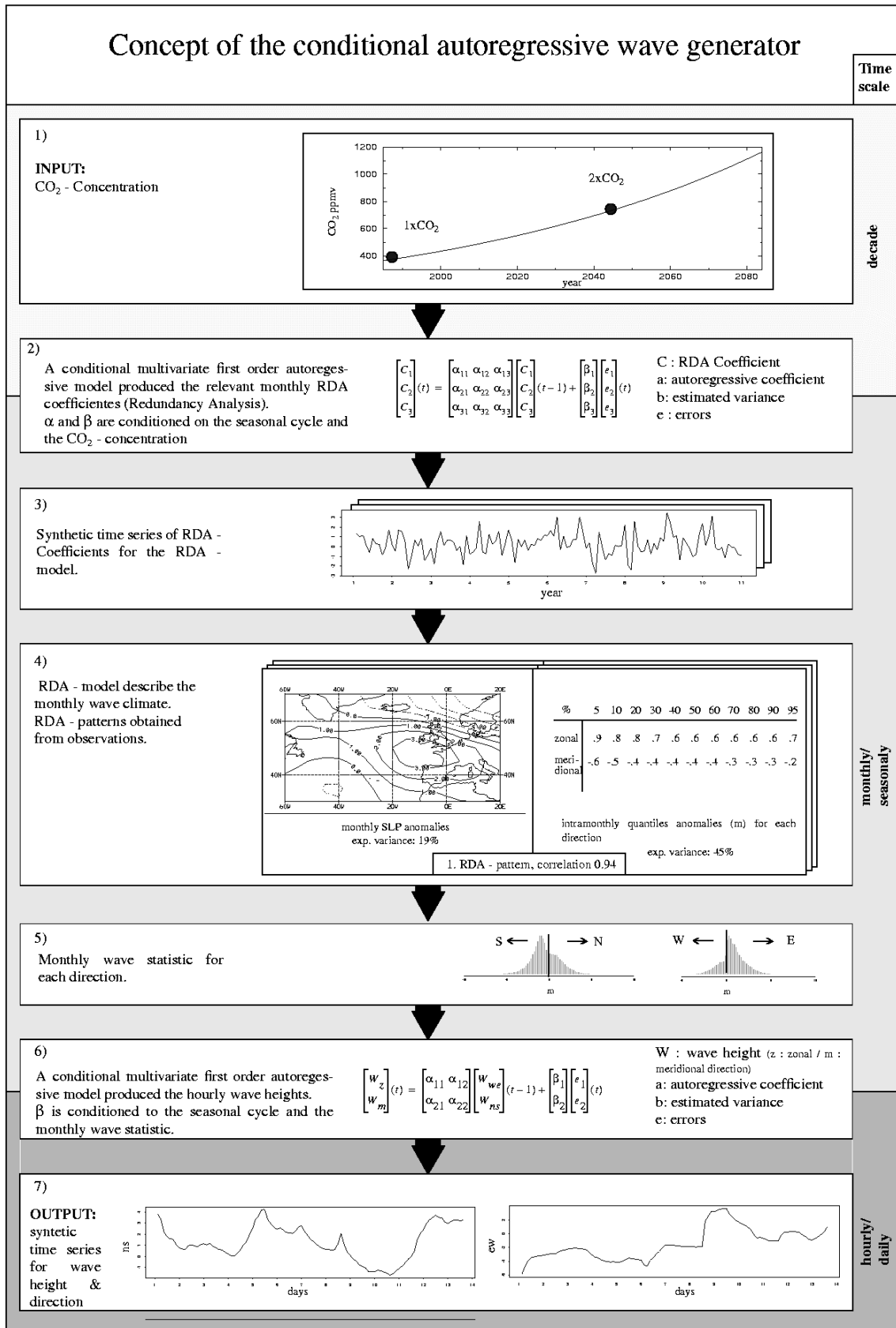


Fig. 6. Conceptual diagram of a wave generator conditioned on the CO₂ concentration.

As a preliminary result Figure 7 shows the mean difference between the control and $2 \cdot \text{CO}_2$ experiment over the 30 years of the SLP (top) for the winter half year. For the northern N-Atlantic and NW-Europe we expected a decrease of the mean pressure state indicating more storm tracks for this area. It is associated with a slight decreases of the lower percentiles (2 - 8 cm) and an increase for the higher percentiles (13-17 cm) for the distribution of wave heights in north - south direction (Fig. 7, bottom). This means a minor increase in the height of south- and northward waves. For the distribution in west - east direction a complete shift about 40 cm is expected, i.e. fewer waves and decreased extreme values for westward waves and more waves and increased extreme values for eastward waves.

Investigations for the mean wave heights and intramonthly wave frequency for the directions show that we have to expect an increase of the mean eastward wave heights and also an increase of the duration of these waves.

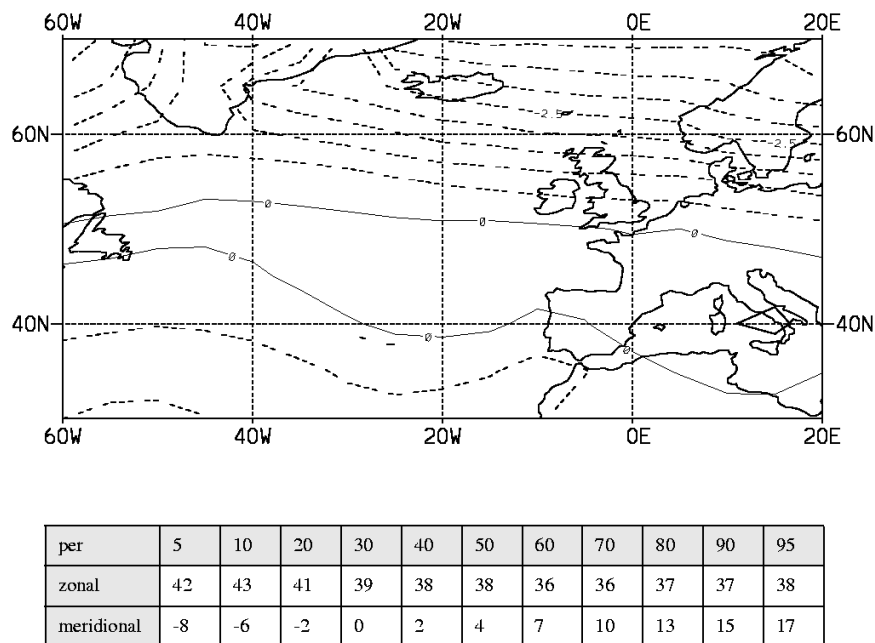


Fig. 7. Mean SLP difference (top) between the control and $2 \cdot \text{CO}_2$ run for the winter (ONDJFM) and the connected change of the percentiles of the wave distributions (bottom).

2. Detection of recent anthropogenic influence on the wave climate.

One actual question in climate research is, if the observed climate trends over the last few decades are unlikely to be caused by natural variability. With our wave generator we have investigate the recent and future development of the monthly probability of eastward waves. A detailed description can be found in Pfizenmayer and von Storch (2000).

In this paper we have examined the evolution of the monthly wave statistic in the central North Sea. Rather than the common variables like the mean wave height and extreme values, we decided to investigate the frequency of intramonthly wave-direction. It was found that in the recent decades

(1955-94) the monthly average time of eastwards waves is around 22.5 days with a positive trend of 3.5 days during this period.

To estimate the significance of this regional event four decades are too short. To obtain a longer period we used a statistical model to reconstruct the local wave climate for this century. As forcing we used the observed monthly SLP over the North Atlantic and Western Europe (1900-1996). With the available long time series for the SLP we were able to reconstruct the past century.

By comparing with the reconstruction of this century we found that the latest reconstructed 30 year mean probability of monthly wave direction, seems inconsistent with natural variability. The 30 - years low-pass filter of the reconstruction is shown in Figure 8 (solid line). However if the change is unlikely it is not impossible in the presence of natural variability.

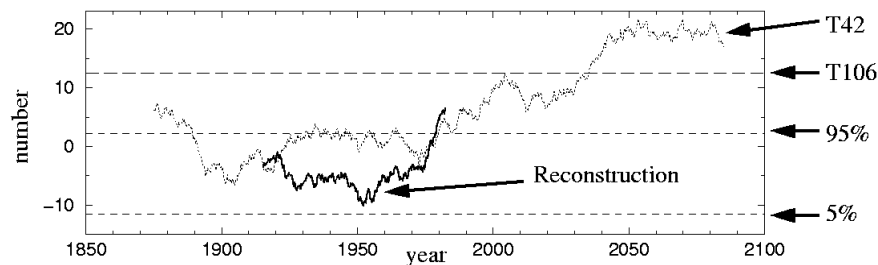


Fig. 8: Comparison of the 30 - year running-mean of the intramonthly time steps of eastward waves. Reconstruction of this century (solid line), the transient T42 run (dotted line) and the time-slice experiment (long dashed line). Dashed line is the estimated 5% and 95% confidence interval from the reconstruction.

To attribute this significant local climate change to an anthropogenic cause, we compared the reconstruction with the results of GCMs under increased greenhouse gas concentrations and aerosols. A 260 year transient run and one high-resolution time slice experiment were used as input for our statistical model.

The enhanced greenhouse effect and changed aerosol concentration in the transient GCM run produced the same qualitative characteristic (Fig. 8) as we found in the last decades of our local wave climate, with an upward trend of intramonthly eastward waves. The change in the time slice experiment is analogical. So it seems highly probable, that the wave climate in the North Sea is influenced by a recent change of anthropogenic emissions.

Plan for the year 2000

In the future a wave generator such as the one described here shall be used to obtain scenarios of the daily/hourly wave statistics in the North Sea and the Mediterranean might evolve under a transient climate change.

This final model will be developed using the T106 time-slice experiment from DMI and the wave simulations performed as part of this project by the partners from UP and DNMI.

Aspects of the socio-economic implications of expected change in wave statistics will be dealt with in a cooperation with the Max-Planck-Institute for Meteorology.

References

Bauer, E. and G. Buerger, 1998: Linking North Sea waves with North Atlantic winds on daily time scales.

Pfizenmayer A. and H. von Storch, 2000: Signature of changing wave climate in the North Sea. GKSS report, in press.

von Storch H. and F.W.Zwiers, 1999: Statistical Analysis in Climate Research. Cambridge University Press..

The WASA Group, 1998: Changing Waves and Storms in the North Atlantic? in: Bulletin of the American Meteorological Society, 79, No.5, 741-760.

STOWASUS-2100

Contract no. ENV4-CT97-0498



National Institute for Coastal and Marine Management (RIKZ).

Contribution to progress report for the second project year (1/12 1998-30/11 1999)

By John de Ronde, Marc Philippart and Stephanie Holterman

Background

The task for the National Institute of Coastal and Marine Management/RIKZ in this project is to develop a specific downscaling approach relating surge levels in deep water (North Sea) to surge levels in the Wadden Sea (task 7 of the work programme) to estimate local variations.

The development of an algorithm can be done in two different ways (also described in the work programme):

- Method 1. Developing a relationship with surge models
- Method 2. Downscaling with statistics

For the approach with surge models, two times 30 year T106-time slice simulations have to be computed with a local high (<1 km) resolution model. This is computationally rather expensive.

Also a combined dynamical/statistical downscaling technique can be used. By scaling of about 10 storms a data set of approximately 150 storms can be generated. This can be done by changing the storm parameters:

- phasing of the storm relative to the tide
- duration of the storm
- height of the wind strength

After computing these storms statistical relations can be derived between the surge levels at deep water and at the Wadden Sea. These relationships are finally used to downscale the surges simulated in the 2*30 year T106-time slice surge simulations with the coarse deep water model of POL.

Before starting the computations, RIKZ has to decide which surge model or surge model configuration should be used for the huge number of computations with a local very high resolution model. So a sensitivity study was carried out first.

Sensitivity study: In surge/search of a model (completed in April 1999)

RIKZ started with a sensitivity study, to investigate which high resolution surge model RIKZ should use for the computations needed for the development of the downscaling algorithm. After inventoring the short-term surge models of the Wadden Sea available for RIKZ, a storm period is

simulated with 5 different model configurations. The 5 model configurations are based on three different surge models nested in different ways, see figure 1:

- The Dutch Continental Shelf Model (DCSM):
This polar coordinated model is used by RIKZ for operational waterlevel predictions and storm surge forecasts. The modelled area of the DCSM contains the North West European Shelf, including the British Isles with grid $1/8^\circ$ longitude and $1/12^\circ$ latitude (~8 kilometers).
- Southern North Sea model (ZNZ):
A new curvilinear model which covers the area from the Southern North Sea, from Aberdeen (Great Britain) to Cherbourg (France).
- Kuststrook model:
This curvilinear model covers the whole Dutch Coast, from Zeebrugge (Belgium) to Norderney (Germany) and the adjoining part of the North Sea. For this model the grid of the Southern North Sea is three times condensed. For this project only the area of interest (the Wadden Sea) is used from the Kuststrook model. This model is called the Wadden Sea Model from which we have two versions, the ZNZ-model 1.5 times condensed is the Wadden Sea model_coarse, 3 times condensed is Wadden Sea model_fine.

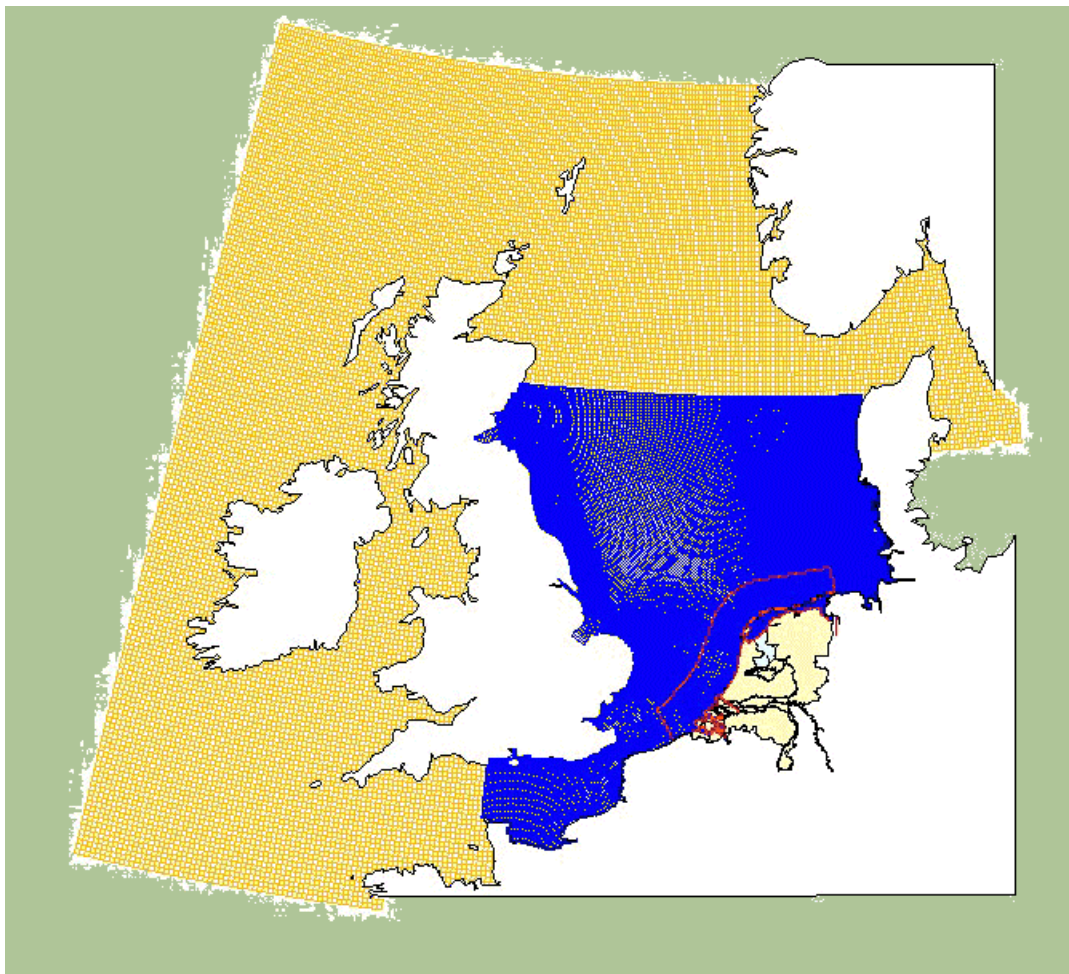


Fig. 1. Range of models RIKZ, from Continental Shelf (yellow contours) via the Southern North Sea model (blue contours) to the Kuststrook area (red contours)

The model configurations, in which boundary conditions, i.e. water levels are passed from coarser to the finer grid are:

1. Continental Shelf Model⇒Southern North Sea
(DCSM ⇒ ZNZ)
2. Continental Shelf Model⇒Southern North Sea⇒Wadden Sea Model_fine
(DCSM ⇒ ZNZ ⇒ Wad_fine)
3. Continental Shelf Model⇒Southern North Sea⇒Wadden Sea Model_coarse
(DCSM ⇒ ZNZ ⇒ Wad_coarse)
4. Continental Shelf Model⇒Wadden Sea Model_fine
(DCSM ⇒ Wad_fine)
5. Continental Shelf Model⇒Wadden Sea Model_coarse
(DCSM ⇒ Wad_coarse)

With these 5 model configurations the following simulations were done:

- period of December 28, 1994 - January 12, 1995, astronomical tide.
- storm period of December 28, 1994 - January 12, 1995.

For the earlier mentioned period predicted astronomical tide and water level measurements at 10 water level stations, see figure 2, were used.

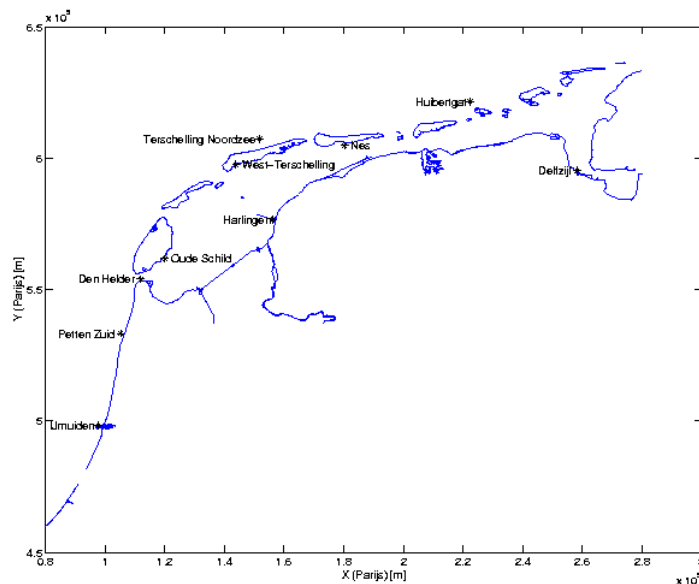


Fig. 2. Water level stations in the Wadden Sea

During and after the computations attention to the following points/requirements was given (in this overview, no attention will be given to points 3, 4 and 5 mentioned below):

1. accuracy and sensitivity of the different models regarding the water levels in the Wadden Sea
2. comparison of the calculation time (CPU-time) of the models

3. check velocity fields to examine possible circular flow on the boundaries
4. regarding the boundary conditions:
 - how to generate the boundary conceptions for the different models
 - how much time and effort it costs generating these boundary conditions
5. regarding the wind fields:
 - how to generate the wind fields for the different models
 - how much time and effort it costs generating these wind fields
6. regarding the different model configurations:
 - how the train of actions can be made automatic

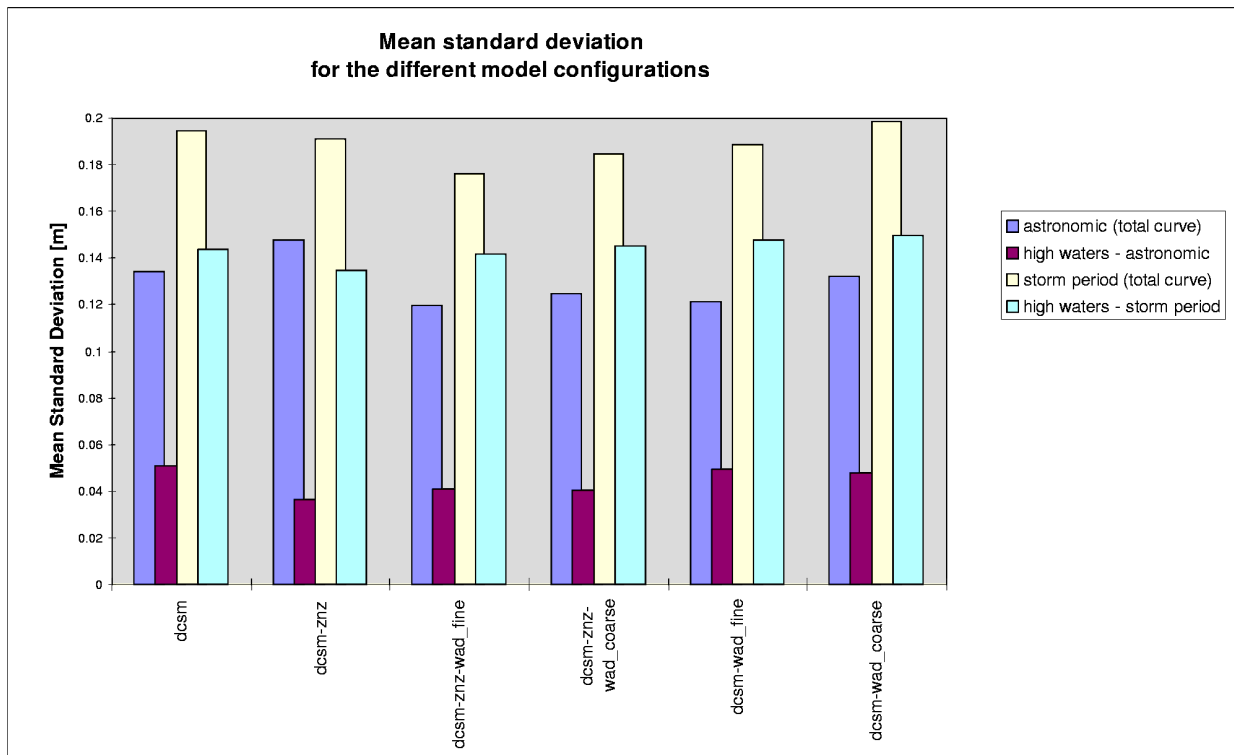


Fig. 3. Mean standard deviation for the different model configurations

After comparison of the simulated astronomic tide with the predicted astronomic tide and the comparison of the simulated storm period with the measurements at the 10 different water level stations the following conclusions can be drawn:

1. With respect to the accuracy and sensitivity of the different models regarding water levels in and around the Wadden Sea:

Because it is hard to determine visually which surge model configuration gives the best results, in figure 3 the mean standard deviation [m] for the different model configurations are given. In this figure the standard deviation is not only shown for the simulated period (pure astronomical

and with wind input), also the standard deviation for the high water situations in this period is presented.

The configurations DCSM-ZNZ and DCSM-ZNZ-Wad_fine give the best results, but no unequivocal conclusion can be drawn after these exercises.

2. Regarding the computation time:

In table 1 the CPU-time needed to compute a specific period for the different surge model configurations is presented. First of all the CPU-time needed to simulate a period of 1 day is presented in table 1 for the 5 surge model configurations. In these computations the boundary conditions are passed from DCSM to several finer models. In the next column the CPU-time needed to simulate a period of 1 day is given for all surge model configurations, but now the computations are made without the use of DCSM. In the last column the CPU-time needed to simulate a period of 30 days, without the use of DCSM, is presented. (N.B. In this project two periods of 30 years has to be simulated!)

Taking the duration of this project into account (01/12/1997 - 01/12/2000), it's not recommended to use surge model configuration 2,3 and 4.

	CPU-time [s] for a period of 1 day with DCSM	CPU-time [s] for a period of 1 day without DCSM	CPU-time [days] for a period of 30 year without DCSM
DCSM-ZNZ	1018	867	55
2. DCSM-ZNZ-Wad_fine	7737	7555	479
3. DCSM-ZNZ-Wad_coarse	1752	1600	101
4. DCSM-Wad_fine	7096	6914	438
5. DCSM-Wad_coarse	921	739	47

Table 1 CPU-time for the different model configurations

The main conclusion is that the Southern North Sea model meets the requirements earlier stated. Therefore it's decided to use the Southern North Sea model during the development of the statistical downscaling algorithm.

Development of a downscaling algorithm (September 1999 - May 2000)

In the beginning of the project it seemed that is was not possible to develop a downscaling algorithm with method 1, because of the amount of needed CPU-time. On the other hand, method 1 is the most suitable method. Therefore we decided in the summer of 1999 to go for method 1, with the restriction to simulate only the storm seasons (period Oktober 1 - March 15) of every year.

The following simulations are planned:

1. 30 storm seasons 'control'¹ scenario, surge only
2. 30 storm seasons 'control' scenario, tide + surge
3. 30 storm seasons '2*CO₂'¹ scenario, surge only
4. 30 storm seasons '2*CO₂'¹ scenario, tide + surge
5. test run (storm season 2088 - 2089), surge only

After receiving the wind, pressure and surge data of the two data sets of 30 year time slice simulations of POL in August/September we were able to set-up the Southern North Sea model for the two 30 year data sets.

1. The development of the downscaling algorithm is divided in two parts:
 - a) Model set-up and computations
 - b) The making and control of the ZNZ boundary conditions
 - c) The running of the simulations and the control of the output
 - d) Post-processing and data storage
2. Statistical processing of the output-data

The making and control of the ZNZ boundary conditions (completed in November 1999)

The boundary conditions for the Southern Sea Model are derived from the ECHAM4 model (wind and pressure), the NEAC model (surges) and from the Southern Sea Model itself (astronomic tide).

The properties of the different models are:

Model	grid	resolution	definition of 1 year	output
ECHAM4	spherical	1.125 degrees	360 days (12 months of 30 days)	6-hourly
NEAC	linear	about 35 km	365 or 366 days	every hour
ZNZ	curvi-linear	varies between 300 and 10000 metres, see figure 4	365 or 366 days	every hour: mapfiles of water levels every 10 minutes: timeseries of water levels and velocities at a few strategic output points for verifying the computations every 10 minutes: water level timeseries at defined locaties every 10 minutes: velocity time series at 20 locations along the Dutch Coast

The main actions were:

- To synchronise the different time conventions from the surge, wind and astronomical data
 - Check time and geographical conventions
 - Change of date convention wind data
 - Change date convention surge data
- To make boundary conditions (time series) for tide, surge and the combination of tide and surge for each winter season.

¹ The first time slice data set is statistically representative of the climate for the 30 years from 1970 to 1999, referred to as the 'control' scenario; the second set represents the climate under conditions of double atmospheric carbon dioxide in the years from 2060 to 2089, referred to as '2*CO₂' scenario. For both datasets the astronomical boundary conditions are equal.

- Interpolate the surge data of 79 points (from POL) to the 33 boundary points of the ZNZ model
- Make tidal time series from astronomical components
- Make boundary conditions by adding astronomical tide and surge time series

All these actions took place before November 15.

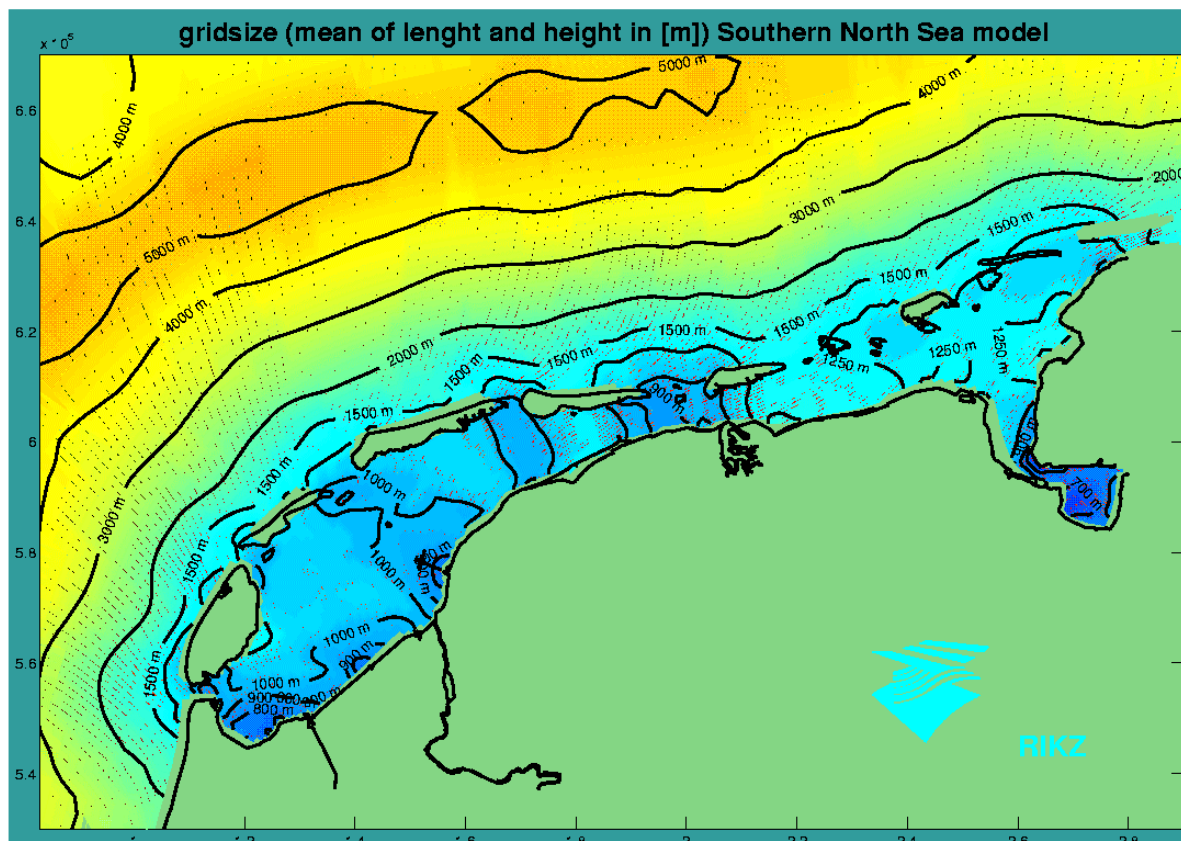


Fig. 4. Grid size Southern North Sea model, Wadden Sea area

The running of the simulations and the control of the output (November 1999 - completed in January 2000)

For each year of the two times 30 year time slice simulations the storm period (October 1 - March 15) has to be simulated; this means 165 or 166 days a year. Due to the availability of faster computers the duration of a simulation of one storm period is about 12 hours/storm period. By using more than one computer, the duration of all the above planned simulations is 1.5 month.

The output of the simulations will be checked random at a couple of strategically defined water level output stations.

For every simulation the following output will be written to the hard disk (and later stored on CD-ROM's):

- Mapfiles with water levels with an interval of 1 hour

- Timeseries of water levels and velocities with an interval of 10 minutes at a couple of strategic defined water level output stations to check the model simulations
- Timeseries of water levels with an interval of 10 minutes at 61 water level stations, see figure 5a and 5b
- Timeseries of velocities with an interval of 10 minutes at 20 locations along the Dutch Coast, see figure 6

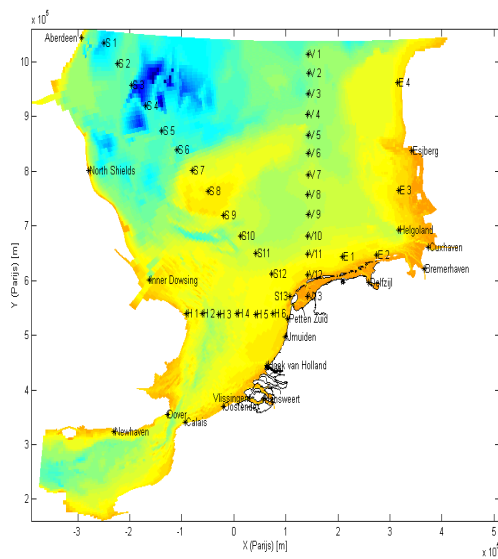


Fig. 5a. Water level output stations ZNZ model

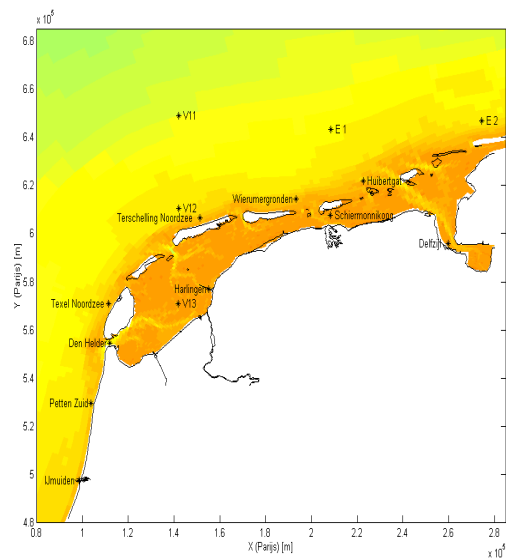


Fig. 5b. Water level output stations Wadden Sea area

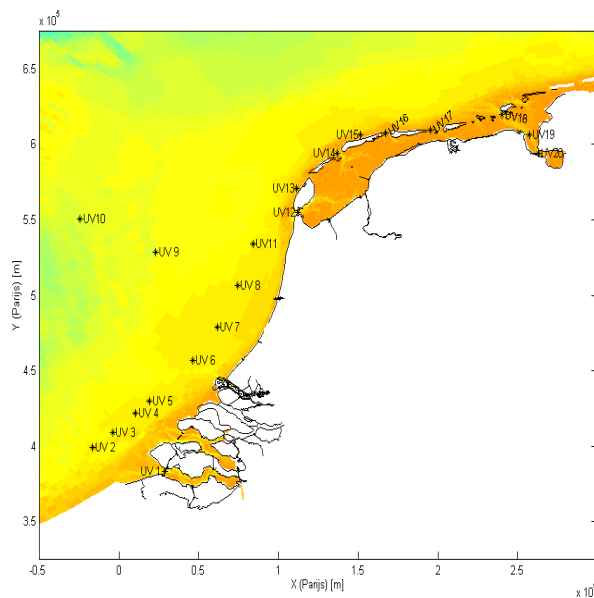


Fig. 6. Velocity output stations along the Dutch Coast

At this moment half of the computations are carried out. The forecast is that all the computations will be finished in the middle of January 2000. In figure 7 the first results of two months (January -

March 2061, 2*CO₂ scenario) are plotted for the storm period 2060 - 2061 for the water level stations Terschelling Noordzee en Harlingen.

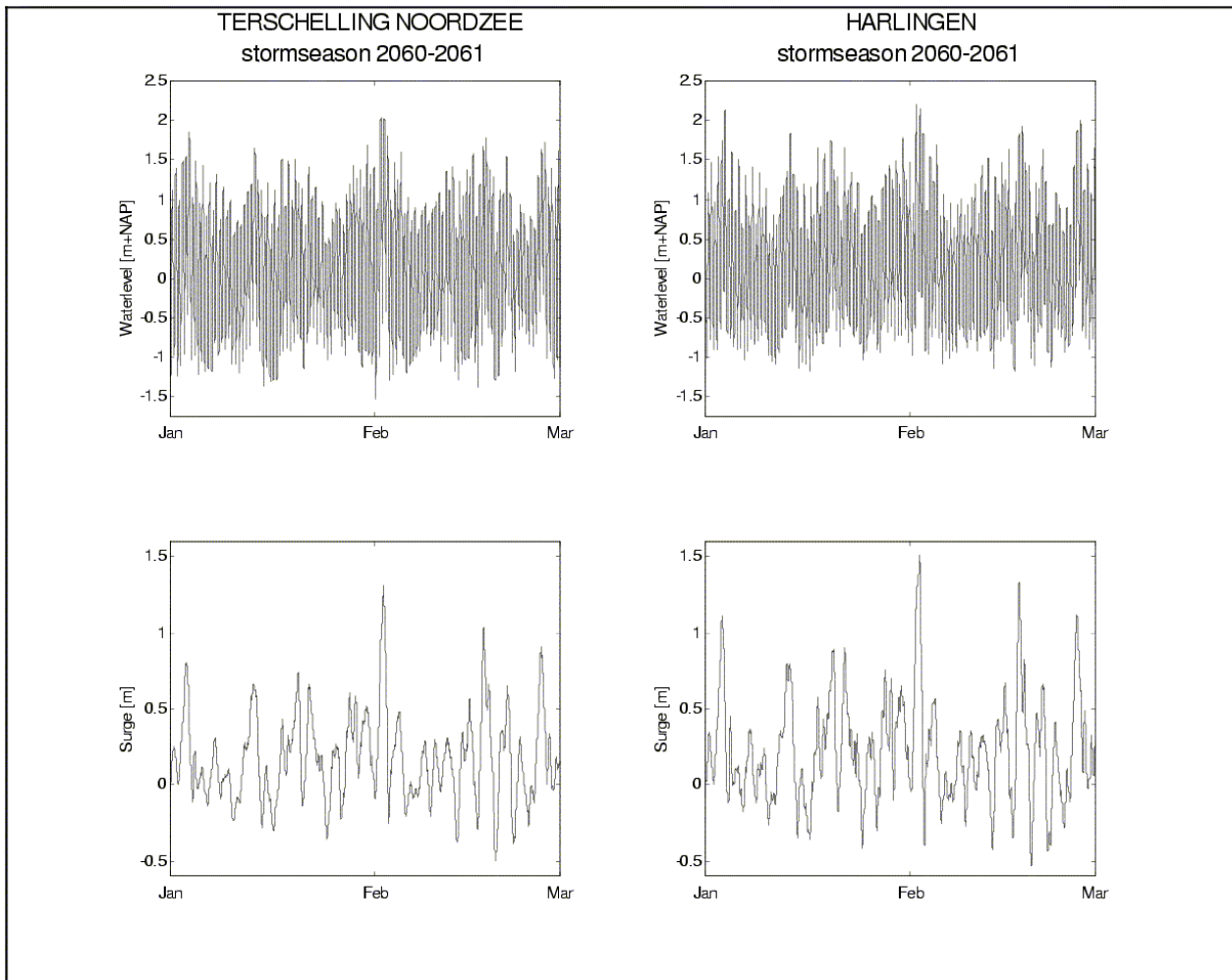


Fig. 7. Total water level and surge for the water level stations Terschelling Noordzee and Harlingen for the period of January - March 2061 (2*CO₂ scenario)

Postprocessing and data storage (December 1999 - completed in January 2000)

During the computations, postprocessing and data storage is an important part of this project because of the huge amount of data and needed disk space. It is necessary to decrease the needed disk space and to transport the data to another disk during the computations, otherwise the computers will be jammed.

To decrease the amount of needed disk space some post-processing programs are written in MATLAB-software.

For example:

One mapfile with water level data = +/- 574 kb

The same mapfile after post-processing = +/- 50 kb

At this moment all the post-processing software, to decrease the amount of data, is written. A part of the data is already processed. All the data and used programmes will be stored at CD-ROM's.

Statistical processing of the output-data (December 1999 - completed May 2000)

During the computations software to process the statistical output is developed.

Progress and future work

We are still on schedule, so there are no deviations from the work plan.

Our time schedule for the next seven months:

	December 1999	January 2000	February 2000	March 2000	April 2000	May 2000	June 2000
Running of the simulations and control of the output	X	X					
Post-processing and data storage	X	X					
Statistical processing of the output-data	X	X	X	X	X	X	
Reports						X	X

Logistics

John de Ronde and Stephanie Holterman attended the meeting in Bergen in June 1999.

STOWASUS-2100

Contract no. ENV4-CT97-0498



Norwegian Meteorological Institute (DNMI).

Contribution to progress report for the second project year (1/12 1998-30/11 1999)

By Magnar Reistad, Knut Helge Midtbø, Ole Vignes, Hilde Haakenstad, Bruce Hackett and Ingerid Fossum.

Part 1: Polar lows

Progress of the work

A statistical analysis of the frequency of polar lows in the control scenario and in the two times CO₂ (CO₂) scenario has been carried out. This analysis has enabled us to indicate that a climate change will increase the frequency of polar lows in the actual sea areas north and east of Norway. Cases have been chosen and listed for the high resolution (10 km grid) simulations from both T106 runs. The high resolution runs have not yet been carried out.

Achievements and results obtained

The main goal for the task was to establish criteria for polar low risk and to apply those criteria to the T106 runs in order to quantify the polar low activity in the climate scenario compared to the control run.

To do so the data from the T106 runs were inspected for parameters quantifying precursors and stability parameters for detecting polar low events. Several methods for quantifying the precursor have been tested ending up with use of quasi-geostrophic omega equation. As discussed previously, it was decided to use polar low trajectory data from the Norwegian Polar Lows Project (Lystad, 1986) together with reanalysed ERA-data from ECMWF to test the methods.

Testing polar low criteria on the data from the Polar Lows Project using ERA-data from ECMWF

The Norwegian Polar Lows Project established elements of a polar low climate for the so called "Norwegian waters" for three winter seasons in the period 1982-1985.

ECMWF re-analysis project has established ERA-15 T106 global analysis in their archive. We retrieved wind and geopotential in standard pressure levels from this archive. Polar lows are not resolved in the T106 but are occasionally recognised as smoothed troughs. An example of a polar low case is shown in figure 1. In this case a trough is seen, but carefully analyses as carried out in the Polar Lows Project (Hoem and Hoppestad, 1985) shows an intense small-scaled cyclone in the position marked by the cross marked with N, W, S, E in the figure.

The method for computing a parameter quantifying the precursor has been based on the quasi-geostrophic omega equation in the form:

$$\kappa \nabla_p^2 \omega + f \cdot (f + \zeta) \cdot \frac{\partial^2 \omega}{\partial p^2} =$$

$$f \cdot \frac{\partial}{\partial p} (\mathbf{v}_g) \cdot (\nabla_p (2\zeta_g + f))$$

where subscript g refers to geostrophic values. The above form has been chosen in order to avoid calculation of terms, which are known to partly cancel. Textbook analysis of the equation shows that rising motion and surface convergence is found in areas where the left hand side of the equation is predominantly positive. Instead of solving the equation we have used the right hand side in a somewhat crude way as we have taken the value of the right hand side calculated in the grid point as a parameter in the polar low risk criterion. The right hand side has been evaluated in the 700 hPa level while the vertical derivatives has been taken from 500 to 1000 hPa.

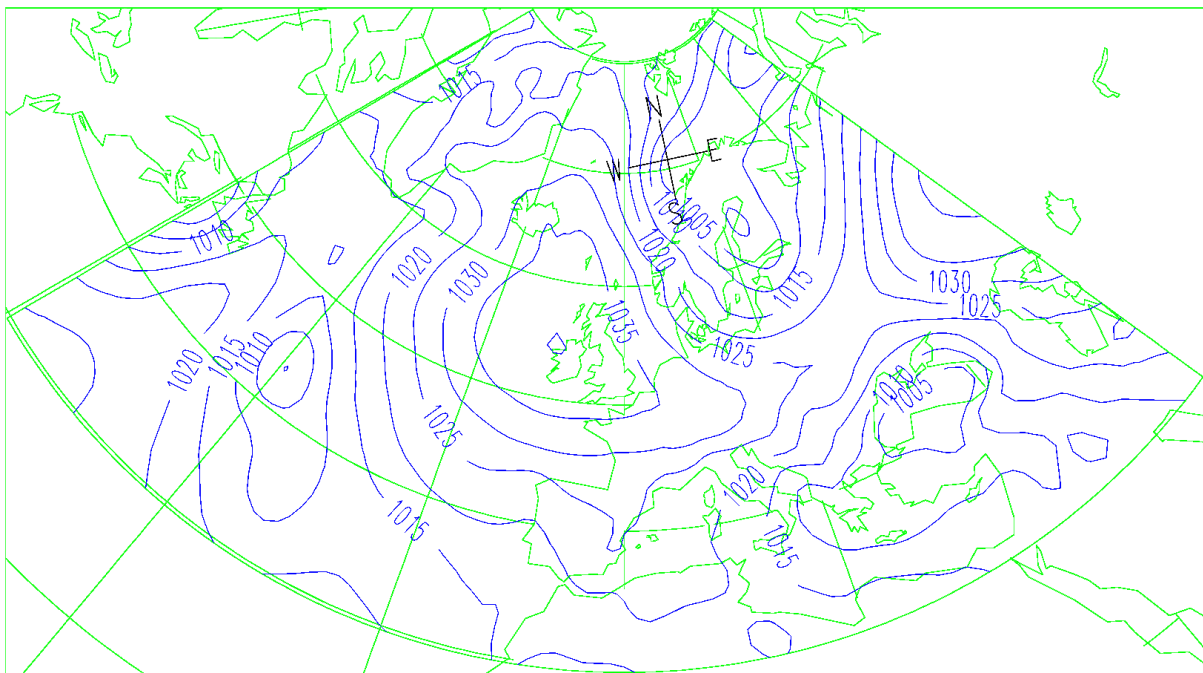


Fig. 1. ERA reanalysis of MSLP valid 00 UTC 7th March 1984. Position of the polar low is marked with a cross (see text).

A stability parameter is included, as polar lows are known to owe their rapid development to strong convection requiring a low 500 hPa temperature. The parameter for stability is taken as the difference between the 500 hPa temperatures and the temperature at the surface. The necessary value of the difference is difficult to establish from the literature. As will be discussed later a limit is difficult to establish from the present data as well.

Limits on the four parameters has been tested together as a criterion in each grid point:

- omega parameter,
- stability parameter,
- northerly wind component,
- surface temperature (0-metre temperature)

In addition the area is restricted to the area over sea within 56 degrees north and 78 degrees north and 21 degrees west and 52 degrees east.

Both ERA analysis and polar low events has been looked up on a 12 hour cycle. Polar lows were not observed outside the period October to April in the three winter seasons so the study has omitted the other months. The number of termins is totally 1293 for the three years. In 288 of those polar lows are observed somewhere in the area giving a little less than 100 each year as a mean.

In order to check the criterion a square area is defined by the start and stop point of the polar low trajectory for all the termins of the life of the low (unfortunately only start and stop point are available from the Polar Lows Project). The square is extended with 5 degrees of latitude to the north and the south and 10 degrees of longitude to the west and the east. The criterion is tested on all grid points inside this square. If at least one point satisfies the criterion the actual termin is a polar low termin. If not, the termin is not. The problem is then a yes/no problem, which can be presented in a contingency table. We have varied the criterion carefully to try to end up with an as good selection as possible. The actual values used for the four parameters listed above in SI-units are: 4.E-6, 36, above 0., above 268.. The cases that were not selected has been inspected and a description of the cause(s) has been included in a list in the report of this task.

The result is shown in table 1.

	Polar low observed	Polar low not observed
Polar low detected by criterion	70	242
Polar low not detected by criterion	218	763

Table 1. Results from the tests selecting polar low cases from the ERA data.

The result is considered as somewhat disappointing. However the selection is based on data with a horizontal resolution of 100 km, which is too large to resolve polar lows. The use of three vertical levels to compute the omega parameter does also contribute to the uncertainties. The rather rough representation of the polar low trajectories does also enlarge the uncertainties of the method. An additional argument is that the polar low phenomenon is rather small scaled and that convection plays an important part in the development. It might therefore be argued that the selection of polar low cases on the basis of 100 km data in three vertical levels is of a probabilistic nature, which cannot arrive at a deterministic selection. The result obtained here with relatively large number of unsuccessful selections is therefore the type of result one must expect.

Polar low frequencies computed from the T106-data for the climate scenarios

The criterion used on the polar low data has been used to compare the control scenario with the climate change scenario. The weakness of the criteria is not so important in this case as it is used to compare two long time series of data. As long as the criterion to some extent selects polar low cases the use of it should enable us to select the one with the largest number of polar low events.

The result of the comparison is presented in several ways. Here we only give the number of termins which are selected as polar low cases. For the control scenario the number is 3646 and for the CO₂ scenario 4972. Looking at the data in table 1 we see that the criteria selects approximately the same number of polar low events in the test data set as actually observed. The numbers given should then not need to be adjusted to estimate the polar low frequency. This means that the climate scenario as a mean has 166 termins with polar lows and the control scenario 122 each year. Both estimates are higher than the 100 termins as a mean for the winter 1982-1985. The number 166 can be interpreted as a significant increase of polar lows in the CO₂ scenario. The reference for only three years is however a little too short to draw too firm conclusions on this point. The data can also be presented as distribution in space of the number of termins selected for each grid point. This type of result is included in the report of this task.

Selection of cases from the T106-runs for running high-resolution experiments.

To select cases for running high resolution (10 km grid) experiments we have looked for a parameter to sort the cases in an objective way. We have ended up with sorting the cases according to the number of grid points at a certain termin, which satisfies the polar low criterion. The list we will take cases from is given in the report. The cases on the top of this list are:

CO₂ scenario: 6th of February year 15

Control scenario: 10th of February year 13

Deviations from the work plan

Problems with the method for selecting polar low cases outlined in the project plan lead to including use of polar low trajectory data and ERA 15 data for testing of the method. This was done as a DNMI contribution to the project and has delayed the work with the task a little.

Modifications of the work for the next period

Simulation of the cases with the high resolution model (10 km grid) will be carried out in the first quarter of year 2000.

References

Hoem, V. and Hoppestad, S., Polar lows case studies III, Technical Report No. 12, the Polar Lows Project, the Norwegian Meteorological Institute, Oslo, 1985

Lystad, M.(editor), Polar Lows in the Norwegian, Greenland and Barents Sea, Final report of the Polar Lows Project, the Norwegian Meteorological Institute, Oslo, 1986

Part 2: Waves

Progress of the work

The numerical wave model WAM is used to study changes in ocean waves. The WAM model was set up on a rotated spherical grid covering the North Sea, the Norwegian Sea, the Barents Sea and a part of the North Atlantic. The grid area is considered to be large enough to catch most of the wave energy affecting the Northwestern European shelf seas. The grid area is shown in Figure 2. The grid resolution is 0.7 degrees or approximately 77 km. There are 2767 sea points in the grid. The model is set up with 25 frequencies, logarithmically spaced from 0.042 to 0.411 Hz, and 24 directions, equally spaced. The monthly ice information used in the time slice experiments is also used as input to the WAM model. Grid points with 40 per cent or more ice coverage are treated as land points in the WAM model.

The following wave parameters are stored for all grid points every 6 hours:

- 1) Wind speed
- 2) Wind direction
- 3) Significant wave height, total sea

- 4) Peak wave period, total sea
- 5) Mean wave period, total sea
- 6) Peak wave direction, total sea
- 7) Mean wave direction, total sea
- 8) Significant wave height, wind sea
- 9) Peak wave period, wind sea
- 10) Peak wave direction, wind sea
- 11) Mean wave direction, wind sea
- 12) Significant wave height, swell
- 13) Peak wave period, swell
- 14) Mean wave period, swell
- 15) Peak wave direction, swell
- 16) Mean wave direction, swell

The full two dimensional wave spectrum is stored in 40 selected grid points.

During the second year of the project the WAM model has been run with for 2X30 years with wind input from the two 30 years T106 time slice experiments.

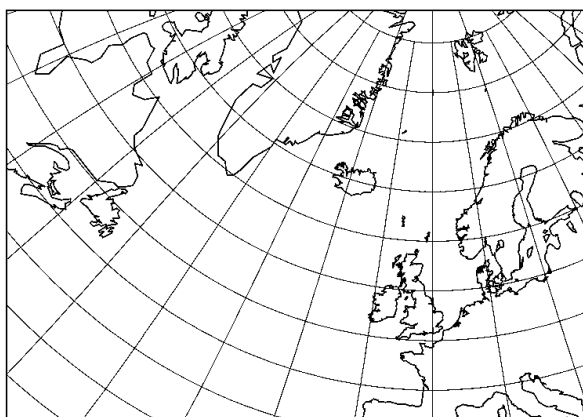


Fig. 2. The integration area for the WAM model.

Achievements and results obtained

The main achievement this period is the production of 2X30 years of wave data by running the WAM model with wind data from the T106 time slice experiments. Only preliminary analyses of the wave data are done. More detailed analyses of the wave data will be done during the last year of the project. Figure 3 shows the difference in average significant wave height between the 2XCO₂ run and the control run. The differences are small, mostly less than 0.15m. There is an increase in the average significant wave height in the North Sea, the Norwegian Sea, the Barents Sea and the area north of the British Isles. Further west there is a small decrease in significant wave height. Table 2 shows some statistics of significant wave heights for 8 positions. For the first two positions, Ekofisk and Statfjord, we have reliable wave measurements for the years 1980-1999 and we see that the model wave climate is not so far from the observed climate for these 19

years, but there is a certain overestimation of the high waves at both positions. In the North Sea (Ekofisk and Statfjord), the Norwegian Sea (Mike) and the Barents Sea (Ami) there seems to be an increase in significant wave height in the 2XCO₂ compared to the control run. The largest increase is in the 99 percentiles. This indicates that the high wave heights are more frequent with a doubling of CO₂. For the other four positions the differences are small.

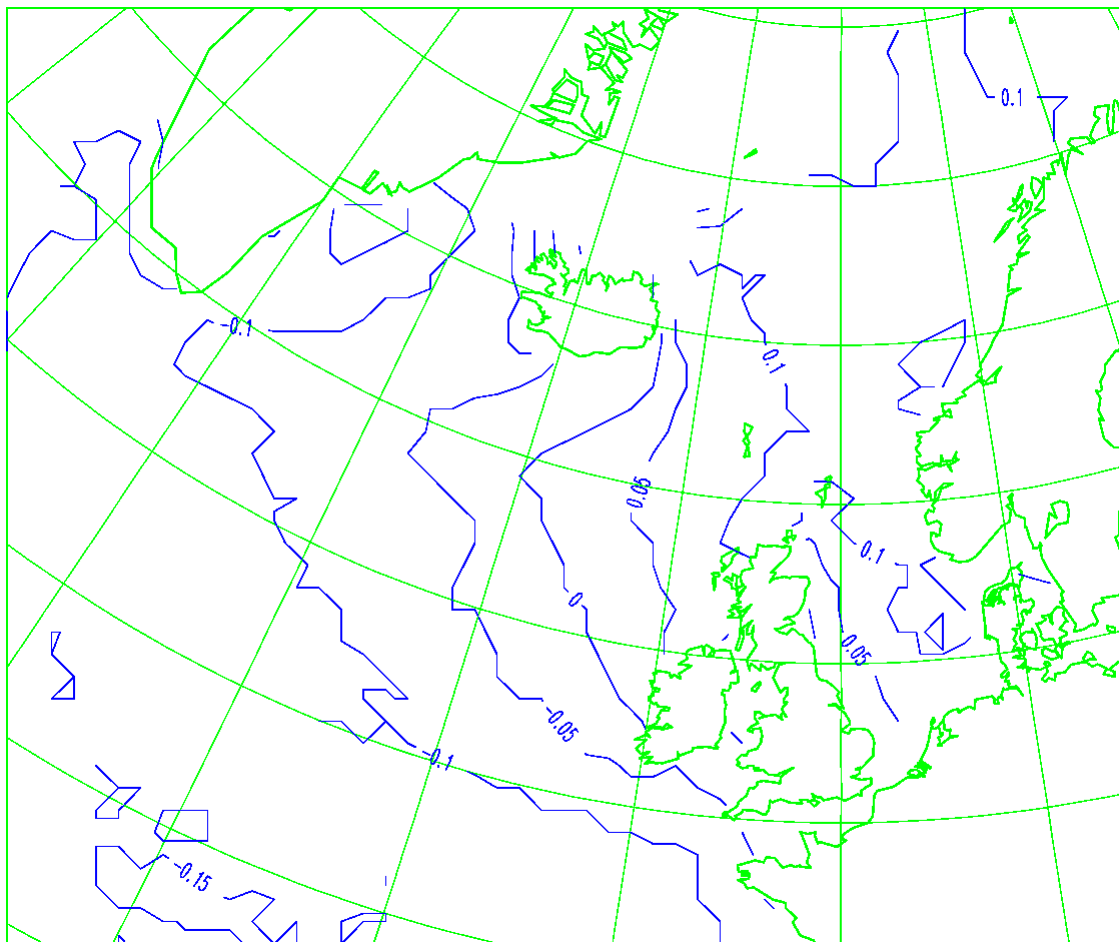


Fig. 3. The difference between average significant wave height in the 2XCO₂ run and the control run for the 30 years. Equidistance 0.05m.

Wave height statistics Ekofisk (56.5 N, 3.2 E)				
	Mean	50%	90%	99%
Ctr. year 1-30	2.09	1.7	4.1	6.7
CO ₂ year 1-30	2.19	1.8	4.3	7.0
Obs. 1980-98	2.07	1.8	3.8	6.2
Wave height statistics Gullfaks (61.2 N, 2.3 E)				
	Mean	50%	90%	99%
Ctr. year 1-30	2.89	2.5	5.4	8.5
CO ₂ year 1-30	3.02	2.6	5.6	8.8
Obs. 1980-98	2.74	2.4	4.9	7.6

Wave height statistics Mike (66.0 N, 2.0 E)				
	Mean	50%	90%	99%
Ctr. year 1-30	2.87	2.5	5.3	8.2
CO ₂ year 1-30	3.00	2.6	5.5	8.9
Wave height statistics Ami (71.5 N, 19.0 E)				
	Mean	50%	90%	99%
Ctr. year 1-30	2.42	2.0	4.5	7.6
CO ₂ year 1-30	2.53	2.1	4.7	8.3
Wave height statistics Charlie (52.5 N, 33.5 W)				
	Mean	50%	90%	99%
Ctr. year 1-30	3.33	2.9	5.8	9.3
CO ₂ year 1-30	3.22	2.8	5.7	8.9
Wave height statistics Lima (56.5 N, 20.0 W)				
	Mean	50%	90%	99%
Ctr. year 1-30	3.45	3.0	6.1	9.7
CO ₂ year 1-30	3.42	3.0	6.1	9.9
Wave height statistics Juliette (52.5 N, 20.0 W)				
	Mean	50%	90%	99%
Ctr. year 1-30	3.27	2.9	5.7	9.1
CO ₂ year 1-30	3.19	2.8	5.7	8.9
Wave height statistics India (59.0 N, 19.0 W)				
	Mean	50%	90%	99%
Ctr. Year 1-30	3.41	3.0	6.1	9.7
CO ₂ year 1-30	3.41	2.9	6.1	10.0

Table 2: Statistics of significant wave height (m): Mean values, 50, 90 and 99 percentiles for control run, 2XCO₂ run. For Ekofisk and Gullfaks also for observations from years 1980-1998.

Deviations from work plan

The 2X30 years runs with the WAM model was finished somewhat before the planned schedule since more computer resources became available during this period.

Modifications of work for the next period

In the project proposal it was planned to run the wave model for at least 2X10 years with wind data from the T106 time slice experiments and to run some selected cases with finer resolution. Now we have run 2X30 years with wind data from the time slice experiments. We decided to give this higher priority than running selected cases with finer resolution. At the moment we are not sure if we will rerun the wave model for a few selected cases. It depends on the results from tasks 2 and 3.

Part 3: Surge

Progress of the work

The surge effort at DNMI in the second annual period has been devoted to Task 5: Surge statistics based on 30 year T106 time slices: Northwestern European shelf seas. In this task, DNMI has obtained tidal residual water level fields from three runs of POL's 35 km NEAC model: the 43-year Hindcast run using DNMI's hindcast wind and mslp fields, and the two 30-year scenario runs forced by the T106 time slice atmospheric

data ("Control" as today's climate and "Scenario" as the 2xCO₂ climate). The work has consisted of two sub-tasks: completing the validation of the Hindcast against Norwegian coastal and offshore observations, and performing comparisons of the Control and Scenario runs against the Hindcast and against each other.

Validation of the Hindcast against Norwegian coastal stations was largely performed in the first year; this included eight stations, most with records covering the entire hindcast period. In the present reporting period, attention has been given to offshore observations. These data are difficult to obtain and analyse, and an effort has been made to obtain results from previous statistical studies. The validation has focussed on surge variability and extreme surge statistics. In addition to extreme value extrapolations such as 50-year return levels, alternative statistical measures of extreme surges have been considered.

Comparison of the time slice runs is nearing completion, and covers Norwegian coastal and offshore sites. So far, statistical comparisons of extremes have been carried out for the same sites as used for the hindcast validation.

In preparation for Tasks 7 and 8, a preliminary comparison of DNMI's surge model with the POL/NEAC model has been carried out.

Achievements and results obtained

The comparison of the NEAC Hindcast surge statistics and coastal observations shows that the model tends to overestimate the 50-year return surges (see Table 3). The agreement is best on the west coast, and overestimation is greatest in the Skagerrak and northern Norway. An alternative measure - the 99.99 percentile - shows a similar overestimation by the model. For the offshore site Frigg, the comparison is quite different, with the model underestimating. However, the quality of the observed values at this site is much less certain, since the time series are shorter and of poorer quality. The overall conclusion is that the NEAC model statistics agree fairly well with the observations, with a bias of about +10% or less. Keeping this in mind, the model is an acceptable tool for realistically estimating surge statistics from atmospheric forcing.

Site	Mean		Std. Dev.		50-year return		99.99 %-ile	
	Obs	Model	Obs	Model	Obs	Model	Obs	Model
Helgeroa	-0.040	0.039	0.172	0.207	1.21	1.54	0.960	1.181
Tregde	0.012	0.019	0.138	0.132	1.02	1.12	0.736	0.847
Måløy	0.016	0.047	0.162	0.145	0.99	1.02	0.771	0.805
Kristiansund	0.024	0.052	0.171	0.151	1.10	1.12	0.860	0.901
Rørвик	-0.005	0.058	0.173	0.161	1.28	1.41	1.036	1.079
Bodø	-0.004	0.074	0.179	0.170	1.22	1.56	0.971	1.082
Narvik	0.000	0.082	0.185	0.178	1.36	1.71	0.989	1.170
Frigg					0.93	0.73		

Table 3: Comparison of residual water level statistics from POL/NEAC Hindcast (1955-97) and observations. Note that the 50-year return and 99.99 %-ile values are adjusted for the mean. All values in meters.

Comparison of the Control and Scenario time slice simulations, as well as the Hindcast, for selected sites is summarized in Figure 4. First of all, the Control and Hindcast mean sea levels are about the same, indicating that the starting point for the simulation is right. The extreme values (50-year return and 99.9 %-ile) for the Control and Scenario are both considerably lower than the Hindcast, as much as 0.2 m. This indicates that the wind forcing from the T106 time slices is generally weaker than in DNMI's Hindcast Archive. However, in light of the validation of the Hindcast, it appears that the Control may be closer to today's (observed) climate than the Hindcast. Second, the Scenario extreme values are almost all higher than the Control, indicating a more severe surge climate in the 2xCO₂ future. Note that the mean sea level is everywhere

higher than the Control, such that the total extreme water levels are all at least as large as the Control. The overall sea level variability, as measured by the standard deviation, is quite similar in all three runs, except that the Control has lower values on the west coast. Comparing the time slices, the sea level variability is greater in the future Scenario. Details of the differences in the distributions of sea level are revealed in Figure 5, which shows quantile-quantile plots of the residual sea level at Tregde and Kristiansund for the Control and Scenario. The middle range of the distributions in both locations are quite similar, with a tendency for the points to lie just above the 1:1 line, reflecting the difference in mean sea level. The most striking differences are at the tails of the plot. In the Skagerrak (Tregde), the Scenario distribution is broadened with respect to the Control, i.e., the Scenario has higher high sea levels and slightly lower low sea levels than the Control. On the west coast (Kristiansund), the Scenario distribution is shifted toward high sea levels, i.e., the Scenario has higher values for both high and low extreme water levels.

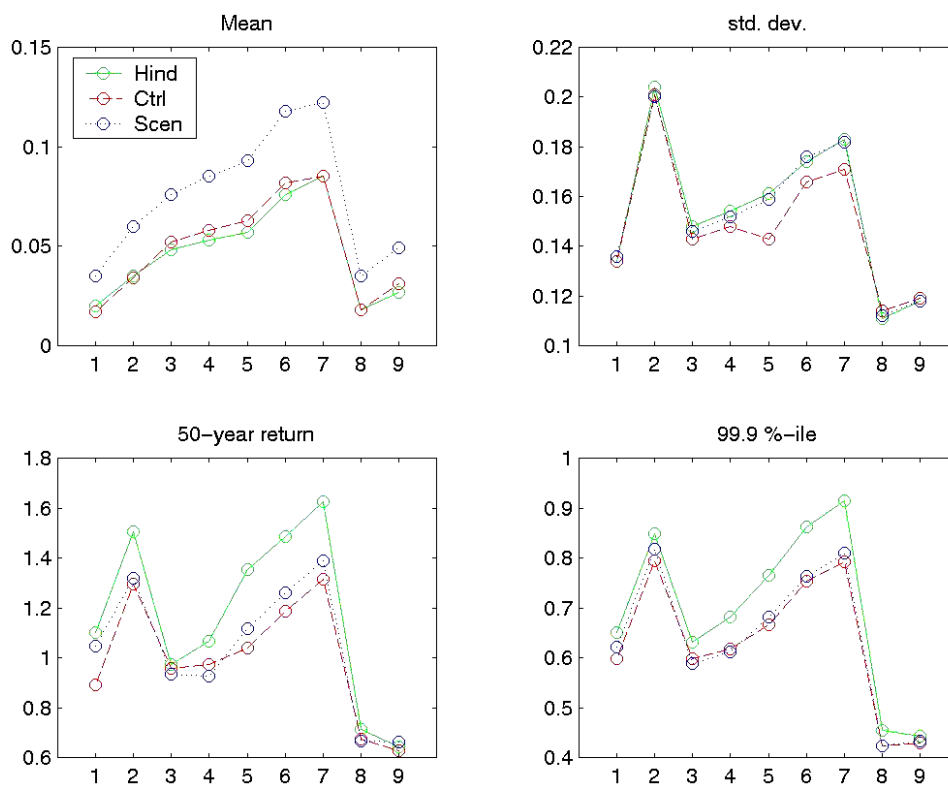


Fig. 4. Comparison of water level statistics from POL/NEAC runs: Hindcast, Control and Scenario. Horizontal axis is site number: 1,2 are in the Skagerrak; 3-7 run northward along the coast; 8,9 are North Sea offshore sites. Note that the 50-year return and 99.9 %-ile are adjusted for the mean.

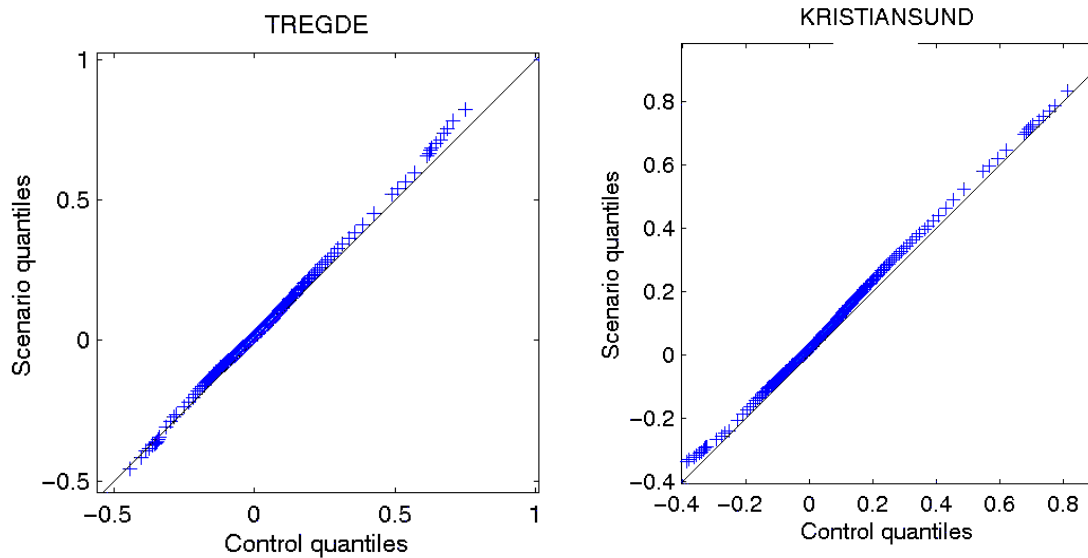


Fig. 5. Quantile-quantile plot of residual water level distribution from POL/NEAC Control and Scenario runs for Tregde (Skagerrak) and Kristiansund (Norwegian west coast). All values in meters.

Deviations from work plan

The work plan is unchanged, but the work is somewhat behind the planned schedule, partly due to delays in obtaining Control and Scenario results and partly due a shortage of manpower in the middle of 1999. The backlog will not jeopardize the completion of the work plan.

Modifications of work for the next period

No changes to the work are envisaged, but sufficient manpower resources for completion of Tasks 7 and 8 have been allotted for 2000.